AD_____

Award Number: DAMD17-00-1-0052

TITLE: Permanent Implantation Brachytherapy for Prostate Cancer Using a Mixture of Radionuclides with Different Half Lives

PRINCIPAL INVESTIGATOR: Ravinder Nath, Ph.D.

CONTRACTING ORGANIZATION: Yale University School of Medicine
New Haven, CT 06520-8047

REPORT DATE: March 2004

TYPE OF REPORT: Final

PREPARED FOR: U.S. Army Medical Research and Materiel Command
Fort Detrick, Maryland 21702-5012

REPORT DOCUMENTATION PAGE

Form Approved
OMB No. 074-0188

1. AGENCY USE ONLY (Leave blank)	2. REPORT DATE	3. REPORT TYPE AND DATES COVERED
	March 2004	Final (1 Mar 2000 - 29 Feb 2004)

4. TITLE AND SUBTITLE
Permanent Implantation Brachytherapy for Prostate Cancer Using a Mixture of Radionuclides with Different Half Lives

5. FUNDING NUMBERS
DAMD17-00-1-0052

6. AUTHOR(S)
Ravinder Nath, Ph.D.

7. PERFORMING ORGANIZATION NAME(S) AND ADDRESS(ES)
Yale University School of Medicine
New Haven, CT 06520-8047

E-Mail: ravinder.nath@yale.edu

8. PERFORMING ORGANIZATION REPORT NUMBER

9. SPONSORING / MONITORING AGENCY NAME(S) AND ADDRESS(ES)
U.S. Army Medical Research and Materiel Command
Fort Detrick, Maryland 21702-5012

10. SPONSORING / MONITORING AGENCY REPORT NUMBER

11. SUPPLEMENTARY NOTES

12a. DISTRIBUTION / AVAILABILITY STATEMENT
Approved for Public Release; Distribution Unlimited

12b. DISTRIBUTION CODE

13. ABSTRACT (Maximum 200 Words)

Overall objective of this project was to test whether the therapeutic effectiveness of permanent implant brachytherapy for prostate cancer can be improved by using a combination of short and long half life radionuclides simultaneously. A theoretical model for continuous low dose rate irradiation (CLDRI) using a mixture of radionuclides was developed. Experiments were performed using BA1112 tumor and Chinese Hamster cells in vitro and BA1112 cells in vivo as solid tumors in WAG/rij rats. Radiobiology parameters for these cells were determined and used in the theoretical radiobiology model to improve our understanding of the experimental observations. Afterloading applicators for in vivo irradiations as well as animal care procedures were developed. In vivo experiments for tumor growth studies using the BA1112 rat model with ^{125}I, ^{103}Pd and a 50:50 mixture of the two were performed. Irradiations at 8 cGy/hr did not result in any tumor cures. At 16 cGy/hr tumor cures were observed in ^{125}I alone, ^{103}Pd alone and in the 50:50 mixture. A higher than expected tumor cure rate was observed in the CLDRI using a 50:50 mixture of ^{125}I and ^{103}Pd seeds. More experiments are required to prove and quantify this observation.

14. SUBJECT TERMS
cancer therapy, radiation therapy, radiobiology, radiation physics

15. NUMBER OF PAGES
110

16. PRICE CODE

17. SECURITY CLASSIFICATION OF REPORT	18. SECURITY CLASSIFICATION OF THIS PAGE	19. SECURITY CLASSIFICATION OF ABSTRACT	20. LIMITATION OF ABSTRACT
Unclassified	Unclassified	Unclassified	Unlimited

Table of Contents

INTRODUCTION

The objective of the project was to test whether the therapeutic effectiveness of permanent implant brachytherapy for prostate cancer can be improved by using a combination of short and long half life radionuclides simultaneously. Specific aims of the proposed project were:

1. To test theoretically the potential of a mixture of radionuclides in permanent implants, using the linear quadratic model, as a function of T_{pot}, potential tumor doubling time.

2. To test experimentally the validity of this concept by *in vitro* irradiation of BA1112 sarcoma cells at a continuous low dose rate (CLDR) with ^{125}I (60 d half life), ^{103}Pd (17 d half life) and a 50:50 mixture of ^{125}I and ^{103}Pd under aerobic conditions leading to exponential growth at different rates (from near quiescence to full exponential growth at a maximal rate, with a doubling time of approximately 14 hours).

3. To measure the radiobiology parameters such as alpha, beta, half life of repair for the BA1112 sarcoma cells under different growth conditions and develop a theoretical model to predict expected levels of cell killing using ^{125}I, ^{103}Pd or a mixture of these isotopes.

4. To use immunohistochemical techniques to measure, in solid BA1112 tumors *in vivo*, the proportion of cells in S phase, the proportion proliferating and non-proliferating cells and the tumor doubling time.

5. To test the therapeutic effectiveness of ^{103}Pd, ^{125}I and a Pd/I mixture in the BA1112 *in vivo* tumor system;

6. To test the therapeutic effectiveness of ^{103}Pd, ^{125}I and a Pd/I mixture in human prostate carcinoma xenografts in nude mice, using a slow growing and a fast growing carcinoma.

7. To evaluate the clinical potential and feasibility of this approach in the treatment of human prostate cancer.

BODY OF THE REPORT

We have developed a theoretical radiobiology model for cell killing by continuous low dose rate irradiation (CLDRI) using a mixture of radionuclides. Theoretical studies were performed to investigate the hypothesis and to plan *in vitro* and animal studies. Experiments have been performed using BA1112 tumor cells and Chinese Hamster cells growing *in vitro* and BA1112 cells growing *in vivo* as solid tumors in WAG/rij rats. Radiobiology parameters for these cells have been determined and used in the theoretical radiobiology model to improve our understanding of the experimental observations.

The linear-quadratic model of cell-killing by CLDRI Using a Mixture of Radionuclides

We have developed a theoretical model for CLDRI using a mixture of radionuclides with different half lives. This model is described in the attached manuscript entitled "Biologically effective dose (BED) for interstitial seed implants containing a mixture of radionuclides with different half lives" by Zhe Chen and Ravinder Nath (Appendix I). Briefly, the purpose of this project was to develop a tool for evaluating interstitial seed implants that contain a mixture of radionuclides with different half-lives and to examine the clinical implications of prescribing to an isodose surface for such an implant. Using a generalized equation for the biological effective dose (BED)[1-5], the effects of cell proliferation and sub-lethal damage repair were examined systematically for implants containing a mixture of radionuclides (Figure 1). The results were contrasted with those for implants using a single type of radionuclide. A clinical permanent seed implant that contained a mixture of ^{125}I and ^{103}Pd seeds was used to examine the clinical implications of the isodose prescription for such implants. An equation of BED for implants containing any number of radionuclide types was obtained. For implants containing a mixture of radionuclides with different half-lives such as ^{125}I and ^{103}Pd, the dose as well as its temporal delivery pattern to a point is dependent on the relative dose contributions from different types of radionuclides. It can vary from point to point throughout the implant volume. Therefore the quantitative effects of cell proliferation and sub-lethal damage repair are spatially dependent in such an implant. For implants containing a mixture of ^{125}I and ^{103}Pd seeds, the prescription to an isodose surface becomes non-unique. If the prescription dose was based on existing clinical experience of using ^{125}I seeds alone, mixing ^{103}Pd seeds with ^{125}I seeds would decrease the cell survival in such implant. On the other hand, if the prescription dose was based on existing clinical experience of using ^{103}Pd seeds alone, mixing ^{125}I seeds with ^{103}Pd seeds in a same implant would create radiobiologically "cold" spots (i.e. an increase in cell survival from the clinical expectation) at locations where a major portion of prescription dose is contributed by the ^{125}I seeds. For fast-

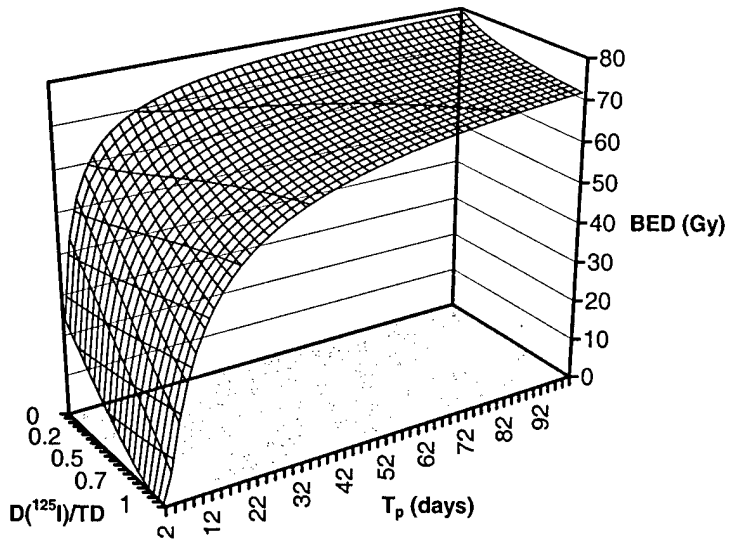

Figure 1

growing tumors, these "cold" spots can become significant. From this theoretical investigation, we conclude that when cell proliferation and sub-lethal damage repair are present during dose delivery, total dose alone is no longer sufficient for a complete characterization of an interstitial seed implant. In order to avoid radiobiological "cold" spots when radionuclides of different half-lives are mixed in a permanent implant, the dose prescription should be based on the clinical experience of using the longer half-life radionuclide. Biologically effective dose provides a tool to start examining the radiobiological effects of mixing different type of radionuclides in the same implant.

A manuscript on the model has been published in the International Journal of Radiation Oncology Biology Physics (*Int J Radiat Oncol Biol Phys* 2003, **55,** 825-834) (Appendix I).

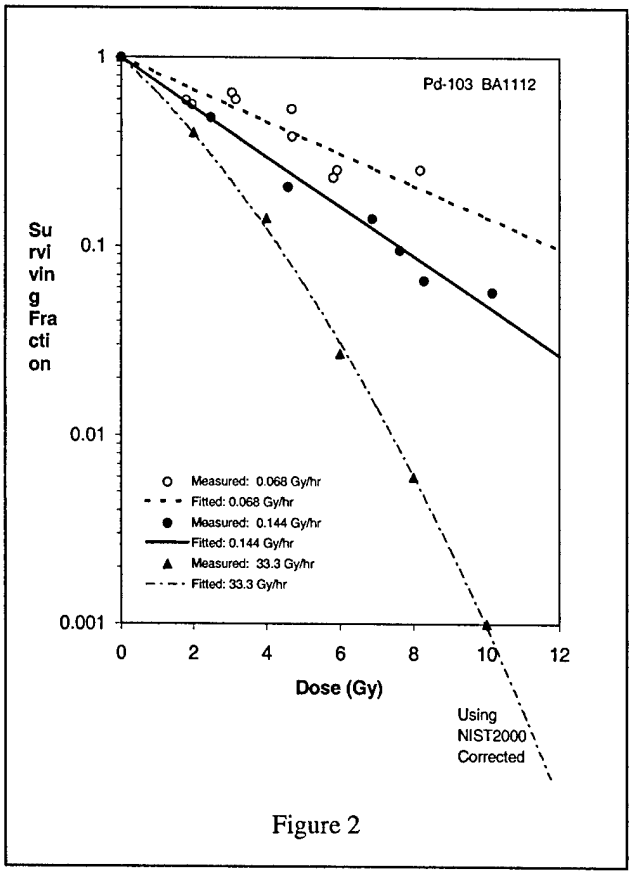

Figure 2

In vitro CLDRI studies

BA1112 tumors were grown between the ears of the a 14 week old male WAG/rij rats by interdermal inoculation from a single cell suspension of BA1112 cells obtained from a 21 day BA1112 tumor growing on the head of a previously inoculated rat.[6-10] A tumor cell suspension was made from the BA1112 tumor and between $1.5x10^5$ and $5.0x10^5$ cells were plated into petri dishes. These cells were allowed to settle and reach logarithmic growth, (48-72 hrs), before they were used in a continuous low dose rate experiment.

Monolayers of rat rhabdomyosarcoma cells (BA1112) were irradiated *in vitro* by ^{103}Pd sources in a polystyrene phantom. Colony formation ability of irradiated cells under aerobic conditions was measured for graded doses, at a dose rate of 8 cGy/hr. Dose to the cell monolayers was determined using $FeSO_4$ Fricke dosimetry, with a calculated correction for interface effects due to photoelectric effect in the tissue culture dishes. The sources (up to 80 in one experiment) were arranged in concentric circles in such a way as to provide a dose uniformity of better than ± 5% across the dishes. Some of the results are shown in Figure 2. Comparison of the surviving fraction as a function of dose calculated for the BA1112 cells to that measured by using CLDRI ^{103}Pd irradiation is also shown in Figure 2. The lines through the data points represent the calculated survival curves the symbols represent the measured data The parameters of α, β, repair half-time, and tumor doubling time were determined directly from the

measurements performed on the BA1112 cells, as described later in the report. A profound dose rate effect was observed at low dose rates in the range of 6.8 to 14.4 cGy/h that are typical of permanent interstitial brachytherapy. At cell-surviving fraction of 0.01, the relative biological effectiveness (RBE) of CLDRI at 6.8 and 14.4 cGy/h using ^{103}Pd sources was reduced by a factor of 3 and 2, respectively, relative to the acute exposure. This observation is in good agreement with the *in vivo* tumor cure studies performed on BA1112 tumor to be described later in the report.

A manuscript entitled "Dose rate dependence of the relative biological effectiveness of ^{103}Pd for Continuous Low Dose Rate Irradiation of BA1112 Rhabdomyosarcoma Cells *in vitro* relative to Acute Exposures" has been submitted to Int. J. Radiat. Biol. (Appendix II).

In vitro studies at an acute dose rate using simulated x-ray beams

To study the radiobiological characteristics of the cells under acute exposure condition, simulated x-ray beams with average energies equivalent to that emitted by ^{125}I (27.2 – 35.49 keV with an average of 27.4) and ^{103}Pd (20 – 22.7 keV with an average of 20.5 keV) were established on a new orthovoltage unit. The simulated beams not only have the average energies similar to that given by the radioactive isotopes but also have a narrow photon energy spectrum. The narrow photon energy spectrum was achieved by optimizing the tube voltage (which determines the upper limit of the produced photon energy) and the added filtration (which filters out the low-energy Bremsstrahlung photons), following the work of Muench et al.[11].

Aluminum filters from Pantak was used to construct a customized filter for the DXT 300 unit that has a desired filtration thickness. A set of aluminum filters (with thickness of 0.1 to 1.0 mm) from Nuclear Associates (AL Filter Set 07-430) were used to determining the half-value-layer (HVL) of a simulated beam using a customized filtration. The thicknesses of the aluminum sheets were measured by using a Mitutogo micrometer (Serial # 2032360) with accuracy of 0.001 mm). The aluminum HVL for a given beam was determined by in-air ionization chamber measurement under the narrow beam geometry. An air-equivalent Spokas chamber (Exradin, Model No: A1 (0.5 ml, AE plastic)) was used to measure the ionization at a fixed source to chamber distance (SCD) of 50 cm in air. The ionization charge was measured by a Keithley electrometer (model 35614E SN 43075) with –300 V bias potential. Due the energy dependence of the chamber at the low energies, the measured ionization were converted to corresponding exposure and the HVL is then determined from the relative exposure as a function of aluminum filter thickness. A narrow circular beam, with a diameter of 6 cm at SCD of 50 cm, was generated by using a homemade lead collimator mounted to DXT 300's accessory mount. The aluminum sheets added to the beam for the HVL measurement were taped to the bottom of the lead collimator.

The HVL as a function of mono-energetic photon beam energy for aluminum is taken from Johns and Cunningham[12]. The expected HVL for a simulated ^{125}I (^{103}Pd) beam with average energy of 27.4 keV (20.5 keV) is 1.84 mm (0.82 mm) aluminum. With the expected HVL in mind, the tube kV, mA and the thickness of the added filtration were

optimized for a simulated ^{125}I and a simulated ^{103}Pd x-ray beam. The optimum setting determined for the DXT 300 unit is summarized in the following table I.

Table I. Radiation characteristics of simulated x-ray beams

Beam	kV	mA	Added Filter (mm AL)	Beam HVL (mm AL)	Energy Homogeneity (%)	Equivalent Energy (keV)	<E> from isotope (keV)
^{125}I Equivalent	43	20	3.545	1.851	86.9	27.45	27.4
^{103}Pd Equivalent	29	25	1.826	0.82	88.6	20.5	20.5

The two simulated beams were used to provide reference acute high dose rate irradiations (AHDRI) for the *in vitro* radiobiological studies using BA1112 and CCL-16 cells and radioactive sources of ^{125}I and ^{103}Pd. Data obtained from AHDRI provides a unified description of the relative radiobiolocal effectiveness (RBE) and its dependence on dose rate and linear energy transfer (LET) of the ^{125}I and ^{103}Pd photons. Details are given in Appendix II.

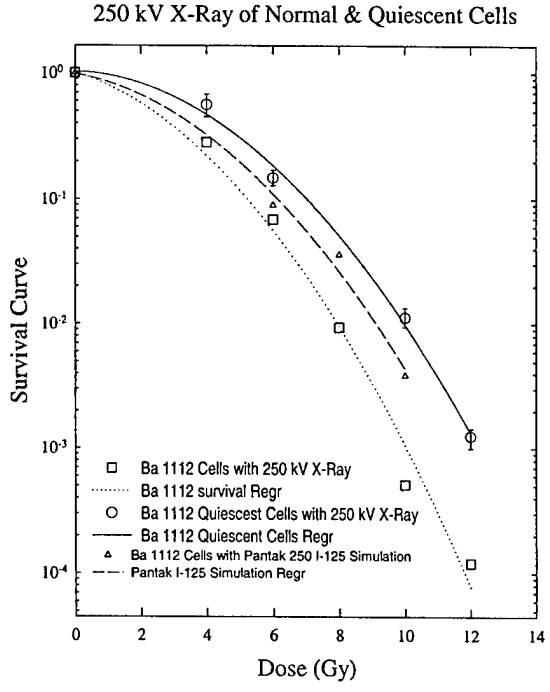

Figure 3

In vitro studies for quiescent BA1112 cells

Animals were implanted with transplanted BA1112 rhabdomyosarcomas by inoculation, into a subcutaneous site on the heads. The tumors were allowed to grow for 3 weeks, to an experimental volume of approximately 199-200mm^3. The animals chosen for the quiescent cell experiments were euthanized by anesthetic overdose and the tumor cells will then be removed using aseptic techniques. A single-cell suspension of tumor cells was suspended, counted, and assayed for viability using the same colony formation assay used for cells in cultures. 1.5 x10^5 cells were plated into a flask with 13 ml of DMEM for cell growth. These cells will then be passed twice a week for approximately 4-8 passages. The cells are transplanted for 2-4 weeks to assure a homogeneity

population of BA1112 cells. When the first line has reached passage 5 the cells were counted and $1.0x10^7$ plated into 5 petri dishes for a cell survival experiments with either normal or quiescent cells. We know from our previous quiescent cell induction experiments that between Days 5-7 were optimal to assure cells in a healthy quiescent state. If we waited past Day 7 we will be in past are optimal window and exhibiting the cell death phase.

The quiescent cells are irradiated on Day 6 or 7, and the response of tumors to irradiation will be assessed by the ability of the BA 1112 tumor cells to form colonies in cell culture after *in vitro* irradiations. A single-cell suspension of the tumor cells will be counted, and assayed for viability and appropriate cell numbers plated in each petri dish as determined by the specific dose given to the BA1112 cells in the petri dish. Therefore multiple platings from a single cell suspension are mandatory to ensure an adequate countable number of colonies. After these dishes are allowed to grow for 14 days in a controlled environment, 37^0C incubator with 95% air/5% CO_2, they are stained with crystal violet. Analysis of cell yield is performed.

Radiological Parameters for CCL-16 and BA1112 cells

In order to measure the radiological parameters of the cells used in these studies, the acute exposure survival curves were measured using 250 kV x-rays. Split dose experiments were conducted to measure the half time of sublethal damage repair. Results are described in Appendix II and IV. The following tables summarize the results obtained for BA1112 and CCL-16 cells.

Radiobiological Parameters Determined from Acute Exposure Experiments

Beam	Parameters for Ba-1112				
	α (Gy^{-1})	β (Gy^{-2})	α/β (Gy)	Tumor Doubling Time (day)	Sub-lethal Damage Repair Half-time (hr)
250 kV old	0.25	0.041	6.1	3.0	0.33
^{125}I equivalent	0.26	0.043	6.1	3.0	0.33
^{103}Pd equivalent	0.29	0.048	6.1	3.0	0.33
250 kV old	0.23	0.044	5.1	3.0	0.33
^{125}I New	0.25	0.044	5.6	3.0	0.33
^{103}Pd New	0.32	0.044	7.3	3.0	0.33

Beam quality	Parameters for CCL-16				
	α (Gy^{-1})	β (Gy^{-2})	α/β (Gy)	Tumor Doubling Time (day)	Sub-lethal Damage Repair Half-time (hr)
250 kV	0.17	0.037	4.7	0.55	0.21
^{125}I equivalent	0.12	0.025	4.7	0.55	0.21
^{103}Pd equivalent	0.16	0.033	4.7	0.55	0.21
250 kV	0.23	0.031	7.4	0.55	0.21
^{125}I equivalent	0.07	0.031	2.1	0.55	0.21
^{103}Pd equivalent	0.18	0.031	5.7	0.55	0.21

IUdR and BrdU Labeling For Flow Cytometric Analysis

We have developed protocols for *in vitro* IUdR labeling and *in vivo* BUdR labeling for flowcytometric analysis of CCL-116 and BA1112 cells based upon a protocol from Dr. Hong Sun at Yale. Several studies on CCL-116 and BA1112 cells have been performed and results are being analyzed. An example is shown below.

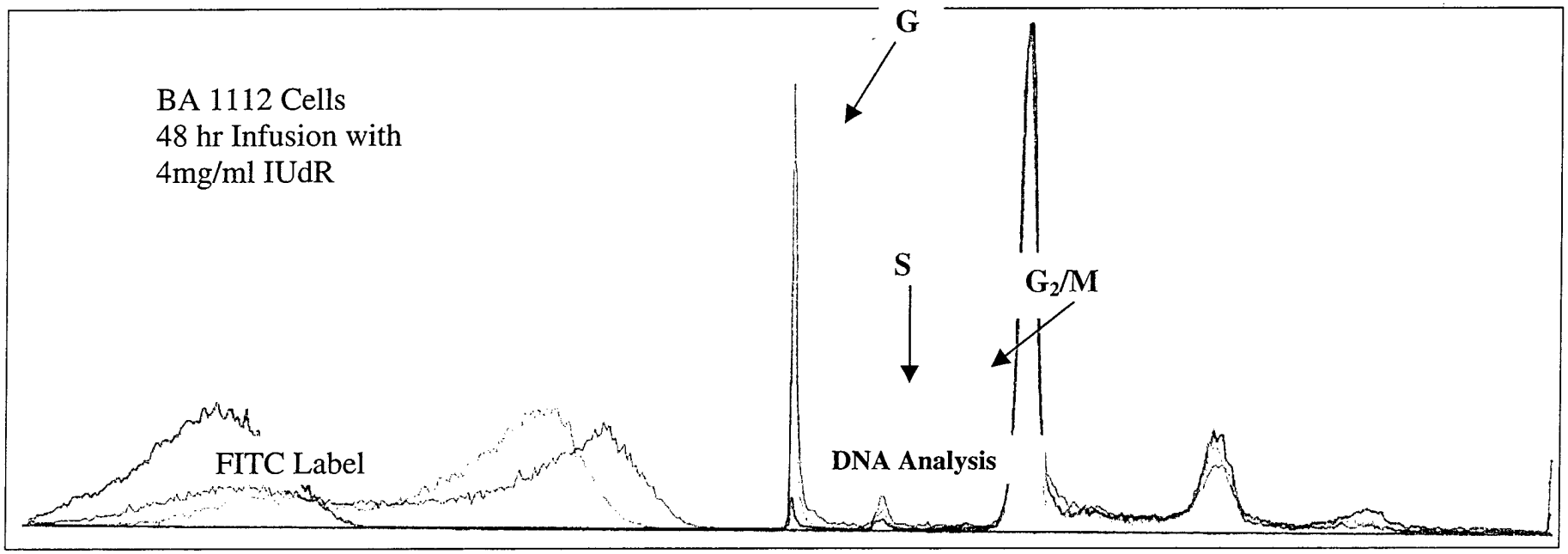

Figure 4

Infused Sample: IUdR Incorporation: Rat 2021: Time 0 hr: G_1 =80% S = 82% G_2M = 78%

Rat 2031: Time 0 hr: G_1 =70% S = 72% G_2M = 68%

Control Sample: IUdR Incorporation: Rat 201 Time 0 hr: G_1 =0.2% S = 0.3% G_2M = 0.3%

In vivo studies using an *in vitro* assay

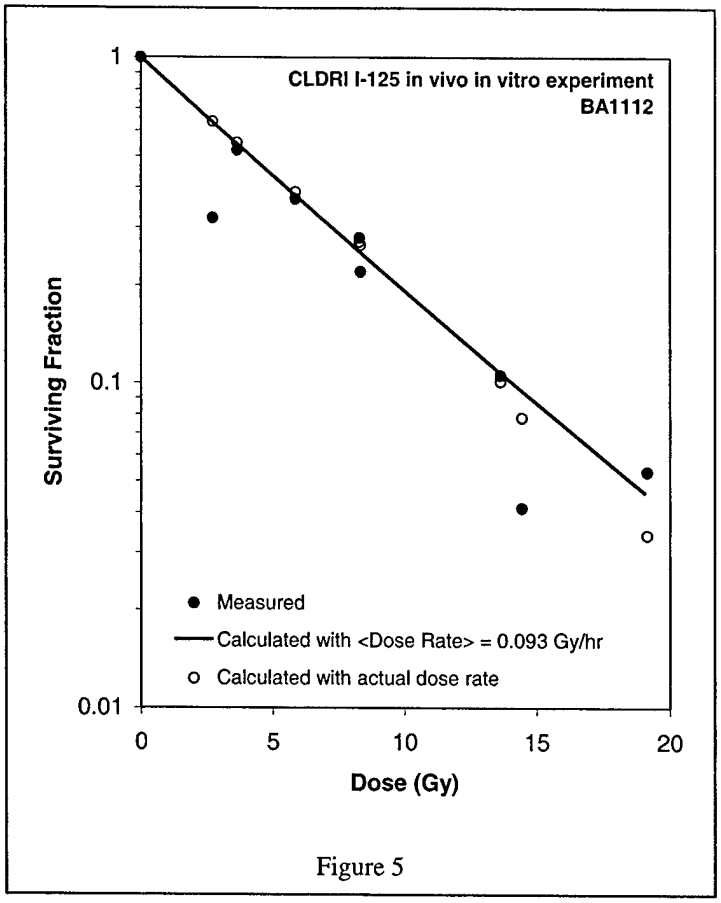

Figure 5

In this experiment, BA1112 tumor cells were irradiated *in vivo* to graded doses from 2 to 20 Gy. Following irradiation at low dose rate, the tumours were removed and their colony formation ability was measured using our *in vitro* assay techniques.[13] Figure 5 shows a comparison of the surviving fraction as a function of dose calculated for the BA1112 cells to that measured in an *in vivo*/*in vitro* experiment using CLDRI ^{125}I irradiation. The solid line represent the calculated survival curve using the average initial dose rates used in the experiments. The open circle represent calculation using the actual initial dose rate for each experiment. The parameters of α, β, repair half-time, and tumor doubling time were determined directly from the measurements performed on the BA1112 cells (as described earlier).

In vivo tumor growth studies

Study of the *in vivo* tumor growth under CLDRI is one of the key experiments of this project and is also the most labor intensive one. Over five consecutive months of time was needed for each experiment condition.

In order to produce a consistent dose distribution to irradiate the tumors transplanted to different animals and to minimize radiation exposure to personnel

handling the radioactive seeds, an afterloading seed applicator was designed and fabricated based upon the work of Peschel et al.[14] The applicator was made of polystyrene with loading ports for nine seeds. The central portion of the applicator was open and has a dimension large enough for tumor to grow. Equal source strength was assigned to all nine seeds in order to minimize the possible confusion of handling variable source strengths. The seeding configuration was optimized to produce an, as uniform as possible, dose distribution to the central portion of the applicator and to be usable for both ^{125}I and ^{103}Pd seeds. Details are described in Appendix III.

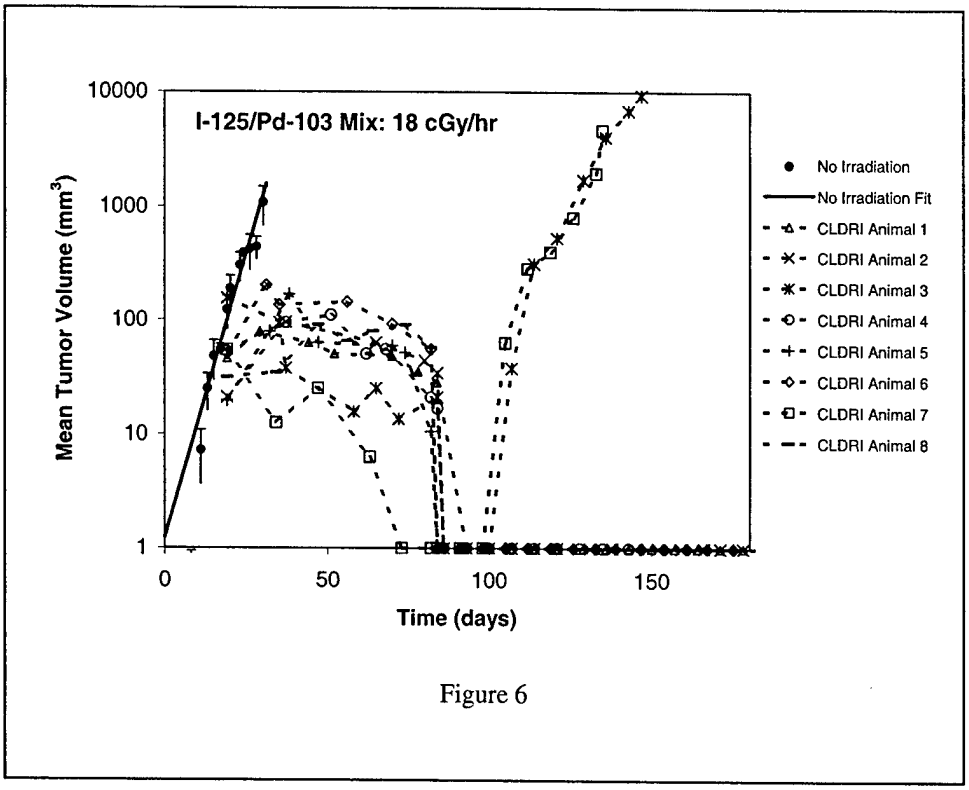

Figure 6

In vivo tumor cure experiments were conducted using ^{125}I seeds with initial dose rates of 8 cGy/hr and 18 cGy/hr, using ^{103}Pd seeds with initial dose rate of 20 cGy/hr, and using a mixture of ^{125}I and ^{103}Pd seeds with initial dose rate of 18 cGy/hr. Eight tumors were treated for each condition. The tumor growth during the irradiation and following the termination of irradiation were measured as a function of elapsed time. The following figure shows a typical result for tumors irradiated by a mixture of ^{125}I and ^{103}Pd seeds with initial dose rate of 18 cGy/hr. The results from this study show that the probability of tumor cure is strongly dependent on both the total delivered dose and the initial dose rate. For CLDRI using ^{125}I, tumor cure was not attainable at initial dose rate of 8 cGy/hr; and was 75% for 146 Gy delivered dose with initial dose rate of 18 cGy/hr. For CLDRI using ^{103}Pd, the probability of tumor cure was 62% at total dose of 112 Gy with initial dose rate of 20 cGy/hr. Interestingly, the tumor cure was 75% for CLDRI using a mixture of ^{125}I and ^{103}Pd at initial dose rate of 18 cGy/hr for a total dose of 146 Gy. This observed tumor cure for the mixed seeds was higher than expected since half of the initial dose rate was contributed by ^{103}Pd, which had a lower tumor cure when used alone at initial dose rate of 20 cGy/hr. These results are highly relevant to the main hypothesis

of this project. More experiments are required to determine if this observation is real and on the possible causes. Details are described in a manuscript entitled "Development of a Rat Solid Tumor Model for Continuous Low Dose Rate Irradiation Studies using ^{125}I and ^{103}Pd Sources" which has been submitted for publication in Brachytherapy (Appendix III).

Nude Mice Studies

One of the specific aims in the proposal was to test the therapeutic effectiveness of ^{103}Pd, ^{125}I and a Pd/I mixture in human prostate carcinoma xenografts in nude mice, using a slow growing and a fast growing carcinoma. This was to be followed depending upon the successful completion of the BA112 in rats studies and to be initiated near the end of the project. Some experimental design studies were performed to investigate the feasibility of using the applicator. Several different designs were considered from a dosimetric point of view. Because of the smaller size of mice and the limitations in reducing the applicator size and weight, we were unable to reach a practical solution. From these initial studies, we have concluded that xenografts studies on nude mice would not be feasible at this stage. A different animal model and brachytherapy applicator would be needed to investigate this issue further.

KEY RESEARCH ACCOMPLISHMENTS

- A theoretical model based on incomplete repair during CLDRI has been developed for addressing the questions raised in the project. The BED for implants with a mixture of two radionuclides has been derived as an analytical expression. A manuscript describing this work has been published in International Journal of Radiation Oncology (Appendix I).

- Cell survival curves for both ^{125}I and ^{103}Pd were measured using monolayers of Chinese hamster cells in a petri dish irradiated at low dose rates using ^{125}I and ^{103}Pd sources. The dose sparing effect of 7 cGy/hr relative to 12 cGy/hr can be expressed by dose modifying factors of 2 ±0.6 and 1.5 ±0.5 for ^{103}Pd and ^{125}I, respectively. The RBEs of ^{103}Pd relative to ^{125}I were 1.2 ± 0.4 and 2.0 ± 0.5 for 7 and 12 cGy/hr, respectively. In our system, the RBE of ^{103}Pd at 19.7 cGy/hr relative to ^{125}I at 7.72 cGy/hr is estimated to be 3±1. A manuscript describing this work has been submitted for publication (Appendix IV).

- Cell survival curves for ^{103}Pd were measured using monolayers of BA1112 cells in a petri dish irradiated at low dose rates using ^{103}Pd sources. An orthovoltage x-ray machine was adapted to produce nearly monoenergetic 21 keV photons, which simulates ^{103}Pd photon energies. Using this x-ray beam, cell survival curves for the BA1112 cells in a petri dish irradiated at an acute dose rate were also measured. We have successfully tested our theoretical model for predicting the CLDRI survival curves *in vitro* for ^{103}Pd sources from the acute dose rate exposure data. A manuscript entitled "Dose rate dependence of the relative biological effectiveness of ^{103}Pd for Continuous Low Dose Rate Irradiation of

BA1112 Rhabdomyosarcoma Cells *in vitro* relative to Acute Exposures" has been submitted to Int. J. Radiat. Biol.. (Appendix II).

- Cell survival curves for ^{125}I were measured using of BA1112 cells irradiated *in vivo* at low dose rate of 8 cGy/hr using the afterloading rat applicator with ^{125}I sources. An orthovoltage x-ray machine was adapted to produce nearly monoenergetic 28 keV photons, which simulates ^{125}I photon energies. Using this x-ray beam, cell survival curves for the BA1112 cells in a petri dish irradiated at an acute dose rate were also measured. Using the parameters derived from the acute exposures, our theoretical model was able to predict the *in vivo-in vitro* CLDRI survival curves. The results are included in the manuscript "Development of a Rat Solid Tumor Model for Continuous Low Dose Rate Irradiation Studies using ^{125}I and ^{103}Pd Sources" that has been prepared for submission to Brachytherapy (Appendix III).

- In order to produce a consistent dose distribution to irradiate the tumors transplanted to different animals and to minimize the radiation exposure to personnel handling the radioactive seeds, an afterloading seed applicator has been designed. *In vivo* tumor cure studies have been performed on live BA1112 tumors treated with CLDRI using these applicators containing ^{125}I and ^{103}Pd seeds. At 8 cGy/hr using ^{125}I, tumor growth was significantly slowed by CLDRI, from a tumor doubling time of 2.7 days in controls to 13 days in the treated animals. However, no tumor cures were observed at 8 cGy/hr. Experiments conducted at 18 cGy/hr for ^{125}I alone, 20 cGy/hr for ^{103}Pd alone, and 18 cGy/hr for a 50:50 mixture of ^{125}I and ^{103}Pd seeds have revealed interesting dependence of tumor cures on the initial dose rate, total delivered dose, and on the mixing of ^{125}I and ^{103}Pd seeds. The relative magnitude of tumor cure observed in the CLDRI of a 50:50 mixture of ^{125}I and ^{103}Pd seeds is one of the primary research objective of this project. Although we are at the end of grant period for this project (due to long duration required for each experiment), more studies are planned to substantiate the observation of the tumor cure from mixed seeds and the possible causes. A manuscript entitled "Development of a Rat Solid Tumor Model for Continuous Low Dose Rate Irradiation Studies using ^{125}I and ^{103}Pd Sources" has been submitted Brachytherapy (Appendix III).

REPORTABLE OUTCOMES

A manuscript entitled "Biologically effective dose (BED) for interstitial seed implants containing a mixture of radio-nuclides with different half lives" by Zhe Chen, Ph.D. and Ravinder Nath, Ph.D. has been published in the International Journal of Radiation Oncology (*Int J Radiat Oncol Biol Phys* 2003, **55** 825-834). The manuscript is attached as an Appendix I.

A manuscript entitled "Dose rate dependence of the relative biological effectiveness of ^{103}Pd for Continuous Low Dose Rate Irradiation of BA1112 Rhabdomyosarcoma Cells *in vitro* relative to Acute Exposures" has been submitted to Int. J. Radiat. Biol. (Appendix II).

A manuscript entitled "Development of a Rat Solid Tumor Model for Continuous Low Dose Rate Irradiation Studies using ^{125}I and ^{103}Pd Sources" has been submitted to Brachytherapy (Appendix III).

A manuscript entitled "Relative biological effectiveness of ^{103}Pd and ^{125}I photons for continuous low Dose rate irradiation of Chinese Hamster cells" is being prepared and will be submitted to Int J of Radiat. Biol. (Appendix IV).

CONCLUSION

We have made considerable progress towards the specific aims of the project. Theoretical model for continuous low dose rate irradiation using a mixture of radionuclides has been developed. Experiments have been performed using BA1112 tumor cells and Chinese Hamster cells growing *in vitro* and BA1112 cells growing *in vivo* as solid tumors in WAG/rij rats. Radiobiology parameters for these cells have been determined and used in the theoretical radiobiology model to improve our understanding of the experimental observations. We have designed and fabricated applicators for *in vivo* irradiations as well as developed the animal care procedures. We have performed *in vivo* experiments for tumor growth studies using the BA1112 rat model with ^{125}I, ^{103}Pd and a 50:50 mixture of the two seeds. A higher than expected tumor cure rate was observed in CLDRI using a 50:50 mixture of ^{125}I and ^{103}Pd seeds, which was the main hypothesis of this project. More experiments are required to prove and quantify the observation and evaluate its clinical implications.

REFERENCES

1. Dale RG. The application of the linear-quadratic dose-effect equation to fractionated and protracted radiotherapy. *Brit J Radiol, 1985;* **58**:515-528.

2. Dale RG. Radiobiological assessment of permanent implants using tumor repopulation factors in the linear-quadratic model. *Brit J Radiol. 1989;* **62:**241-244.

3. Ling CC. Permanent implants using Au-198, Pd-103, and I-125: radiobiological considerations based on the linear quadratic model. *Int. J. Radiat. Oncol. Biol. Phys.1992;* **23:**81-87.

4. Dale RG, Jones B. The clinical radiobiology of brachytherapy. *British J. Radiol,* 1998; 71: 465-483.

5. Thames HD. An "incomplete-repair" model for survival after fractionated and continuous irradiation, *Int. J. Radiat. Biol.* 1985;**47:**319-339.

6. Reinhold, H.S., Quantitative evaluation of the radiosensitivity of cells of a transplantable rhabdomyosarcoma in the rat. Europ. J. Cancer, 2: 33-42, 1966

7. Reinhold, H.S., DeBree, C., Tumor cure rate and cell survival of a transplantable rat rhabdomyosarcoma following x-irradiation. Europ. J. Cancer 4: 367-374, 1968

8. Fischer JJ, Reinhold HS, The cure of rhabdomyosarcoma BA1112 with fractionated radiotherapy. Radiology 105: 429-433, 1972.

9. Moulder JE, Fischer JJ, Determination of an optimal treatment plan for rat rhabdomyosarcoma. Radiology 107: 439-441, 1973.

10. Moulder JE, Fischer JJ, Milardo R, Time-dose relationships for the cure of an experimental rat tumor with fractionated radiation. Int. J. Radiat. Oncol. Biol. Phys. **1**, 431-438, 1976.

11. Muench PJ, Meigooni AS, Nath R, McLaughlin WL. Photon energy dependence of the sensitivity of radiochromic film and comparison with silver halide film and LiF TLDs used for brachytherapy dosimetry. Med Phys. 18:769-75 1991.

12. H. Johns and J. R. Cunningham, The Physics of Radiology, 4th edition, p. 732, 1983.

13. Nath R, Bongiorni P, Rockwell S, The relative biological effectiveness of iodine-125 and americium-241photons relative to radium-226 photons for continuous low dose rate irradiations at dose rates of 0.17 to 0.73 Gy/hr, Endocurie, Hypertherm, Oncol. 681-91, 1990.

14. Peschel RE, Martin DF, Fischer, Tumor cure studies on the rate sarcoma BA1112 using continuous low-dose-rate radiation. Radiology 152, 801-803, 1984.

Int. J. Radiation Oncology Biol. Phys., Vol. 55, No. 3, pp. 825–834, 2003

0360-3016/03/$–see front matter

ELSEVIER

doi:10.1016/S0360-3016(02)04282-7

PHYSICS CONTRIBUTION

BIOLOGICALLY EFFECTIVE DOSE (BED) FOR INTERSTITIAL SEED IMPLANTS CONTAINING A MIXTURE OF RADIONUCLIDES WITH DIFFERENT HALF-LIVES

ZHE CHEN, PH.D., AND RAVINDER NATH, PH.D.

Department of Therapeutic Radiology, Yale University School of Medicine, New Haven, CT

Purpose: To develop a tool for evaluating interstitial seed implants that contain a mixture of radionuclides with different half-lives and to demonstrate its utility by examining the clinical implications of prescribing to an isodose surface for such an implant.

Methods and Materials: A linear-quadratic model for continuous low dose rate irradiation was developed for permanent implants containing a mixture of radionuclides. Using a generalized equation for the biologically effective dose (BED), the effects of cell proliferation and sublethal damage repair were examined systematically for implants containing a mixture of radionuclides. A head-and-neck permanent seed implant that contained a mixture of ^{125}I and ^{103}Pd seeds was used to demonstrate the utility of the generalized BED.

Results: An equation of BED for implants containing a mixture of radionuclides with different half-lives was obtained. In such an implant, the effective cell kill was shown to depend strongly on the relative dose contributions from each radionuclide type; dose delivered by radionuclides with shorter half-life always resulted in more cell kill for any given sublethal damage repair and cell proliferation rates. Application of the BED formula to an implant containing a mixture of ^{125}I and ^{103}Pd seeds demonstrates that the conventional dose prescription to an isodose surface is not unique for such an implant. When the prescription dose was based on existing clinical experience of using ^{125}I seeds alone, mixing ^{103}Pd seeds with ^{125}I seeds would increase the cell kill. On the other hand, if the prescription dose were based on existing clinical experience of using ^{103}Pd seeds alone, mixing ^{125}I seeds with ^{103}Pd seeds in the same implant would create radiobiologically "cold" spots (i.e., an increase in cell survival) at locations where a major portion of the prescription dose is contributed by the ^{125}I seeds. For fast-growing tumors, these "cold" spots can become significant.

Conclusions: Total dose alone is no longer sufficient for a complete characterization of a permanent seed implant containing a mixture of radionuclides with different half-lives due to the presence of cell proliferation and sublethal damage repair in the protracted dose delivery. BED provides a tool for evaluating the radiobiologic effects of mixing different type of radionuclides in the same implant. When radionuclides of different half-lives are mixed in a permanent implant, using the dose prescription established from existing clinical experience of implants with the longer half-life radionuclide would help to avoid radiobiologic "cold" spots. © 2003 Elsevier Science Inc.

Interstitial implant, Biologically effective dose, Iodine-125, Palladium-103, Brachytherapy, Radiobiology.

INTRODUCTION

Permanent implantation of encapsulated radioactive seeds in tumors has been used widely as a primary or adjuvant therapy for treating prostate and head-and-neck cancers (1–5). At present, seeds that contain the radionuclide of ^{125}I or ^{103}Pd are routinely used in permanent interstitial implants (6). ^{125}I seed has been introduced since the late 1960s to replace ^{198}Au seeds due to its long half-life [59.4 days (7)], which is convenient for storage, and its low photon energy, which is easy for radiation protection. It has remained a popular choice for permanent interstitial implant (8). ^{103}Pd seed, which has an average photon energy close to ^{125}I and a shorter decay half-life [16.991 days (7)], was introduced for clinical implant about a decade ago. It is generally considered that ^{103}Pd seeds, due to their short half-lives, are more effective for fast growing tumors, whereas ^{125}I seeds are better for slow growing tumors (9). The decision regarding which radionuclide to use for a given implant has been influenced largely by the historical development of radioactive seeds and, recently, by the radiobiologic considerations for each radionuclide (9). Nonetheless, seeds containing different radionuclide types have never been reported in the same clinical implant. For tumors that may contain both fast and slow growing cells, it would seem desirable to use

Reprint requests to: Ravinder Nath, Ph.D., Department of Therapeutic Radiology, Yale University School of Medicine, 333 Cedar Street, New Haven, CT 06510. Tel: (203) 688-2951; Fax: (203) 737-4252; E-mail: Ravinder.Nath@yale.edu

Supported in part by DOD grant DAMD 17-00-1-0052.

Acknowledgment—The authors would like to thank Dr. Y. Son for many interesting and helpful discussions on the clinical head-and-neck implant used as an example in this article.

Received Mar 26, 2002, and in revised form Sep 17, 2002. Accepted for publication Oct 14, 2002.

repair model (13), takes into account both the cell proliferation and sublethal damage repair during the dose delivery characterized by a simple exponential function. Ling has used the model to study the relative radiobiologic effectiveness (RBE) of permanent implants using ^{198}Au, ^{125}I, or ^{103}Pd seeds (9) and to examine the biologic effects of dose heterogeneity inherent in interstitial implants (16). In this article, we generalize Dale's BED formula for implants containing a mixture of radionuclides with different half-lives. The potential of using the generalized BED formula as a tool for evaluating implants containing a mixture of radionuclides is examined. Its usage is demonstrated by examining the clinical implications of isodose prescription for a head-and-neck implant containing a mixture of ^{125}I and ^{103}Pd seeds.

METHODS AND MATERIALS

Implants containing a mixture of radionuclides

For simplicity, let us consider an implant containing two types of radionuclides (e.g., ^{125}I and ^{103}Pd). Assume that there are N_1 seeds of radionuclide type 1 and N_2 seeds of radionuclide type 2. In such an implant, the instantaneous dose rate to a point $\vec{r}$ at time t after implantation is given by

$$\dot{D}(\vec{r},t) = \sum_{i=1}^{2} \dot{D}_{0i}(\vec{r}) e^{-\lambda_i t} \tag{2a}$$

where $\dot{D}_{0i}(\vec{r})$ denotes the total initial dose rate produced by the seeds of radionuclide type i. It depends on the spatial locations of all type i seeds. It is clear from Eq. 2a that the overall temporal pattern in such an implant depends on the value of $\dot{D}_{0i}(\vec{r})$;, which can be variable throughout the implant volume. For point-like sources, $\dot{D}_{0i}(\vec{r})$ is approximately equal to (17)

$$\dot{D}_{0i}(\vec{r}) \approx \sum_{l=1}^{N_i} \frac{S_{il}\Lambda_i {r_0}^2}{|\vec{r}_{il} - \vec{r}|^2} g_i(|\vec{r}_{il} - \vec{r}|)(\bar{\phi}_{an})_i \tag{2b}$$

In the above equations, the index i labels the radionuclide type and l labels the individual seeds. S_{il} denotes the air-kerma strength for the seed l of radionuclide type i. Λ_i, λ_i, $(\bar{\phi}_{an})_i$, and $g_i(r)$ denote the dose rate constant, the radioactive decay constant, the anisotropy constant, and the radial dose function, respectively, for the seeds of radionuclide type i. r_0 denotes the reference distance (usually 1 cm) at which the dose rate constant was determined. In this work, the delivered dose, isodose distribution, and dose–volume histograms used in conventional implant dose evaluation were computed by using Eq. 2 with appropriate parameters for ^{125}I and ^{103}Pd seeds (17).

Linear-quadratic model for CLDRI

Dale's work on BED for implants containing a single type of radionuclide (11, 12) is generalized in this paper for implants containing a mixture of radionuclides of different half-lives. To model the kinetics of sublethal damage repair, Dale has invoked the assumption that radiation-induced cell inactivation is caused by the damage of two critical targets in a cell to model the kinetics of sublethal damage repair. Under this assumption, when a radiation event damages only one critical target, the cell is considered sublethally damaged, which is repairable. Cell kill occurs only when the other critical target is damaged before the existing damage is fully repaired. By assuming sublethal damage repairs exponentially with time, i.e., if a sublethal damage was inflicted at time t_0, then the probability for it persisting to time t is $e^{-\mu(t-t_0)}$, the rate of sublethal damage repair can be characterized by a single parameter, repair half-time $T_{1/2}^{(R)} = \dfrac{\text{Ln } 2}{\mu}$. Average repair half-times reported for mammalian normal and tumor tissues vary from 0.5 to 3 h with normal tissues usually possessing longer repair half-time (18). For "generic" tumors, a repair half-time of 1.5 h has often been used in model calculation (19). The rate of cell proliferation was also modeled by a single parameter, the tumor potential doubling time T_p. This model assumes that the cells in a target volume all proliferate at the same rate and cell loss from the tumor volume is negligible. The tumor potential doubling time is tumor-type dependent and may vary from patient to patient even among the same tumor type. For squamous cell head-and-neck cancer, a "typical" T_p of 5 days has been quoted in literature (19). For prostate carcinoma, T_p values ranging from 10 to 60 days have been reported in the literature (20). Using these simple models for sublethal damage repair and cell proliferation, Dale derived an analytic expression of BED for interstitial implants containing a single type of radionuclide as follows,

$$BED = D(T_{eff})\,RE - \frac{0.693 T_{eff}}{\alpha T_p} \tag{3}$$

where RE is given by

$$RE = 1 + 2\left(\frac{\beta}{\alpha}\right)\frac{\gamma}{D(T_{eff})} \tag{4a}$$

with

$$\gamma = \frac{\dot{D}_0^2}{\mu - \lambda}\left\{\frac{1}{2\lambda}(1 - e^{-2\lambda T_{eff}}) - \frac{1}{\lambda + \mu}(1 - e^{-(\mu+\lambda)T_{eff}})\right\} \tag{4b}$$

In the above equations, $\dot{D}_0$ denotes the initial dose rate, $\dot{D}(T_{eff}) = \dfrac{\dot{D}_0}{\lambda}(1 - e^{-\lambda T_{eff}})$ is the dose delivered up to T_{eff}, and α and β are coefficients of the LQ model. The effect of sublethal damage repair is captured by the factor RE, and the effect of cell proliferation is characterized by the second term on the right-hand side of Eq. 3. This analytic form of

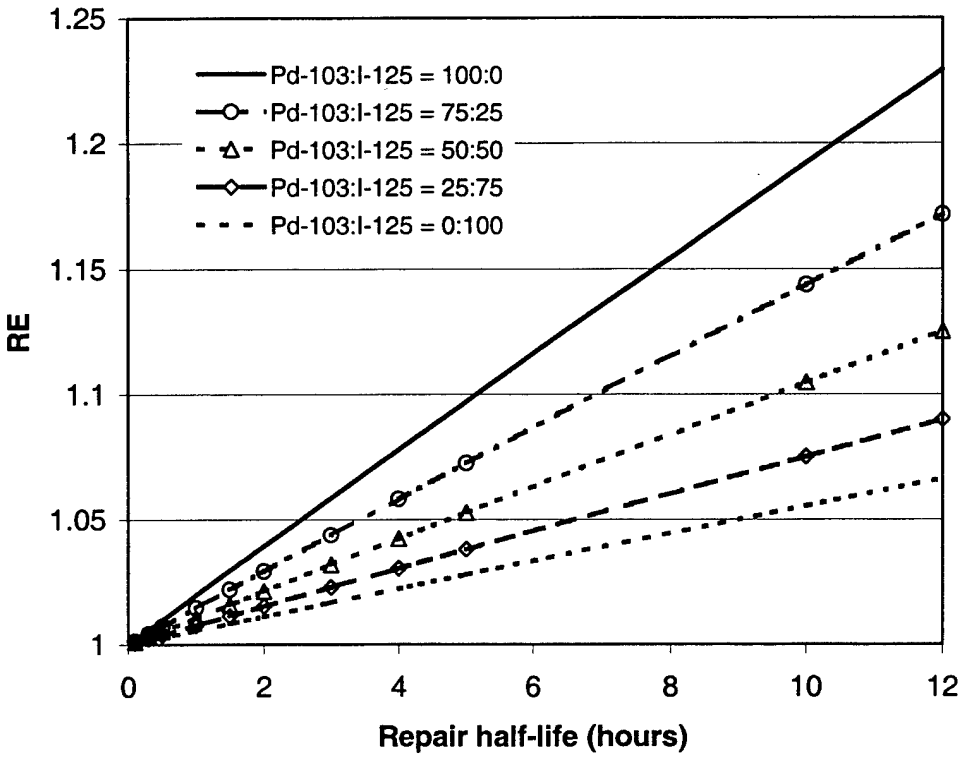

Fig. 2. Relative effectiveness, RE, calculated as a function of repair half-time for implants using a mixture of ^{125}I and ^{103}Pd seeds. The BED is the product of RE and the total delivered dose.

Total delivered dose is 80 Gy. When the relative dose contribution by ^{125}I and ^{103}Pd seeds is fixed, the BED is shown to increase with T_p. For a given T_p, BED is always larger when the same dose is delivered by the radionuclide with shorter half-life (^{103}Pd in this case). The difference in BED between dose delivered by ^{103}Pd and ^{125}I alone is most significant for fast growing tumors and becomes less significant for slower growing tumors.

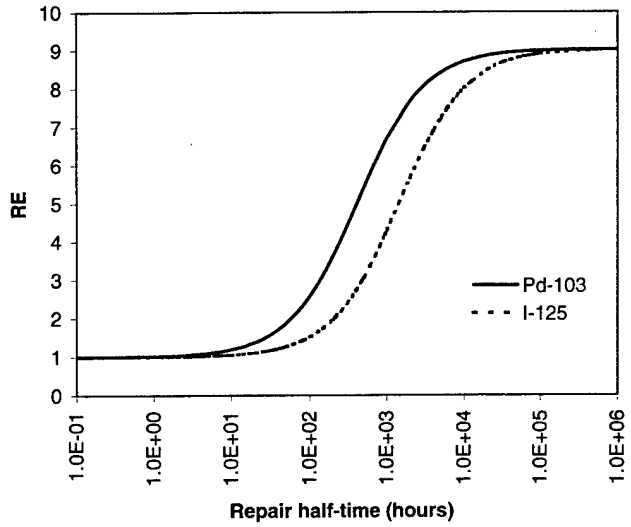

Fig. 3. Relative effectiveness (RE) over the entire range of possible repair half-time for implants using ^{125}I or ^{103}Pd alone.

An application of the generalized BED: Inadequacy of isodose prescription in mixed seed implant

The basic issue regarding the isodose prescription for an implant containing seeds of different half-lives is as follows. For a permanent implant using only a single type of radionuclide, the total dose, TD, at any given point is related to the initial dose rate, $\dot{D}_0$,

$$TD = 1.44 T_{1/2} \dot{D}_0 \tag{7}$$

For this type of implant, a prescription to an isodose surface is equivalent to a prescription to an isodose rate surface. In other word, the initial dose rate is fixed once a prescription of total dose is established. The temporal dose delivery pattern in such an implant follows a simple exponential function and is the same throughout the implant volume. For an implant containing a mixture of two radionuclides, however, Eq. 7 becomes

$$TD = 1.44 T_{1/2}^{(1)} \dot{D}_0^{(1)} + 1.44 T_{1/2}^{(2)} \dot{D}_0^{(2)} \tag{8}$$

The total dose is now dependent on the initial dose rates, $\dot{D}_0^{(1)}$ and $\dot{D}_0^{(2)}$, produced by the two types of radionuclide, respectively. According to Eq. 8, a prescription to an isodose surface can now be fulfilled by many different combinations of $\dot{D}_0^{(1)}$ and $\dot{D}_0^{(2)}$. Therefore the prescription to an isodose surface is not unique with respect to the initial dose rates produced by the two types of radionuclides. Further-

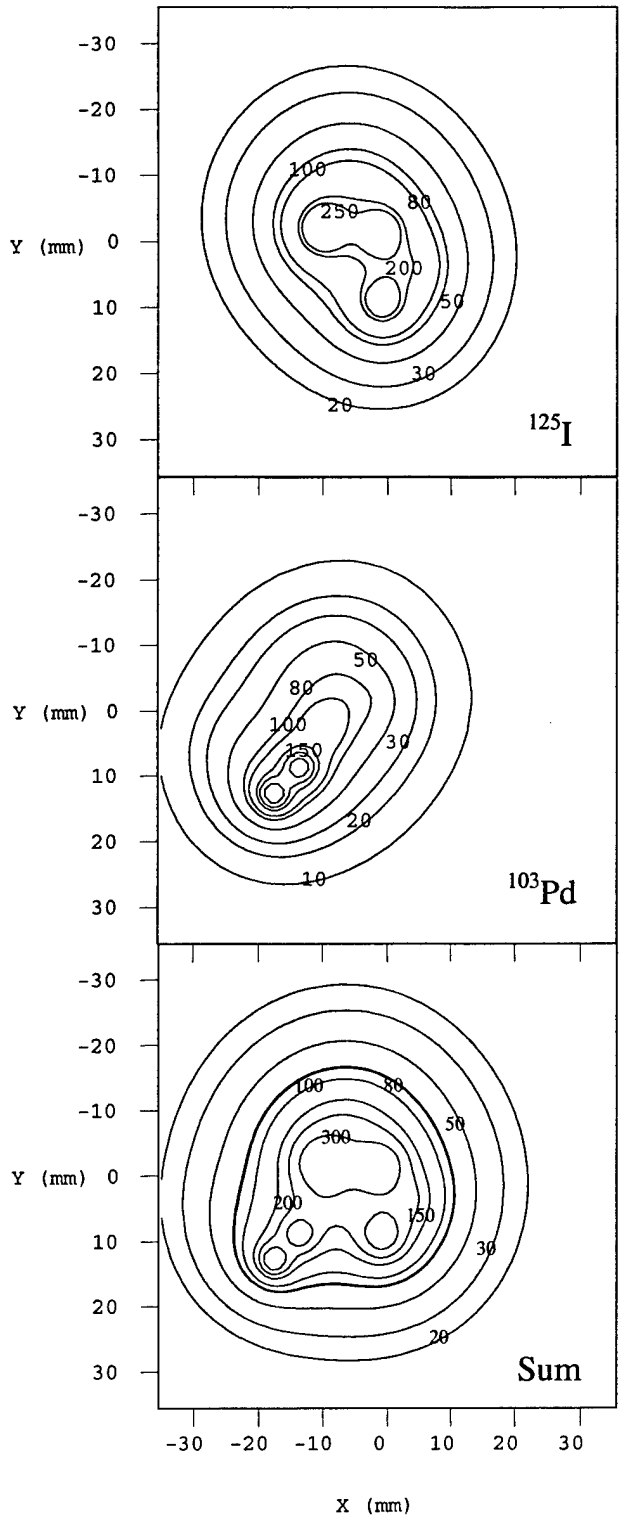

Fig. 5. Dose distribution on the *x-y* plane for a head-and-neck implant using ^{125}I and ^{103}Pd seeds: ^{125}I seeds alone (top), ^{103}Pd seeds alone (middle), and from the actual implant with mixed seeds (bottom). The 80 Gy isodose line on the bottom panel was chosen as the clinical prescription isodose.

time-dependent in the permanent implants. Parenthetically, *in vitro* measurements have shown that the RBE for ^{103}Pd is greater than that for ^{125}I (22). If the RBE of ^{103}Pd and ^{125}I were taken into account in the model calculation, the observations made in this article would have been further reinforced.

Although the general conclusions drawn from the model calculation conform to common intuition, it should be emphasized that the quantitative numbers of BED should always be viewed in the context of the limitations inherent in the models. Many other factors that affect the radiobiologic responses of human tissues, such as the cell cycle effects (24), radiation-induced apoptosis (25, 26), and tissue architecture, were not considered in the current model. Even then, for the calculated BED to be clinically meaningful, one would have to know the patient-specific tumor potential doubling time, sublethal damage repair half-time, and other required model parameters. Given the simplistic nature of the biologic model and the lack of reliable means of determining the patient-specific model parameters at present, it would be inappropriate to treat the calculated BED as a quantitative predictor of the clinical outcome for a patient implant. Taking the current model as an example, the relative uncertainty in the calculated BED is determined by the relative uncertainty of each model parameter:

$$\frac{\Delta BED}{BED} = A\frac{\Delta\alpha}{\alpha} + B\frac{\Delta(\alpha/\beta)}{(\alpha/\beta)} + A\frac{\Delta T_p}{T_p} + C\frac{\Delta\mu}{\mu} \qquad (9)$$

where the coefficients A, B, and C are given by

$$A \equiv \frac{0.693T_{eff}/T_p}{D(T_{eff})\,RE - 0.693T_{eff}/T_p}, \qquad (10a)$$

$$B \equiv \frac{D(T_{eff})(1-RE)}{D(T_{eff})\,RE - 0.693T_{eff}/T_p}, \qquad (10b)$$

$$C \equiv \frac{D(T_{eff})\,\mu\dfrac{\partial RE}{\partial\mu}}{D(T_{eff})\,RE - 0.693T_{eff}/T_p}. \qquad (10c)$$

These coefficients determine the sensitivity of the calculated BED to the relative uncertainties that may incur in determining each model parameter. Because A, B, and C are functions of the model parameters $\{\alpha, \alpha/\beta, T_p, \mu\}$, the influence of the relative uncertainty of a given model parameter on the calculated BED, in fact, depends on the characteristics of the tumor being studied. For example, the relative uncertainty associated with the potential tumor doubling time has a negligible effect on slowly growing tumors (i.e., A $\rightarrow$ 0, for $T_p \rightarrow \infty$) but can be appreciable on fast growing tumors. Similarly, relative uncertainty incurred in determining α/β would have less effect on tumors with larger α/β than on tumors with small α/β. For the repair time constant, however, BED is insensitive to $\Delta\mu/\mu$ when repair is extremely slow or fast and is most sensitive at intermediate repair kinetics (see coefficient C and Fig. 3). Therefore, the numerical values of the calculated BED can not and should not be taken as a quantitative indicator of the

with different half-lives. The generalized BED provides a tool for evaluating the radiobiologic effects of mixing different types of radionuclides in the same implant. Model calculation performed in this paper suggests that adding the ^{103}Pd to the ^{125}I implant would increase the effectiveness of cell kill, whereas the opposite is not true if the dose prescription was based on the clinical experience established with the ^{125}I implants. It is hoped that this work will stimulate further research interest in improving the radiobiologic modeling.

REFERENCES

1. Blasko JC, Grimm PD, Ragde H, Schumacher D. Implant therapy for localized prostate cancer. In: Ernstoff MS, Heaney JA, Peschel RE, editors. Prostate cancer. Cambridge, Massachusetts and Oxford, England: Blackwell Science; 1998. p. 137–155.
2. Lefebvre JL, Coche-Dequeant B, Castelain B, Prevost B, Buisset E, Ton Van J. Interstitial brachytherapy and early tongue squamous cell carcinoma management. *Head Neck* 1990;12:232–236.
3. Son YH, Sasaki CT. Nonsurgical alternative therapy for bulky advanced head and neck tumors. *Arch Otolaryngol Head Neck Surg* 1995;121:991–993.
4. Vikram B, Mishra S. Permanent iodine-125 implants in postoperative radiotherapy for head and neck cancer with positive surgical margins. *Head Neck* 1994;16:155–157.
5. Wilson LD, Chung JY, Haffty BG, Cahow EC, Sasaki CT, Son YH. Intraoperative brachytherapy, laryngopharyngoesophagectomy, and gastric transposition for patients with recurrent hypopharyngeal and cervical esophageal carcinoma. *Laryngoscope* 1998;108:1504–1508.
6. Nath R. New directions in radionuclide sources for brachytherapy. *Semin Radiat Oncol* 1993;3:278–289.
7. Kinsey RR. The NuDat Program for Nuclear Data on the Web. National Nuclear Data Center, Brookhaven National Laboratory. (http://www nndc bnl gov/nndc/nudat/). Database last updated August 12, 1999.
8. Hilaris BS, ed. Handbook of interstitial brachytherapy. Acton, MA: Publishing Science Group; 1975.
9. Ling CC. Permanent implants using Au-198, Pd-103, and I-125: Radiobiological considerations based on the linear quadratic model. *Int J Radiat Oncol Biol Phys* 1992;23:81–87.
10. Hall EJ. Radiobiology for the radiologist. 4th ed. Philadelphia: Lippincott; 1994.
11. Dale RG. The application of the linear-quadratic dose-effect equation to fractionated and protracted radiotherapy. *Br J Radiol* 1985;58:515–528.
12. Dale RG. Radiobiological assessment of permanent implants using tumor repopulation factors in the linear-quadratic model. *Br J Radiol* 1989;62:241–244.
13. Thames HD. An. "incomplete-repair" model for survival after fractionated and continuous irradiation, *Int J Radiat Biol* 1985;47:319–339.
14. Fowler JF. The linear-quadratic formula and progress in fractionated radiotherapy. *Br J Radiol* 1989;62:679–694.
15. Barendsen GW. Dose fractionation, dose rate and iso-effect relationships for normal tissue response. *Int J Radiat Oncol Biol Phys* 1982;8:1981–1997.
16. Ling CC, Roy J, Sahoo N, Wallner K, Anderson L. Quantifying the effect of dose inhomogeneity in brachytherapy: Application to permanent prostatic implant with 125I seeds. *Int J Radiat Oncol Biol Phys* 1994;28:971–978.
17. Nath R, Anderson LL, Luxton G, Weaver KA, Williamson JF, Meigooni AS. Dosimetry of interstitial brachytherapy sources: Recommendations of the AAPM radiation therapy committee task group 43. *Med Phys* 1995;22:209–234.
18. Dale RG, Jones B. The clinical radiobiology of brachytherapy. *Br J Radiol* 1998;71:465–483.
19. Orton CG. Update on time-dose models. In: Purdy JA, editor. Advances in radiation oncology physics dosimetry, treatment planning, and brachytherapy. : American Institute of Physics; 1992. Woodbury, NY: p. 374–389.
20. Haustermans KMG, Hofland I, Van Poppel H, *et al.* Cell kinetic measurements in prostate cancer. *Int J Radiat Oncol Biol Phys* 1997;37:1067–1070.
21. Dale RG, Coles IP, Deehan C, O'Donoghue J. The calculation of integrated biological responses in brachytherapy. *Int J Radiat Oncol Biol Phys* 1997;38:633–642.
22. Ling CC, Li WX, Anderson LL. The relative biological effectiveness of I-125 and Pd-103. *Int J Radiat Oncol Biol Phys* 1995;32:373–378.
23. Hall EJ. Radiation dose rate: A factor of importance in radiobiology and radiotherapy. *Br J Radiol* 1972;45:81–97.
24. Knox SJ, Sutherland W, Goris MC. Correlation of tumour sensitivity to low dose rate irradiation G2/M phase block and other radiobiological parameters. *Radiat Res* 1993;135:24–31.
25. Ling CC, Chen CH, Fuks Z. An equation for the dose response of radiation-induced apoptosis: Possible incorporation with the LQ model. *Radiother Oncol* 1994;33:17–22.
26. Ling CC, Chen CH, Li WX. Apoptosis induced at different dose rates: Implication for the shoulder region of cell survival curves. *Radiother Oncol* 1994;32:129–136.
27. Martel MK, Narayana V. Brachytherapy for the next century: Use of image-based treatment planning. *Radiat Res* 1998;150: S178–188.
28. Lee SP, Len MY, Smathers JB, McBride WH, Parker RG, Withers HR. Biologically effective dose distribution based on the linear quadratic model and its clinical relevance. *Int J Radiat Oncol Biol Phys* 1995;33:375–389.

APPENDIX

Equation 5 can easily be derived following the work of Dale (11, 12) for implants containing a single type of radionuclide. The reader is referred to Dale's original articles (11, 12) for the detailed steps and the rationale underlying the derivation. The main derivation steps are outlined below.

Dale has invoked the assumption that a lethal radiation damage is caused by the damage of two critical targets in a cell. When the two critical targets are damaged simultaneously by a radiation event, the resulting lethal damage is termed type A damage. When a radiation event damages only one critical target, the cell is considered sublethally damaged, which is repairable. In the latter case, a lethal damage results when the second critical target is damaged before the existing sublethal damage is fully repaired. This type of lethal damage is termed type B damage. Type A damage is always proportional to the total delivered dose irrespective of dose rate, whereas the type B damage is dose

Dose rate dependence of the relative biological effectiveness of ^{103}Pd for continuous low dose rate irradiation of BA1112 rhabdomyosarcoma cells in vitro relative to acute exposures

Ravinder Nath, Paul Bongiorni, Zhe Chen, Jillian Gragnano, and Sara Rockwell

Department of Therapeutic Radiology, Yale University School of Medicine, 333 Cedar Street, New Haven, Connecticut 06510

Corresponding author:

Ravinder Nath, Ph.D.

203-785-2971 (tel)

203-688-8682 (fax)

ravinder.nath@yale.edu (email)

(Submitted to International Journal of Radiation Biology on March 1, 2004)

Supported in part by DOD grant no. DAMD 17-00-1-0052, awarded by the Department of Army

Abstract

The relative biological effectiveness (RBE) of continuous low dose rate irradiation (CLDRI) using ^{103}Pd sources was measured relative to acute exposures from a 250 kVp x-ray beam and a simulated x-ray beam with an equivalent mono-energetic photon energy equal to the average energy of the ^{103}Pd source. For acute irradiation, the RBE of the simulated ^{103}Pd beam was 1.24 relative to 250 kVp x-rays. A profound dose rate effect was observed at low dose rates in the range of 6.8 to 14.4 cGy/h that are typical of permanent interstitial brachytherapy. At cell-surviving fraction of 0.01, the RBE of CLDRI at 6.8 and 14.4 cGy/h using ^{103}Pd sources was reduced by a factor of 3 and 2, respectively, relative to the acute exposure. This observation is in good agreement with recent in vivo tumor cure studies performed on BA1112 tumor.

Key words: LET, RBE, palladium-103, ba1112, radiobiology, prostate implants.

Introduction

Radioactive seeds containing ^{125}I and, recently, ^{103}Pd have been used successfully in interstitial brachytherapy for prostate cancer [1-2] and head and neck cancers [3-5]. Permanent interstitial implantation of the ^{125}I or ^{103}Pd seeds provides a distinct irradiation environment to tumors as compared to conventional fractionated external beam radiotherapy (EBRT). In a permanent implant, the tumor cells are subjected to continuous low dose rate irradiation (CLDRI) over a period of several months by low-energy photons (20 - 35 keV) with initial dose rates of 7 – 22 cGy/h. In theory, the secondary electrons produced by the low-energy photons give rise to higher linear energy transfer (LET) than those from the high-energy photons used in external beam radiotherapy and therefore are biologically more effective [6]. However, the advantage of high LET in determining the relative biological effectiveness (RBE) can be quickly negated by the lower dose rate of irradiation utilized in the implants, as the repair of sublethally damaged cells and continued cell repopulation during the protracted irradiation become important [7]. A proper characterization of the RBE of the brachytherapy implants using ^{125}I or ^{103}Pd sources requires the consideration of both the effect of LET as well as the dose rate of irradiation.

Many studies that focus on the LET-induced RBE (which will be labeled as RBE_{LET} for clarity) have been performed for ^{125}I irradiations using reference radiations of ^{137}Cs [8, 9], ^{192}Ir [10, 11], ^{226}Ra [12], and ^{60}Co [13, 14]. In these studies, the dose rate of the reference irradiation was matched to that of the ^{125}I irradiation. The reported values of RBE_{LET} varied from 1.0 to 1.5 over a range of dose rates from 3 cGy/h to 9 Gy/h. The RBE_{LET} of 1.0 reported by De Silva et al [11] for ^{125}I relative ^{192}Ir for an *in vivo* mouse brachytherapy tumor model should have been 1.2 according to a re-analysis by Ling et al [14] of the ^{125}I dosimetry. Relative to ^{60}Co, a recent measurement by Ling et al [14] gave a RBE_{LET} of 1.4 for ^{125}I for REC:ras cells in cell culture, in both exponential and plateau phase at a dose rate of approximately 7 cGy/h. Despite of the diverse biological test systems and reference irradiations used in these studies, the reported RBE_{LET} values for ^{125}I fall within a fairly narrow range of 1.2 to 1.5, confirming a definite biological advantage of the higher LET associated with the low-energy photons.

For ^{103}Pd sources, there was only one reported measurement of RBE_{LET} by Ling et al [14]. The measured RBE_{LET} was 1.9 relative to ^{60}Co for REC:ras cells in the dose rate range of 7

to 14 cGy/h [14]. The RBE_{LET} is higher than that of ^{125}I for the same reference radiation and cell line. A higher RBE_{LET} from ^{103}Pd is expected as the photon energies emitted by ^{103}Pd (average energy of 20.8 keV) are lower than those emitted by the ^{125}I (average energy of 29 keV). A theoretical calculation by Wuu et al [15,16] based on microdosimetric analysis placed a value of 1.6 on the RBE_{LET} of ^{103}Pd relative to ^{60}Co in the low dose and/or low dose rate limit.

The reported RBE_{LET} clearly demonstrated a LET-induced RBE advantage of using ^{125}I or ^{103}Pd. However, it does not include the influence of dose rate on RBE and it is therefore insufficient for comparing, for example, the RBE of permanent implants to that of external beam radiotherapy. Quantitative knowledge about the influence of dose rate on RBE is required if the observed clinical efficacies of the two modalities are to be exploited to provide radiobiological insights into the disease, for example, the α/β ratio of prostate cancer [17, 18]. The aim of this work is to measure the RBE as a function of LET and dose rate for CLDRI using ^{103}Pd sources with reference to the standard 250-kVp acute x-ray irradiation [6]. A customized ^{103}Pd irradiator was built to provide CLDRI using ^{103}Pd at different dose rates to BA1112 rhabdomyosarcoma cells growing in exponential phase in culture. A special x-ray beam that simulates the photon energies emitted by the ^{103}Pd source was also developed to provide acute irradiation. The RBE with respect to acute irradiation with standard 250 kVp x-rays was then measured for dose rates relevant to interstitial brachytherapy.

Methods and Materials

Preparation of the BA1112 rhabdomyosarcomas cells

The BA1112 rhabdomyosarcomas cells used for the in vitro irradiation were obtained from the exponentially growing cell lines maintained in our laboratory [19]. For each experiment, BA1112 cells were harvested from a BA1112 tumor growing on a WAG/Rij rat. The tumor had been initiated by inoculation of approximately 7500 tumor cells, suspended in 0.05 ml of sterile cell culture medium, into a subcutaneous site on the head of a rat at the age of about 14 weeks. At approximately 3 weeks after inoculation, the tumor had grown to a volume of approximately 100-200 mm^3. The rat carrying the tumor was euthanized by anesthetic overdose and the tumor was removed using aseptic techniques. The tumor was chopped into a fine mash with a sterile blade, and the tumor pieces were added to a trypsin solution and stirred at 37° C for 15 minutes. The suspension was filtered to remove pieces of intact tissue and centrifuged at

400g for 10 minutes. The cells were re-suspended in 10 ml of DMEM. This single-cell suspension was counted and assayed for viability using the same colony formation assay used for cells in cultures. Flasks, containing 13 ml of medium, were prepared by seeding cells at concentrations of 2.5×10^6 - 5×10^6. These flask dishes were kept in a humidified 37° C incubator with 95% air and 5% CO_2 and subcultured every 3 or 4 days to keep them in exponential growth. These stock cultures were used to set up experimental dishes for CLDRI cell irradiations, as well as acute high dose rate irradiations. The BA1112 stock in vitro culture was maintained for no longer than 4 weeks before a new BA1112 tumor was harvested to prepare new stock in vitro cultures.

Irradiation techniques

A). ^{103}Pd irradiator for continuous low dose rate irradiation

A customized ^{103}Pd irradiator was built for in vitro continuous low dose rate irradiation using ^{103}Pd source (Fig.1). The irradiator consists of a 20.3 x 20.3 x 10.2 cm polystyrene phantom with a centered 10.2 cm diameter hole, a polystyrene disk loaded with ^{103}Pd sources, and polystyrene spacers for dose rate control. During an experiment, the tissue culture dish was placed on top of the source disk or on top of a polystyrene spacer, depending on the dose rate required for the experiment. The polystyrene source disk has a diameter of 10 cm and a thickness of 1.25 cm. This disk was loaded with 80 ^{103}Pd sources (model 200; Theragenics Corp., Norcross, Atlanta) with an initial activity of 1.9 mCi per source. The sources were arranged in three concentric circles with diameters of 6, 3.5, and 1.3 cm. Different dose rates spanning the range from 6 to 14 cGy/h were obtained by varying the thickness of the polystyrene spacers placed between the sources and the tissue culture dish. During the CLDRI experiment, the ^{103}Pd irradiator was placed in a 37°C water-jacketed incubator and surrounded in lead foil of 1 mm thickness to shield the photons emitted by ^{103}Pd.

The dose to the cells in the dish was determined from the measured average dose to tissue culture medium in the dish using Fricke dosimetry [20], with a calculated correction for interface effects due to photoelectric effect in the tissue culture dish [20]. The uniformity of dose rate across the dish was verified by three independent means: LiF thermoluminescent dosimetry, film dosimetry and dose calculations by a computerized treatment planning package (Theraplan). In all cases, the dose uniformity across the dish was better than $\pm$5%.

B). Simulated ^{103}Pd x-ray beam for acute high dose rate irradiation

A heavily filtered x-ray beam was established on an orthovoltage x-ray unit (Pantek DXT 300, CT) that simulates the x-rays emitted by ^{103}Pd for acute high dose rate irradiation (AHDRI). The Pantek DXT 300 unit provides stable digital tube voltage control to as low as 20 kV. By optimizing the tube voltage (which determines the upper limit of the photon energy spectrum) and the amount of added filtration (which preferentially removes the low-energy bremsstrahlung photons), an x-ray beam with very narrow spectrum was obtained. The equivalent mono-energetic energy of the simulated beam was determined from the measured half-value-layer (HVL) of the beam according to Johns and Cunningham [21]. The HVL was measured under narrow beam condition for each combination of tube voltage and added filtration using an air-equivalent Spokas chamber (Exradin, Model No: A1 [0.5 ml, AE plastic]) and a set of calibrated aluminum sheets (Nuclear Associates). It should be noted that as more aluminum sheets were added into the beam during the HVL measurement, the effective energy of the resulting beam increased. To account for the non-uniform energy response of the Spokas chamber during the HVL measurement, the effective energy of the resulting beam at each aluminum thickness was determined and the energy response for the chamber was then obtained from an energy calibration curve for the Spokas chamber traceable to National Standard of Science and Technology. Figure 2 plots the relative exposure as a function of the thickness of the aluminum absorber for the simulated ^{103}Pd beam. The beam was found to have a HVL of 0.84 mm aluminum and an equivalent mono-energetic energy of 20.5 keV, which is approximately the same as the average energy of the photons emitted by ^{103}Pd source, 20.9 keV. The energy-homogeneity of the beam, as measured by the ratio of the 2nd HVL to the 1st HVL, was 89% indicating a narrow energy spread in the beam's photon energy spectrum. The basic parameters of the simulated ^{103}Pd beam are given in Table I.

Acute irradiations were performed using the simulated ^{103}Pd x-ray beam as well as a standard 250-kVp x-ray beam used in clinical treatment. The 250-kVp beam had a HVL of 1.85 mm Cu. Radiation output for the 250 kVp and the simulated ^{103}Pd beam were determined for the average dose to tissue culture medium in the culture dish, as measured by Fricke dosimetry [20]. Fricke dosimetry was used since it measures dose in the same type of culture dish with approximately the same amount of liquid as was used during cell irradiation. The interface

correction due to photoelectric effect in the polystyrene culture dish was taken as approximately 1.0, in this case, since the cells are located upstream in the irradiation beam, as opposed to the irradiation geometry of the ^{103}Pd irradiator. The radiation output of the two beams for acute irradiation was also checked against measurements using the air-equivalent Spokas chamber and a calibrated parallel-plate soft-energy chamber following the AAPM TG-61 calibration protocol [22]. The dose rate to the dish was determined to be 33.3 Gy/hr for the simulated ^{103}Pd beam and 38.9 Gy/hr for the 250-kVp beam.

Measurement of cell survival curves

All experiments were performed using the cell monolayers that were prepared by plating cells, suspended from exponentially growing stock cultures in flasks. These cells were harvested from the flasks and seeded into 60-mm diameter Falcon tissue culture dishes at cell concentration of $5\times10^5 - 1.5\times10^6$ cells per dish. The cells were seeded 18 hours prior to irradiation, to allow them to attach and to progress into exponential growth. The growth medium was removed and replaced by fresh growth medium just before the beginning of the irradiations, which lasted 1 to 60 hr in CLDRI, and from several minutes to about half of a hour in AHDRI.

For CLDRI, cells were maintained in a humidified 95% air-5% CO_2 environment at 37°C during irradiations. Controls were treated similarly. After irradiation, the cells were washed with Hanks' balanced salt solution, trypsinized, and counted using a Coulter counter, equipped with a Channelizer to allow assessment of and correction for any changes in cell size. Cells were plated for colony formation in at least four dishes per data point and were allowed to grow in a humidified 95% air-5% CO_2 environment at 37°C for 14 days. The colonies were then fixed, stained, and counted. To facilitate accurate counting, the experiments were planned such that approximately 120 colonies were formed in each dish, by adjusting the number of cells plated per dish appropriately. The cell surviving fraction was calculated as the ratio of the plating efficiencies of the irradiated cells relative to those of unirradiated control cells plated at the same time as the irradiated cells. In these experiments, however, the numbers of cells in cultures irradiated with CLDRI were significantly lower than the numbers of cells in control cultures, even though the same numbers of cells were used to initiate the cultures, because of reduced rates of cell division in the irradiated cultures and because some cells died during the prolonged

irradiations. The surviving fractions were therefore corrected to account for the deficit in cell number in the irradiated cultures, using the formula:

$$S = \frac{P_{exptl}}{P_{control}} \times \frac{C_{exptl}}{C_{control}} \qquad (1)$$

where P_{exptl} = plating efficiency of the experimental sample;

$P_{control}$ = plating efficiency of the control sample;

C_{exptl} = number of cells harvested from the experimental sample at the end of irradiation time;

$C_{control}$ = number of cells harvested from the unirradiated control sample assayed at the end of irradiation time.

Plating efficiencies (colonies formed/cells plated) for unirradiated cells were approximately 90% in the experiments reported here.

Determination of RBE

In this work, a surviving fraction of 0.01 (1% of survival) was chosen as the biological endpoint for comparing the relative biological effectiveness of a given irradiation condition on the BA1112 tumor cells. The RBE was defined with respect to a standard reference irradiation condition as follows [6],

$$RBE = \frac{D_{250kV}}{D_T} \qquad (1)$$

where D_{250kV} is the dose required to reduce the cell survival to 1% by using 250 kVp x-rays under acute irradiation condition and D_T is the dose required to produce the same cell survival using ^{103}Pd under a given irradiation condition. The RBE defined by Eq.(1) gives a direct relationship between the biological effectiveness of irradiations using the ^{103}Pd source and of the conventional 250-kVp AHDRI used in the clinic. As pointed out in the Introduction, most of the reported measurements of RBE for ^{125}I and ^{103}Pd captured only the effect of LET. The relationship between the standard RBE definition (Eq.1) and the RBE_{LET} will be discussed in detail in the Discussion section.

Results

The cell survival curves for the BA1112 cells irradiated using the simulated ^{103}Pd x-ray beam and using the 250-kVp x-ray beam under AHDRI condition are plotted in Fig. 3. The dashed lines represent the fit of the experimental data to the linear quadratic equation for cell survival. Note that the cell survival curves exhibit clear curvatures, indicating a significant contribution of cell killing from reparable damages. The doses required to produce a surviving fraction of 1% were 9.2 and 7.4 Gy for the 250 kVp beam and the simulated ^{103}Pd beam, respectively. According to Eq.1, the RBE for the simulated ^{103}Pd x-ray beam, using 1% cell survival as an endpoint, was 1.24 relative to the 250-kVp x-ray beam under AHDRI condition.

Figure 4 compares the survival curves at different dose rates for CLDRI using ^{103}Pd. Note that the survival curves in the semi-log plot were essentially linear at low dose rates, indicating the cell killing from reparable damage is negligible. The lines represent the fit of the measured survival data by the linear-quadratic (LQ) survival model. Figure 4 shows that the cytotoxicity of the irradiation was strongly dependent on the dose rate for CLDRI using ^{103}Pd sources. The dose required to produce a surviving fraction of 1% was 15.2 and 23. 6 Gy for CLDRI at dose rate of 14.4 cGy/h and of 6.8 cGy/h, respectively, as compared to 7.4 Gy for AHDRI by the simulated ^{103}Pd beam. At 1% surviving fraction, the RBE as defined by Eq.(1) decreased from 1.24 at AHDRI to 0.61 at the dose rate of 14.4 cGy/h and to 0.39 at the dose rate of 6.8 cGy/h (Table 2). Compared to AHDRI, the relative biological effectiveness of ^{103}Pd was reduced by a factor of 2 and 3 for the CLDRI using dose rates of 14.4 cGy/h and 6.8 cGy/h, respectively.

Discussions

The results presented in the above shown that the relative biological effectiveness of the photons emitted by ^{103}Pd depends on both the LET of the low energy photons and the dose rate of irradiation. When acute irradiation of 250 kVp x-rays is chosen as the reference, the photons similar to those emitted by ^{103}Pd (using the simulated ^{103}Pd x-ray beam) is biologically more effective in killing BA1112 tumor cells if it is delivered at the same dose rate as the 250 kVp x-rays (a RBE of 1.24). This result confirms the general expectation that irradiation by ^{103}Pd would result in a higher RBE due to the higher LET of its low energy photons as compared to the high-

energy photons used in conventional external beam radiotherapy. As the dose rate of the ^{103}Pd irradiation decreases, however, the relative biological effectiveness decreases rapidly compared to the acute reference 250-kVp x-ray irradiation. In fact, the gain in RBE that results from the higher LET can be quickly negated by the reduced dose rate of the irradiation, resulting in a reduction of the overall RBE by a factor of 2 and 3 at dose rates of 14.4 and 6.8 cGy/h, respectively.

It should be emphasized that the standard definition of RBE (Eq.1), while providing the most direct comparison of the relative biological effectiveness between two different radiation techniques, does consider the influences of both the LET and the dose rate on RBE when different dose rates of irradiation are compared (e.g. between the permanent prostate seed implant using ^{103}Pd and fractionated external beam radiotherapy). Alternative definitions of RBE, which emphasize primarily the effect of LET by matching the dose rate of the reference irradiation to that of the low dose rate irradiation, have been used in literature [8-14]. For example, the relative biological effectiveness defined with a matched dose rate (as denoted by RBE_{LET} in the Introduction) is given by

$$RBE_{LET} = \frac{D_{250kV}(\dot{d})}{D_T(\dot{d})} \qquad (2)$$

where $\dot{d}$ denotes the dose rate of the test irradiation. RBE_{LET} is related to RBE of Eq.1 by a dose rate factor for the reference irradiation, DRF_{250kV}, as follows

$$RBE = \frac{D_{250kV}(\dot{d}_R)}{D_T(\dot{d})} \equiv RBE_{LET} \times DRF_{250kV} \qquad (3)$$

where $DRF_{250kV} = D_{250kV}(\dot{d}_R)/D_{250kV}(\dot{d})$ and $\dot{d}_R$ is the dose rate of the standard reference irradiation. The use of RBE_{LET} is theoretically appealing as it allows one to focus on the effect of LET on RBE for a given dose rate. Previously reported measurements on the relative biological effectiveness of ^{125}I [8-14] and ^{103}Pd [14] sources are, in fact, RBE_{LET}. Nonetheless RBE_{LET} alone does not provide sufficient information to predict the clinical effectiveness of ^{103}Pd or ^{125}I implant from the existing experience of standard EBRT, because the standard EBRT are not delivered at the low dose rates of the implant. As shown in Eq.(3), DRF_{250kV} needs to be determined separately in order to obtain the overall RBE. Furthermore, RBE_{LET} itself can also be dose rate dependent because the sublethal damage repair for high- and low-LET radiations can

be different [6]. From a theoretical point of view, if an RBE_{LET} must be defined for studying primarily the effect of LET on relative biological effectiveness, we propose to define RBE_{LET} at the AHDRI condition, i.e. replace $\dot{d}$ by $\dot{d}_R$ in Eq.(2). Following this definition, equation (3) becomes

$$RBE = \frac{D_{250kV}(\dot{d}_R)}{D_T(\dot{d})} \equiv RBE_{LET}^{Ref} \times DRF_T \qquad (4)$$

where the dose rate factor, $DRF_T = D_T(\dot{d}_R)/D_T(\dot{d})$, is now defined for the test irradiation and contains all the effects caused by the dose rate of the irradiation. In Eq.(4), we have added a superscript *Ref* to RBE_{LET}^{Ref} to emphasize that this LET-induced RBE is defined at the high dose rate of the reference irradiation. The advantage of using Eq.(4) is that the effects of LET and dose rate on RBE can be characterized independently. When comparing AHDRIs, the $DRF_T = 1$. When comparing irradiations of different dose rates, for example, the results obtained for the BA1112 tumor cells in this work, Eq. 4 gives a RBE_{LET}^{Ref} (AHDRI) of 1.24 and DRF_T of 0.49 and 0.31 for CLDRI using ^{103}Pd at dose rates of 14.4 and 6.8 cGy/h, respectively, for achieving a 1% cell survival (Table 2).

To the best of our knowledge, there is only one reported measurement of RBE_{LET} by Ling et al for ^{103}Pd irradiation at low dose rates [14]. The RBE_{LET} was measured by in vitro irradiation of REC:ras cells derived from rat embryo cells with cells in exponential or plateau phase. ^{60}Co gamma rays with matched low dose rates were used as the reference irradiation. Because of the low irradiation dose rates, the measured survival curves were essentially straight lines and the RBE_{LET} was taken as the ratio of the slopes of the fitted survival curves. The reported RBE_{LET} was 1.8 ± 0.6 and 1.9 ± 0.3 at dose rates of about 7 and 14 cGy/h, respectively, with cells in plateau phase and was 2.0 ± 0.8 and 1.8 ± 0.7 at the two respective dose rates with cells in exponential phase. They concluded that the RBE_{LET} of ^{103}Pd relative to ^{60}Co was about 1.9 in the dose rate range of 7 to 14 cGy/h for REC:ras cells. Our measured value cannot be compared directly with Ling's result due to the differences in cell line, reference radiation, and the dose rate of irradiation. Our measured RBE_{LET}^{Ref} of 1.24 at AHDRI relative 250 kVp x-rays, however, is not contradictory to Ling's result because 1) The RBE_{LET} is expected to increase as the dose rate decreases from acute irradiation [6]; 2) the 250 kVp x-ray has a theoretically higher LET than the ^{60}Co gamma rays [6]; and 3) RBE_{LET} is expected to increase at lower doses. A

theoretical calculation by Wuu et al using microdosimetry analysis placed the RBE_{LET} of ^{103}Pd relative to ^{60}Co at about 1.6 in the limit of low dose and /or low dose rate [15,16]. However, as it was pointed out earlier, the clinically relevant value is given by RBE and this work indicates that the overall RBE is only 0.61 and 0.39 at dose rates of 14.4 and 6.8 cGy/h, respectively, for the BA1112 tumor cells.

Although the numerical value of RBE as given in Table 2 was obtained from in vitro irradiation of cell cultures and the endpoint of study was 1% surviving fraction, this RBE was surprisingly consistent with the RBE estimated for in vivo CLDRI using ^{103}Pd for BA1112 tumors grown on the head of WAG/Rij rats using tumor cure rate as the endpoint of study. Based on a recent work of Nath et al [23], the tumor cure rate of in vivo CLDRI using ^{103}Pd sources was approximately 62% with initial dose rate of 20 cGy/h. The duration of in vivo CLDRI for the tumor was 76 days and it corresponded to a total dose of 112 Gy delivered to the tumor. The tumor cure rate for the same in vivo BA1112 tumor model under acute high dose rate irradiation using 250 kVp x-rays had been measured previously by Fischer et al [24]. A total dose of 60 Gy was needed to achieve the same tumor cure rate seen for CLDRI. The RBE of in vivo CLDRI using ^{103}Pd, using 62% cure rate as the study endpoint, would, at a first glance, be 0.53 for BA1112 tumors given the initial dose rate of 20 cGy/h. It should be noted that there exists an inherent uncertainty in calculating the total dose for the CLDRI tumor cure study. The dose rate in CLDRI decreases continuously and there exists an effective treatment time beyond which the rate of cell kill will be insufficient to overcome the rate of repopulation [25]. Dose delivered beyond the effective treatment time would simply be wasted in terms of providing tumor cure. For the BA1112 tumor, the effective treatment time is approximately 46 days for ^{103}Pd with an initial dose rate of 20 cGy/h. The total dose delivered during the effective treatment time is approximately 100 Gy. An RBE calculated using the dose delivered during the effective treatment time would be 0.60. A fit of the in vitro RBE (Table 2) to a logistic function yielded a RBE of 0.71 at initial dose rate of 20 cGy/h, which is approximately 15% higher than the in vivo RBE using the tumor cure as endpoint. Due to the long irradiation time needed in the in vivo tumor cure study, the continued tumor cell proliferation and repair of sublethal damage, which was negligible in the in vitro cell survival study, is expected to reduce the effectiveness of CLDRI, resulting a smaller in vivo RBE, consistent with the above estimate. The presence of hypoxic cells in the tumor, if any, however, could counter the effect of cell proliferation and

sublethal damage repair. The quantitative effects of cell proliferation, sublethal damage repair, and presence of hypoxic tumor cells on the in vivo RBE warrant further study. Nonetheless, the numerical agreement in RBE (~ 15%) between the in vitro and in vivo CLDRI using ^{103}Pd is very good indeed considering the differences in the cell environments and study endpoints.

Still, it should be cautioned that, the numerical value of RBE is strongly dependent on the biological system and the endpoint used in the study in addition to LET and dose rate [6]. For example, the RBE values reported in this study cannot be used directly to evaluate the biological equivalency between clinical permanent implant using ^{103}Pd source and conventional external beam radiotherapy for prostate cancer. Several studies have indicated that the biochemical disease free survival between fractionated EBRT with a total dose of greater or equal to 72 Gy is equivalent to ^{103}Pd permanent implants with total dose of 125 Gy [26]. The initial dose rate for the permanent implants is approximately 21 cGy/h. If the in vivo RBE value (0.60 at 20 cGy/h) were applied to the ^{103}Pd prostate implant, it would have indicated that the 125 Gy implant dose would be equivalent to a 75 Gy single exposure at high dose rate, which should be far more effective than the 72 Gy fractionated radiotherapy. According to the linear quadratic model, the 72 Gy fractionated radiotherapy at 2 Gy per fraction is equivalent to about 18 Gy single exposure for prostate cancer with a α/β of 3 Gy. This large difference cannot be explained by the shorter effective treatment time as discussed earlier. For prostate cancer, the effective treatment time is approximately 60 and 85 days for tumors with potential doubling time of 10 and 30 days, respectively. The doses delivered during the respective effective treatment times are 114 and 121 Gy, neither are consistent with the in vivo BA1112 RBE value. The large difference is presumably due to differences in radiobiological characteristics of two tumor systems such as the much shorter cell cycle time for the BA1112 tumor compared to the human prostate cancer. Further studies are needed to obtain a clinically meaningful RBE for permanent prostate implant using ^{103}Pd for prostate cancer.

The reduction of RBE from 0.61 at the dose rate of 14.4 cGy/h to 0.39 at dose rate of 6.8 cGy/h (by more than 35%) as shown in Table 2 carries some interesting clinical implications for permanent implants. On the one hand, the dose rate of irradiation to organs at risk and normal tissues outside the target volume is always lower than that inside the target volume due to the rapid dose-fall-off around the low-energy photon sources. Therefore permanent implants would provide additional sparing, beyond that indicated by the planned physical dose, to the organs at

risk and the surrounding normal tissues. By the same token, any "cold" spots of dose rate occurring inside the target volume would be worse biologically than what is indicated by physical dose alone. Therefore, both the dose and dose rate should be considered in the planning and evaluation of permanent implants. Ideally, the RBE_{LET}^{Ref} and the DRF_T should be build into the planning and evaluation software for brachytherapy.

Conclusion

The relative biological effectiveness of continuous low dose rate irradiation using ^{103}Pd sources has been measured relative to acute high dose rate irradiation using 250 kVp x-rays and the BA1112 tumor cells. When delivered at AHDRI, the ^{103}Pd photons are biologically more effective due to their higher LET, resulting in a RBE of 1.24. However, this higher RBE can be quickly negated by the low dose rates of irradiation that are used in typical permanent interstitial brachytherapy. At 1% survival level, the RBE of CLDRI at 6.8 and 14.4 cGy/hr using ^{103}Pd sources was reduced by a factor of 3 and 2, respectively, from the RBE of acute irradiations. This observation is in good agreement with recent in vivo tumor cure studies performed on BA1112 tumor.

References

1. Blasko JC, Grimm PD, Ragde H, Schumacher D. Implant therapy for localized prostate cancer. In Ernstoff MS, Heaney JA, Peschel RE, editors. Prostate Cancer. Cambridge, Massachusetts and Oxford, England: Blackwell Science; 1998. p. 137-155.
2. King CR, Sanzone J, Anderson KR, and Peschel RE: Definitive therapy for stage T1/T2 prostate carcinoma: A PSA based comparison between surgery, external beam and implant radiotherapy. *J Brachytherapy Int* **14**, 169-177, 1998.
3. Lefebvre JL, Coche-Dequeant B, Castelain B, Prevost B, Buisset E, Ton Van J. Interstitial brachytherapy and early tongue squamous cell carcinoma management. *Head Neck.* 1990;12:232-6.
4. Son YH, Sasaki CT. Nonsurgical alternative therapy for bulky advanced head and neck tumors. *Arch Otolaryngol Head Neck Surg.* 1995;121:991-3.
5. Vikram B, Mishra S. Permanent iodine-125 implants in postoperative radiotherapy for head and neck cancer with positive surgical margins. *Head Neck.* 1994;16:155-157.
6. Hall EJ. Radiobiology for the radiologist. 4th ed. Philadelphia: Lippincott, 1994
7. Hall, EJ, Radiation dose rate: a factor of importance in radiobiology and radiotherapy. Br. J. Radiol. 45:81-97, 1972.
8. Marchese, MJ, Hall, ER, Hillaris, BS, Encapsulated ^{125}I in radiation oncology. I. Study of the relative biological effectiveness (RBE) using low dose rate irradiation of mammalian cell cultures. Am. J. Clini. Oncol. 7:607-611, 1984.
9. Freeman, ML, Goldhagen, PE, Sierra, E, Hall, ER, Studies with encapsulated I-125 sources. II. Determination of relative biological effectiveness using cultured mammalian cells. Int. J. Radiat. Oncol. Biol. Phys. 8:1355-1361, 1982.
10. Hering, ER, A comparison of the biological effect of I-125 and Ir-192 gamma rays on the roots of Vicia faba using a specifically designed applicator. Br. J. Radiol. 53:255-258, 1980.
11. De Silva, VF; Gutin, PH, Deen, DF, Weaver, KA, Relative biological effectiveness of ^{125}I sources in a murine brachytherapy model. Int. J. Radiat. Oncol. Biol. Phys. 10:2109-2111, 1984.
12. Nath, R, Bongiorni, P, Rockwell, S. The relative biological effectiveness of Iodine-125 and Americium-241 photons relative to Radium-226 photons for continuous low dose rate

irradiation at dose rate of 0.17 and 0.73 Gy/h. Endocuriether./Hyperthermia Oncol. 6:81-90,1990.

13. Zeitz, L, Kim, SH, Kim, JH, Detko, JF, Determination of relative biological effectiveness (RBE) of soft x-rays. Radiat. Res. 70:552-563, 1977.
14. Ling, CC, Li, WX, Anderson, L, The relative biological effectiveness of I-125 and Pd-103. Int. J. Radiat. Oncol. Biol. Phys. 32:373-378, 1995.
15. Wuu, CS, and Zaider, M, A calculation of the relative biological effectiveness of 125I and 103d brachytherapy sources using the concept of proximity function. Med. Phys. 25:2186-2189, 1998.
16. Wuu, CS, Kliauga, P, Zaider, M, Amols, HI, Microdosimetric evaluation of relative biological effectiveness for 103Pd, 125I, 241AM, and 192Ir brachytherapy sources. Int. J. Radiat. Oncol. Biol. Phys. 36:689-697, 1996.
17. Brenner DJ. Hypofractionation for prostate cancer radiotherapy--what are the issues? Int J Radiat Oncol Biol Phys. 57:912-4 2003.
18. Fowler J, Chappell R, Ritter M Is alpha/beta for prostate tumors really low? Int J Radiat Oncol Biol Phys. 50:1021-31 2001.
19. Fischer JJ, Reinhold HS, The cure of rhabdomyosarcoma BA1112 with fractionated radiotherapy. Radiology 105: 429-433, 1972.
20. Nath R, Bongiorni P, Rockwell S. Iododeoxyuridine radiosensitization by low- and high-energy photons for brachytherapy dose rates. Radiat Res. 24:249-58 1990.
21. Johns H and Cunningham J, The Physics of Radiology, 4th ed., Springfield: Thomas 1983.
22. Ma CM, Coffey CW, DeWerd LA, Liu C, Nath R, Seltzer SM, Seuntjens JP; AAPM protocol for 40-300 kV x-ray beam dosimetry in radiotherapy and radiobiology. Med Phys. 28:868-93 2001.
23. Nath R, Bongiorni P, Chen Z, Gragnano J, and Rockwell R, Development of a Rat Solid Tumor Model for Continuous Low Dose Rate Irradiation Studies using ^{125}I and ^{103}Pd Sources, manuscript in preparation for submission to Radiat Res. 2004.
24. Fischer JJ and Moulder JE, "The steepness of the dose-response curve in radiation therapy", Radiology, 117:179-184 1075.
25. Dale RG. The application of the linear-quadratic dose-effect equation to fractionated and protracted radiotherapy. *Brit J Radiol, 1985;* **58**:515-528

26. Kupelian, PA, Potters L, Khuntia, D, Ciezki, JP, Reddy, VA, Reuther, AM, Carlson, TP, and Klein, EA, Radical prostatectomy, external beam radiotherapy < 72 Gy, external beam radiotherapy ≥ 72 Gy, permanent seed implantation, or combined seeds/external beam radiotherapy for stage T1-T2 prostate cancer. Int. J. Radiat. Oncol. Biol. Phys. 58:25-33, 2004.

Figure Captions

Figure 1 A picture and a schematic cross-sectional view of the ^{103}Pd irradiator used for continuous low dose rate irradiation (CLDRI) of the BA1112 cells in culture dishes. The polystyrene spacer is designed to produce different dose rates for the CLDRI experiments. The ^{103}Pd irradiator was placed in a 37°C water-jacketed incubator and surrounded by lead foil of 1 mm thickness (not shown in the sketch) to shield the photons emitted by ^{103}Pd during the experiments.

Figure 2 Relative exposures as a function of added filtration in the simulated ^{103}Pd beam established on an orthovoltage x-ray machine. The half-value-layer thickness was determined from this curve. Its equivalent mono-energetic photon energy and the basic operating parameters are given in Table 1.

Figure 3 Comparison of the cell survival curves of BA1112 cells irradiated using the simulated ^{103}Pd x-ray beam and using a reference 250-kVp x-ray beam with acute exposures. Open triangles represent measured surviving fractions from the 250 kVp x-rays. Filled triangles represent measured surviving fractions from the simulated ^{103}Pd x-rays. Lines represent fits to data using the linear-quadratic model.

Figure 4 Cell survival curves of BA1112 cells irradiated by the simulated ^{103}Pd x-ray beam (filled triangles) and by the ^{103}Pd irradiator at dose rates of 6.8 cGy/h (open circles) and 14.4 cGy/h (filled circles). Lines represent fits to the data using the linear-quadratic model.

Table I. Beam characteristics of the simulated ^{103}Pd x-ray beam

kV	mA	Added Filter (mm AL)	Beam HVL (mm AL)	Energy Homogeneity (%)	Equivalent Photon Energy (keV)
29	25	1.826	0.84	88.6	20.7

Table II. RBE of CLDRI using ^{103}Pd sources

Radiation Source	Dose Rate (Gy/hr)	RBE_{LET}^{Ref}	DRF_T	RBE (1% surviving fraction)
250 kV x-rays	38.9	1.00	1.00	1.00
Simulated Pd-103 x-rays	33.3	1.24	1.00	1.24
Pd-103	0.144	1.24	0.49	0.61
Pd-103	0.068	1.24	0.31	0.39

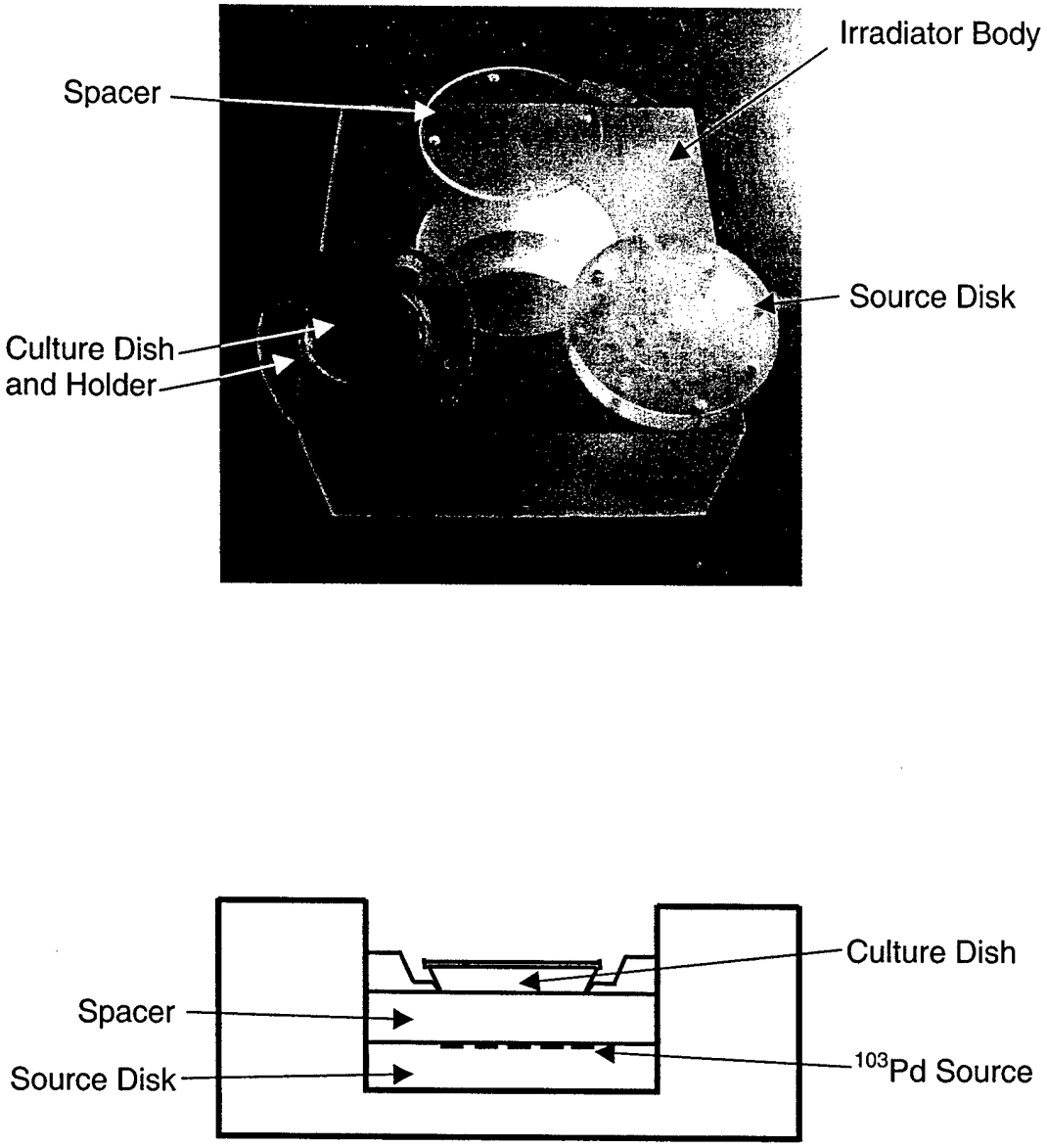
Irradiator Body
Spacer
Source Disk
Culture Dish
and Holder
Culture Dish
Spacer
^{103}Pd Source
Source Disk

Figure 1

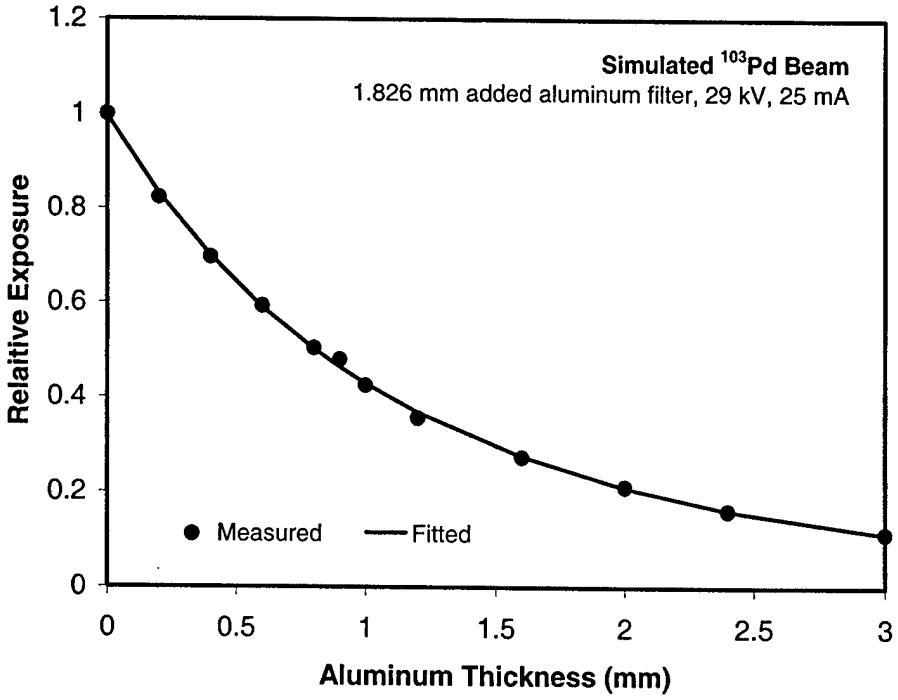
Simulated ^{103}Pd Beam
1.826 mm added aluminum filter, 29 kV, 25 mA
Relaitive Exposure
Aluminum Thickness (mm)
Measured
Fitted
0
0.2
0.4
0.6
0.8
1
1.2
0
0.5
1
1.5
2
2.5
3

Figure 2

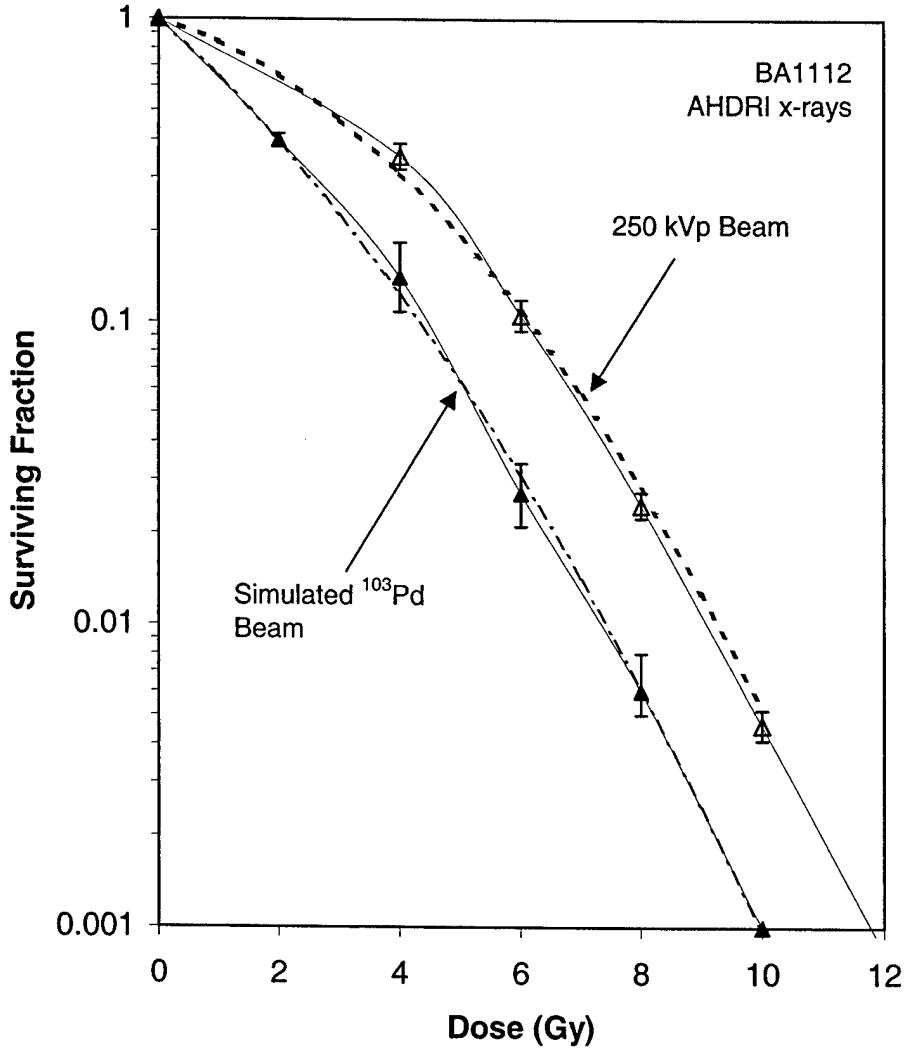
BA1112
AHDRI x-rays
250 kVp Beam
Simulated ^{103}Pd
Beam
Surviving Fraction
1
0.1
0.01
0.001
0
2
4
6
8
10
12
Dose (Gy)

Figure 3

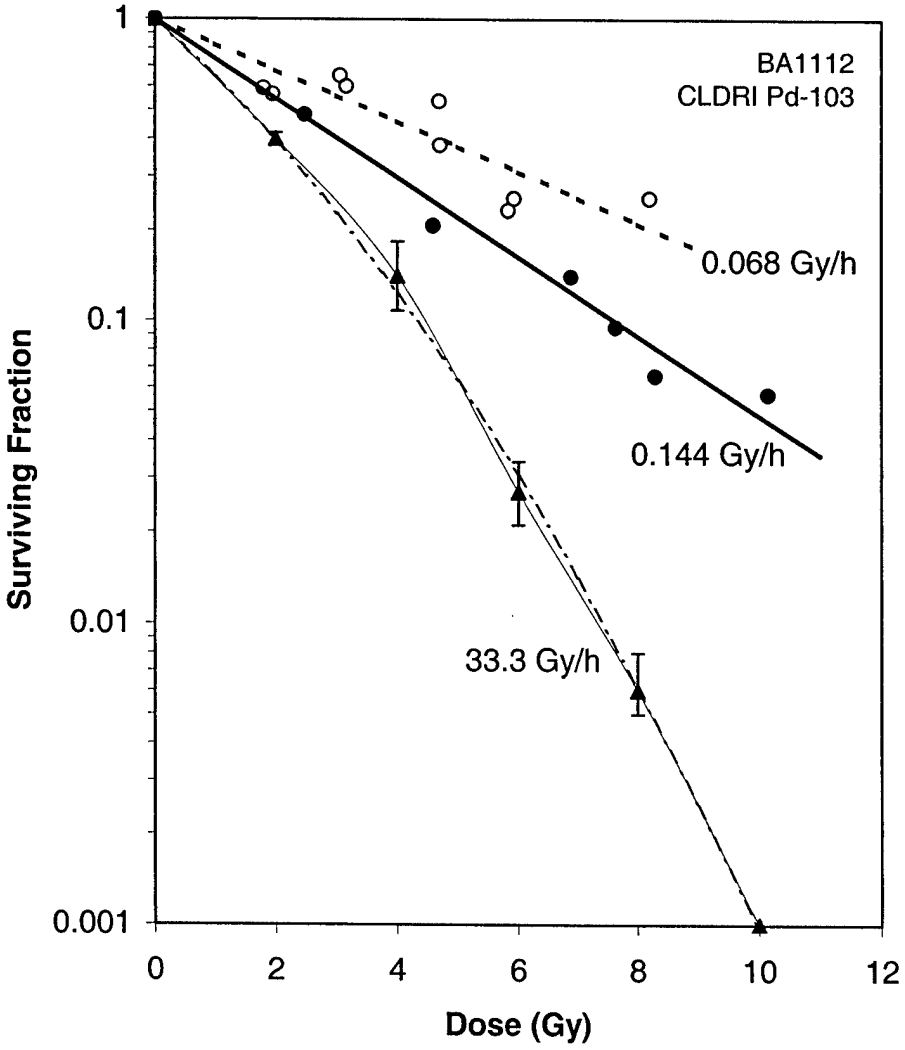
BA1112
CLDRI Pd-103
0.068 Gy/h
0.144 Gy/h
33.3 Gy/h
Surviving Fraction
Dose (Gy)
1
0.1
0.01
0.001
0
2
4
6
8
10
12

Figure 4

Development of a rat solid tumor model for continuous low dose rate irradiation studies using ^{125}I and ^{103}Pd sources

Ravinder Nath, Paul Bongiorni, Zhe Chen, Jillian Gragnano, and Sara Rockwell

Department of Therapeutic Radiology, Yale University School of Medicine, 333 Cedar Street, New Haven, Connecticut 06510

(Submitted to Brachytherapy on March 28, 2004)

Supported in part by DOD grant no. DAMD 17-00-1-0052, awarded by the Department of Army

ABSTRACT

PURPOSE: To develop an experimental technique for studying the radiobiology of continuous low dose rate irradiation (CLDRI) using clinical brachytherapy sources emitting low energy photons for a rat solid tumor model.

METHODS and MATERIALS: BA1112 tumors were grown between the ears of the 14-week old male WAG/Rij rats by interdermal inoculation. A radioactive source afterloading system, which consists of a lightweight helmet sutured to the rat and a nine-source polystyrene applicator, was fabricated for *in vivo* tumor irradiation by ^{125}I and ^{103}Pd brachytherapy sources. This system has a 12 mm × 12 mm opening in the center to accommodate the tumor and its growth during irradiation (the diameter of a typical BA1112 tumor was about 6 mm when radiation was applied). The spatial locations of the nine sources were optimized to produce an as uniform as possible three-dimensional dose distribution to the central portion of the applicator for both the ^{125}I and ^{103}Pd sources. Absolute dose delivered by the applicator was verified by point dose measurements using calibrated TLD in a polystyrene phantom that mimics the scattering environment of the tumor on the rat.

RESULTS: The feasibility of tumor cure experiments using the experimental technique presented in this work was demonstrated. The technique was used to study the influence of initial dose rate on the *in vivo* tumor cure probability of BA1112 tumors irradiated by ^{125}I and ^{103}Pd sources at dose rates varying from 8 to 20 cGy/hr. The technique was also used for studying the *in vitro* tumor cell survival following *in vivo* CLDRI irradiation of the tumor.

CONCLUSION: An experimental technique using an *in vivo* tumor model has been developed for studying the radiobiological effects of continuous low dose rate irradiations using ^{125}I sources alone, ^{103}Pd sources alone or a mixture of ^{125}I and ^{103}Pd sources.

Keywords: Brachytherapy, Ba1112 sarcoma, Tumor cure, Iodine-125, Palladium-103, Continuous low dose rate irradiation, Rat tumor model

Introduction

The dosimetry goal of radiation therapy is to create a uniform dose distribution conforming to the three-dimensional shape of an intended target volume with no or minimum dose to the surrounding normal tissues and critical organs. With external beam radiotherapy (EBRT), even using the most sophisticated intensity modulation technique [1], unwanted radiation doses are inevitably deposited to the normal tissues along the paths of the externally directed radiation beams. On the other hand, interstitial brachytherapy using low photon energy radionuclides, such as ^{125}I (28 keV average energy) and ^{103}Pd (21 keV average energy) implanted directly into the target volume, has provided an alternative method to create highly conformal dose distribution for a target volume while achieving the goal of minimizing radiation exposure to the surrounding normal tissues [2]. In the last two decades, interstitial brachytherapy with permanent implantation of ^{125}I or ^{103}Pd sources has become a popular treatment modality for early stage prostate cancer [3-4]. Interstitial brachytherapy for brain, head & neck, and breast cancers have also been widely reported with good clinical outcomes [5-7].

Theoretically, interstitial brachytherapy using permanent implantation of ^{125}I or ^{103}Pd sources provides continuous low dose rate irradiation (CLDRI) to tumor forever. However, eighty percent of physical dose to full decay is delivered over a time period of 40 days for ^{103}Pd or 140 days for ^{125}I. The time scales of dose delivery have a significant overlap with the potential doubling times of tumor cells, which vary from a few days in head & neck cancers [8] to over 30 days in prostate cancers [9]. As a result, the clinical efficacy of interstitial brachytherapy is affected by the interplay between the tumor cell kinetics (e.g. repopulation, sublethal damage repair, cell cycle redistribution, etc) and the temporal pattern of CLDRI characterized by ever-decreasing dose rate [10-12]. Most of the clinical insights into this complex interplay were obtained through retrospective clinical studies [13-16]. However, due to the ethical constraints inherent in clinical applications and in human clinical trials, quantitative knowledge on the radiobiological interplay between the total dose, initial dose rate, and a given tumor characteristic that is needed to establish an optimal clinical prescription is still lacking. Indeed, the existing clinical prescriptions for CLDRI brachytherapy were guided heavily by model estimates based on empirical time-dose-factors [17] and linear quadratic cell survival models [10-11,18-19]. The aim of this work is to develop an experimental technique for quantitative

study of the radiobiological properties of interstitial brachytherapy with CLDRI using ^{125}I and ^{103}Pd irradiation in a live animal model system.

The technique is based on a well-characterized BA1112 solid tumor which grows on the head of laboratory rats introduced initially in 1966 [20-21]. In the early 1970's, radiobiology group led by Fischer and Moulder used this model for an extensive investigation of the time dose fractionation effects using EBRT [22-24]. In 1984, Peschel et al. reported development of a CLDRI system for this model using high-energy photons emitted by ^{192}Ir [25]. Here we introduce the modification of this system for its use with low photon energy emitters ^{103}Pd and ^{125}I. Customized afterloading applicators for radioactive seeds of ^{125}I and ^{103}Pd were constructed to provide CLDRI for live BA1112 tumors. The experimental technique was applied to study the influence of initial dose rate on the *in vivo* tumor cure probability for BA1112 tumors irradiated by ^{125}I, ^{103}Pd, and a mixture of ^{125}I and ^{103}Pd. The technique was also used to study the *in vitro* tumor cell survival following in vivo CLDRI irradiation of the tumor.

Methods and Materials

In vivo CLDRI technique using ^{125}I and ^{103}Pd sources

In order to perform *in vivo* irradiations of a tumor growing on the head of a laboratory rat and to minimize the personnel radiation exposure by ^{125}I and ^{103}Pd sources, an afterloading applicator system was designed and fabricated (Fig. 1). It consisted of a lightweight metallic helmet and a source applicator. The metallic helmet measuring 2.2 cm (cranial-caudal length) × 2.15 cm (side-side width) × 2.2 cm (height) was sutured to the rat's head prior to the CLDRI experiments. The source applicator was made of clear polystyrene for easy visual verification of the source location and for periodic monitoring of the tumor growth (Figs. 1 and 2). The central portion of the applicator is open with a dimension of 12 mm × 12 mm, large enough for the tumor to grow inside (the diameter of a typical tumor was about 6 mm when radiation was applied). For tumor irradiation, the afterloading applicator was loaded with radioactive sources and then placed and locked to the helmet in a minimal amount of time (< 5 sec). The number and spatial locations of the sources were optimized to produce an as uniform as possible dose distribution to the central portion of the applicator and to be usable for both ^{125}I and ^{103}Pd sources. Although the source strengths for each individual sources can be further optimized for a more uniform dose distribution within the applicator, equal source strengths were chosen for all nine sources in order to minimize possible errors in handling the sources of different strengths.

Because the sources were very close to the tumor, dosimetry data were modeled at distances as short as 1 mm. Dose distribution in the central portion of the applicator was computed from the three dimensional dose distribution pre-calculated for each individual source by Monte Carlo method since most experimental dosimetry data is limited to distances > 5 mm [26-27].

The dose delivered by each applicator to a tumor on the rat was verified by TLD point dose measurements after the applicator was removed from the rat at the completion of each experiment. A jig, which simulates a fully-grown tumor on the head of a rat was used for the TLD measurement. Two 1×1×1 mm^3 micro-TLD cubes were placed in the jig so that the TLD cubes were near the center and 3 mm above the base of the applicator. The applicator and the metallic helmet were placed on the jig during the measurement to simulate the actual dose delivery. Three separate measurements were made for each applicator to minimize the statistical uncertainties from the TLD cubes. The irradiation times were selected so that the cumulative doses delivered to TLDs were about 100 cGy. The use of the TLD dosimetry system follows an existing protocol established in our laboratory [28]. For each batch of TLD, the sensitivity of the TLD cube was determined by irradiating the TLDs to a known dose and comparing the resulting TLD readings. To relate a TLD reading to the dose delivered by ^{125}I or ^{103}Pd seeds, the TLD response was calibrated in a 6 MV photon beam from a Clinac-2100C linear accelerator. An energy correction factor, which takes into account of the energy dependence of the sensitivity of the TLD, was then applied to yield the dose given by ^{125}I or ^{103}Pd sources. The energy correction factor of 1.41 determined by Meigooni and Nath [29] was used for the ^{125}I and ^{103}Pd seeds.

Twelve applicators were built to conduct the tumor cure experiments. Each applicator was paired with a lightweight metallic helmet. Prior to irradiation, the helmet was sutured to the rat's head by four stitches through the cartilage of the ears and two more stitches just behind the head at the neck (Fig.1). A seventh suture was placed under the tumor and tied to the central bar on the top of the helmet, thus ensuring the tumor was pulled up into the center of the irradiation volume. Radioactive sources of ^{125}I or ^{103}Pd were loaded into the afterloading applicator in the hot lab and the applicator was then transported to the animal facility to be loaded into the helmet in less than 5 sec.

Each rat carrying a radioactive applicator was placed in a separate shielded cage. Because the CLDRI experiment lasted over a long period of time (up to 80 days of irradiation and up to

100 days following the termination of irradiation), the door of the cage was built with transparent Pb-lined plastic, which provided adequate light for the rat during the period of experiment. The experimental protocol established for this experiment was reviewed and approved by the Yale University Animal Care and Use Committee prior to the start of the experiments. The attachment of the helmets and suturing during the long irradiations was shown to have no ill effects on the overall health of the rats. The rats gained weight as expected and went on their daily activities in a normal fashion.

BA 1112 tumor model characteristics

Tumors grown on the head of male WAG/Rij rats were used for *in vivo* CLDRI irradiations. The tumor was initiated by implanting of about 5000 tumor cells into the subcutaneous tissues between the ears of a rat at age of approximately14 weeks. The initiation tumor cells were obtained from a single cell suspension of BA1112 cells, which had been harvested from a BA1112 tumor growing on the head of a previously inoculated rat. The BA1112 tumor is a poorly differentiated rhabdomyosarcoma, which is isologous in the WAG/Rij strain of rats [24]. Its properties have been described previously [20-21] and the tumor system has been used extensively in studying the time dose fractionation effects of x-rays [22-24]. The rats were bred and maintained in our breeding colony under SPF conditions.

Typical tumor volume growth characteristics of the BA1112 tumor model under no irradiation is plotted in Fig. 3 as a function of elapsed time after the tumor cell inoculation. The tumor volume was determined using the volume of a half ellipsoid as $4\pi ABC/3$, where A is the tumor length, B is the tumor depth, and C is the tumor height measured by a caliper. The tumor volume growth exhibited two growth phases: an initial fast growing phase and a late slow phase. In the late growth phase, from the elapsed time of about 15 days onward, the tumor volume increases exponentially with an apparent volume-doubling time of about 3 days. This apparent volume-doubling time is significantly longer than the *in vitro* tumor cell doubling time (about 20 hours), reflecting the complex nature of the volume growth in a tumor in a live animal which is affected by such factors as cell loss, cell death, prolonged cell cycle time due to change in local micro-environment as well as the limited supply of nutrients from the tumor cell supporting matrix.

Tumor cure studies under ^{125}I and ^{103}Pd CLDRI

The experimental technique developed in this work can be used to study many radiobiology issues concerning the CLDRI brachytherapy using decaying radioactive sources such as ^{125}I and ^{103}Pd. To demonstrate its application, the influence of initial dose rate on the tumor cure was examined in this work. Experiments were performed using ^{125}I sources with mean initial dose rates of 8 cGy/hr and 18 cGy/hr. For comparison, irradiations using ^{103}Pd sources with a mean initial dose rate of 20 cGy/hr were also performed. For ^{125}I, the irradiation was terminated after a planned total dose of 146 Gy was delivered. It corresponded to approximately 43 days of CLDRI. For ^{103}Pd, the irradiation was terminated after 79 days of irradiation, corresponding to a total delivered dose of 112 Gy. Irradiations of the tumor were initiated at approximately day 21 after the inoculation of the tumor cells in the rat. Typical tumor volume at the onset of irradiation was about 100-200 mm^3. The tumor response to the CLDRI was recorded by measuring the tumor volume twice weekly during the irradiation, until each tumor had reached a maximum volume of 1000 mm^3 (failure) or until the tumor had regressed and the animal had been free of tumor for 100 days (local control). The patterns of tumor volume growth were used to compute the tumor cure probability.

In vivo irradiation and *in vitro* cell survival assay

The experimental system was also used to study the cell survival characteristics using *in vivo* irradiation by ^{125}I or ^{103}Pd sources and an *in vitro* cell survival assay. At approximately 3 weeks after the inoculation of tumor cells to a rat, tumors growing on the rats were irradiated by ^{125}I to a given radiation dose. The rats were then put to death at the end of the irradiation and the tumor cells were suspended, counted, and assayed for viability using the same colony formation assay used for cells from cultures. Analyses of cell yield were performed to account for the loss of cells during the protracted irradiations [30]. A complete cell survival curves after relatively short, graded treatment times (hours to days) under CLDRI of ^{125}I sources were measured. The measured survival curve can be used as a surrogate for the effects of initial dose rate on CLDRI brachytherapy treatment. It can also be used to test theoretical cell surviving models developed for protracted irradiations. Details of the in vitro assay have been discussed previously [31].

Results

Dosimetry properties of the afterloading applicator

The dose distribution within the open portion of the applicator was characterized by the initial iso-dose-rate distributions of sources having unit air-kerma strength. For the ease of visualization, Fig. 4 plots this iso-dose-rate distribution in eight planes parallel to the base of the applicator for ^{125}I seeds (Draximage model LS-1). The distance of each plane relative to the applicator base is –1 mm (A), 0 mm (B), 1 mm (C), 2 mm (D), 3 mm (E), 4 mm (F), 5 mm (G), and 6 mm (H). Note that plane A is 1 mm below the base of the applicator. Fig. 5 shows the initial dose-rate distribution from ^{103}Pd (Theragenics Model 200) seeds. During the irradiation, the tumor was pulled up into the center of the applicator (as described earlier). The dose distribution characteristics in the central opening of the applicator, within a cylindrical volume of 10 mm diameter and 10 mm height is summarized in the cumulative dose volume histogram shown in Fig. 6. Fig.s 4-6 show that the dose-rate distribution within the open portion of the applicator has a uniformity between 95% and 150% for both ^{125}I and ^{103}Pd seeds. Table I compares the dose to water measured in the polystyrene phantom to the dose calculated to water at the same measurement point for six applicators. The measured dose in polystyrene is on the order of 5% higher than the calculated dose.

Tumor cure probability under CLDRI using ^{125}I and ^{103}Pd

Tumor growth under CLDRI using ^{125}I with initial dose rates of 8 cGy/hr is shown in Fig. 7 for a total delivered dose of 146 Gy. The experiment was repeated on eight different rats in order to obtain a statistically meaningful result. In Fig. 7, the solid circles represent the average growth of the tumors under no irradiation and the open triangles represent average tumor size measured at various time during the irradiation. It should be pointed out that most of the tumors irradiated with 8 cGy/hr initial dose rate could not receive the full planned dose of 146 Gy because the tumor had grown too big to fit inside the central opening of the applicator before the planned dose was reached. Fig. 7 shows that tumor cure was not attainable with the initial dose rate of 8 cGy/hr using ^{125}I. The tumors continued to grow during the irradiation, albeit with a much slower "apparent" growth rate. The apparent volume-doubling time for the tumors under irradiation at 8 cGy/hr was approximately 21 days as compared to 3 days for normal growth with no radiation.

At the initial dose rate of 8 cGy/hr, the rate of cell killing inflicted by the irradiation was not sufficient to overcome the rate of cell repopulation by the remaining cells and the repair of sublethally damaged cells. However, when the initial dose rate was increased to 18 cGy/hr, tumor cure was observed in six out of eight rats, resulting in a 75% tumor cure (Fig. 8). It is interesting to note from Fig. 8 that the tumor volumes continued to grow slightly even after the radiation was applied for about 20 days, but soon (after about 30 days) they began to decrease rapidly as irradiation continued. At one time or another within the experimental time span, the tumor volumes of all eight experiments had been reduced to sizes invisible to human eyes (apparent tumor cure). The two failures in Fig. 8 occurred at approximately 42 days after the irradiation was terminated. At the termination of irradiation (with total dose of 146 Gy), one rat had a visible tumor while the other's original tumor was invisible. In either case, the local failures indicate that there were viable tumor cells remaining at the time of radiation termination in these two rats even though the tumor volume was invisible to human eyes. Therefore, delivering 146 Gy total dose with an initial dose rate of 18 cGy/hr using ^{125}I is not sufficient to produce 100% tumor cure in this tumor model system.

The tumor growth characteristics irradiated by ^{103}Pd sources are plotted in Fig. 9 for an initial dose rate of 20 cGy/hr. Five out of eight tumors were cured, resulting in approximately 62% probability of tumor cure. Note that the plots exhibited similar characteristics as those shown in Fig. 8 for ^{125}I. However, the time each tumor took to achieve a rapid tumor volume reduction had shown much wider variation with ^{103}Pd irradiation. The wider variation is most likely caused by the variation of initial tumor burden (100 –200 mm^3) at the onset of the irradiation, given the fact the initial dose rates and the intrinsic tumor cell characteristics were essentially the same for all eight experiments. Such variations in initial tumor burden also existed in the tumors irradiated by ^{125}I. But the effect on the subsequent tumor volume growth was magnified in case of ^{103}Pd because its dose rate decreased much faster due to the shorter decay half-life.

Fig. 10 plots the tumor growth as a function of treatment time when the tumor was irradiated by a mixture of ^{125}I and ^{103}Pd sources to a total dose of 146 Gy. The total initial dose rate was 18 cGy/hr with ^{125}I and ^{103}Pd each contributing 9 cGy/hr. The irradiation was terminated at day 63 or 65 for a total dose of 146 Gy. The probability of tumor cure under this irradiation condition was 75% similar to that achieved with ^{125}I alone with initial dose rate of 18 cGy/hr.

In vivo irradiation and *in vitro* cell survival assay

As a demonstration of another application of the experimental technique, Fig. 11 shows a tumor cell survival curve as a function of dose measured in an *in vivo/in vitro* experiment using ^{125}I sources. The initial dose rate was 8 cGy/hr. Plotted also in the Fig. are the survivals calculated using a theoretical model [18-19]. The solid line represent the calculated survival curve using the average initial dose rates, while the open circles represent calculation using the actual initial dose rate for each experiment. The parameters of α, β, repair half-time, and tumor doubling time were determined directly from the measurements performed on the BA1112 cells. These experiments can provide a set of well-defined cell survival data for testing theoretical radiobiological models and for predicting tumor cure probabilities.

Discussion

The results of tumor cure studies performed in this work indicate that tumor cure was not attainable when the initial dose rate was too low, for example, 8 cGy/hr using ^{125}I. As the initial dose rate was increased, probability of tumor cure increased. For CLDRI using ^{125}I, a 75% tumor cure was achieved with initial dose rate of 18 cGy/hr and a total dose of 146 Gy. It is interesting to examine the pattern of failures in the tumors irradiated with initial dose rate of 18 cGy/hr. One may ask if a failure was due primarily to insufficient initial dose rate or insufficient total dose. To answer this question, one needs to know the cell kill rate at the time of radiation termination. If the cell kill rate caused by the radiation was greater than the cell repopulation rate, then the radiation is theoretically successful in producing a tumor cure. Because the instantaneous dose rate decreases exponentially with irradiation time, there exists an effective treatment time at which the cell kill rate from the instantaneous ^{125}I irradiation equals to the rate of cell repopulation. Within this effective treatment time, the cell kill rate from the delivered radiation is greater than cell repopulation rate resulting in a net tumor cell reduction. A calculation based on the model proposed by Dale [18-19] yielded an effective treatment of approximately 130 days for ^{125}I with an initial dose rate of 18 cGy/hr. Therefore, at the time of irradiation termination (43 days) in our experiment, the cell kill rate was theoretically greater than the cell repopulation rate. If irradiations were kept on to deliver a greater total dose, the two failures might have been eliminated.

As in the case of irradiation with ^{125}I, the tumor volumes in the ^{103}Pd experiments had also reduced to invisible size at one time or another during experimental monitoring. Among the three experiments that failed to achieve a tumor cure, one tumor grew back after the irradiation was terminated and the tumor volume had remained invisible for one week. The other two grew back after the tumor volumes had shrunk to invisible size for over 28 days while irradiation was still on. A similar calculation on the effective treatment time for ^{103}Pd irradiation with initial dose rate of 20 cGy/hr yielded 46 days. The total dose delivered up to the effective treatment time was 100 Gy only about 12% lower than the total dose of 112 Gy achieved at the irradiation termination day 79. Since the irradiation was terminated at day 79, well beyond the effective treatment time, it suggests that the failures in the ^{103}Pd irradiation are due mainly to insufficient initial dose rate. In contrast, the failures in the ^{125}I irradiation with the initial dose rate of 18 cGy/hr were due primarily to insufficient total dose (as the irradiation was terminated at day 43, well before the effective treatment time of 130 days).

Mixing seeds of different decay characteristics provides a way to modulate the temporal pattern of dose delivery. As shown in Fig. 12, the temporal pattern of dose rate for the mixed seed irradiation (each contributing 50% of initial dose rate) is intermediate between that from either ^{125}I or ^{103}Pd alone. Since the tumor cure probability would be less than 62% using ^{103}Pd alone at an initial dose rate of 18 cGy/hr and would be approximately 75% using ^{125}I alone at the same initial dose rate, one would have expected that the probability of tumor cure for the mixed source irradiation to lie in between 62% and 75%. The observed tumor cure probability irradiated by the mixed seed irradiation was higher than expected at 75% similar to that irradiated by ^{125}I alone at the same initial dose rate. This numerical coincidence may be caused by statistical uncertainty of the experiment as only eight rats were used in each irradiation condition. On the other hand, the observed tumor cure rate could be a real manifestation of the presence of other factors in tumors *in vivo*, such as hypoxic cells and re-oxygenation, that may favor irradiations with slower radioactive decay.

The results from the tumor cure experiments for the BA1112 tumors *in vivo* shown that the probability of tumor cure under CLDRI with ^{125}I and ^{103}Pd depends on both the total delivered dose and the initial dose rate. An optimal combination of initial dose rate and total dose may be determined for BA1112 tumors or for other tumors if their basic radiobiological properties are known. Such a study and its clinical implications are being pursued further by our

group. These results have demonstrated that the experimental technique developed here is suitable for detailed study of the radiobiological underpinnings of brachytherapy using radionuclides with different decay characteristics. It also provides a tool for testing the basic radiobiological principles and hypothesis regarding CLDRI using ^{125}I and ^{103}Pd, for example, the efficacy of using mixed radioactive sources in interstitial brachytherapy. We fully realize that the results obtained from the animal tumor model may not be translated directly to human applications. We expect, however, these studies will provide a well-defined data set for testing the theoretical radiobiological models that are used increasingly in interstitial brachytherapy plan evaluations.

Conclusion

An experimental technique using an in vivo model tumor has been developed for studying radiobiological effects of CLDRI using ^{125}I and ^{103}Pd sources. The technique was used to demonstrate the influence of initial dose rate and radionuclide type on the probability of tumor cure for BA1112 tumors grown on the head of laboratory rats. The results shown that the probability of tumor cure is strongly dependent on both the initial dose rate and on the prescribed total-dose. The experimental technique can be used to examine other interesting radiobiological issues related to the CLDRI brachytherapy treatment and the data collected from these experiments may also provide a test bed for theoretical radiobiological models.

References

1. Intensity-Modulated Radiation Therapy – The State of the Art. Edited by Jatinder R. Palta and T. Rockwell Mackie. Medical Physics Publishing; Madison, WI, 2003

2. Hilaris BS, ed. Handbook of interstitial brachytherapy. Acton, MA: Publishing Science Group; 1975.

3. Blasko JC, Grimm PD, Ragde H, Schumacher D. Implant therapy for localized prostate cancer. In Ernstoff MS, Heaney JA, Peschel RE, editors. Prostate Cancer. Cambridge, Massachusetts and Oxford, England: Blackwell Science; 1998. p. 137-155.
4. King CR, Sanzone J, Anderson KR, and Peschel RE: Definitive therapy for stage T1/T2 prostate carcinoma: A PSA based comparison between surgery, external beam and implant radiotherapy. *J Brachytherapy Int* **14**, 169-177, 1998.
5. Lefebvre JL, Coche-Dequeant B, Castelain B, Prevost B, Buisset E, Ton Van J. Interstitial brachytherapy and early tongue squamous cell carcinoma management. *Head Neck.* 1990;12:232-6.
6. Son YH, Sasaki CT. Nonsurgical alternative therapy for bulky advanced head and neck tumors. *Arch Otolaryngol Head Neck Surg.* 1995;121:991-3.
7. Vikram B, Mishra S. Permanent iodine-125 implants in postoperative radiotherapy for head and neck cancer with positive surgical margins. *Head Neck.* 1994;16:155-157.
8. Struikmans H, Kal HB, Hordijk GJ, van der Tweel I, Proliferative capacity in head and neck cancer. Head Neck. 23:484-91, 2001.
9. Haustermans KM, Hofland I, Van Poppel H, Oyen R, Van de Voorde W, Begg AC, Fowler JF. Cell kinetic measurements in prostate cancer. Int J Radiat Oncol Biol Phys. 37:1067-70, 1997.
10. Dale RG, Jones B. The clinical radiobiology of brachytherapy. *British J. Radiol*, 1998; 71: 465-483.
11. Ling CC. Permanent implants using Au-198, Pd-103, and I-125: radiobiological considerations based on the linear quadratic model. *Int. J. Radiat. Oncol. Biol. Phys.1992;* **23:**81-87.

12. Thames HD. An "incomplete-repair" model for survival after fractionated and continuous irradiation, *Int. J. Radiat. Biol.* 1985;**47:**319-339.
13. Sylvester JE, Blasko JC, Grimm PD, Meier R, Malmgren JA. Ten-year biochemical relapse-free survival after external beam radiation and brachytherapy for localized prostate cancer: the Seattle experience. Int J Radiat Oncol Biol Phys. 2003 Nov 15;57(4):944-52.
14. Potters L, Cao Y, Calugaru E, Torre T, Fearn P, Wang XH. A comprehensive review of CT-based dosimetry parameters and biochemical control in patients treated with permanent prostate brachytherapy. Int J Radiat Oncol Biol Phys. 2001 Jul 1;50(3):605-14.
15. RG Stock, NN Stone, A Tabert, C Iammuzzi, and JK DeWyngaert, "A dose-response study for I-125 prostate implants," Int. J. Radiat. Oncol. Biol. Phys. **41**, 101-108, 1998.
16. GE Hanks, AL Hanlon, B Epstein, EM Horwitz. Dose response in prostate cancer with 8-12 years' follow-up. Int J Radiat Oncol Biol Phys 54:427-35, 2002.
17. Orton CG. Time-dose factors (TDFs) in brachytherapy. Br J Radiol. 47:603-7, 1974.
18. Dale RG. The application of the linear-quadratic dose-effect equation to fractionated and protracted radiotherapy. *Brit J Radiol, 1985;* **58**:515-528.
19. Dale RG. Radiobiological assessment of permanent implants using tumor repopulation factors in the linear-quadratic model. *Brit J Radiol. 1989;* **62:**241-244.
20. Reinhold, H.S., Quantitative evaluation of the radiosensitivity of cells of a transplantable rhabdomyosarcoma in the rat. Europ. J. Cancer, 2: 33-42, 1966
21. Reinhold, H.S., DeBree, C., Tumor cure rate and cell survival of a transplantable rat rhabdomyosarcoma following x-irradiation. Europ. J. Cancer 4: 367-374, 1968
22. Fischer JJ, Reinhold HS, The cure of rhabdomyosarcoma BA1112 with fractionated radiotherapy. Radiology 105: 429-433, 1972.
23. Moulder JE, Fischer JJ, Determination of an optimal treatment plan for rat rhabdomyosarcoma. Radiology 107: 439-441, 1973.
24. Moulder JE, Fischer JJ, Milardo R, Time-dose relationships for the cure of an experimental rat tumor with fractionated radiation. Int. J. Radiat. Oncol. Biol. Phys. **1**, 431-438, 1976.
25. Peschel RE, Martin DF, Fischer, Tumor cure studies on the rate sarcoma BA1112 using continuous low-dose-rate radiation. Radiology 152, 801-803, 1984.

26. Williamson JF. Dosimetric characteristics of the DRAXIMAGE model LS-1 1-125 interstitial brachytherapy source design: a Monte Carlo investigation. Med Phys. 2002 29:509-21.

27. Chan GH, Prestwich WV. Monte Carlo investigation of the dosimetric properties of the new 103Pd BrachySeedPd-103 Model Pd-1 source. Med Phys. 2002 29:1984-90.

28. Nath R, Melillo A. Dosimetric characteristics of a double wall 125I source for interstitial brachytherapy. Med Phys. 20:1475-83 1993.

29. Muench PJ, Meigooni AS, Nath R, McLaughlin WL. Photon energy dependence of the sensitivity of radiochromic film and comparison with silver halide film and LiF TLDs used for brachytherapy dosimetry. Med Phys. 18:769-75 1991.

30. Nath R, Bongiorni P, Rockwell S, The relative biological effectiveness of iodine-125 and americium-241photons relative to radium-226 photons for continuous low dose rate irradiations at dose rates of 0.17 to 0.73 Gy/hr, Endocurie, Hypertherm, Oncol. 681-91, 1990.

31. Nath R, Bongiorni P, Chen Z, Gragnano J, Rockwell S, Dose rate dependence of the relative biological effectiveness of ^{103}Pd for continuous low dose rate irradiation of BA1112 rhabdomyosarcoma cells in vitro relative to acute exposures. Submitted to Int. J. Radiat. Biol.

Figure Captions

Fig. 1 Photography of the afterloading device developed for *in vivo* irradiation of BA1112 tumor grown on the head of a laboratory rat. Shown on the left is a matched pair of lightweight metallic helmet and the polystyrene radioactive source afterloader. Shown on the right is the helmet sutured on a rat's head. Note the string used to pull the tumor up into the center of the source applicator (not shown) during the irradiation experiment.

Fig. 2 Schematic drawing of the source afterloader for ^{125}I and ^{103}Pd brachytherapy sources.

Fig. 3 BA1112 tumor volume growth characteristics. The tumor volume is measurable from approximately 10 days after inoculation of the BA1112 tumor cells to the rat. After a brief period fast volume growth, the tumor volume grows exponentially with an apparent volume-doubling time of approximately 3 days with no irradiation.

Fig. 4 Iso-initial-dose-rate plotted at eight different planes parallel to the base of the source applicator for ^{125}I sources of unit air-kerma strength. The distance of each plane relative to the applicator base is –1 mm (A), 0 mm (B), 1 mm (C), 2 mm (D), 3 mm (E), 4 mm (F), 5 mm (G), and 6 mm (H). Note that plane A is 1 mm below the base of the applicator.

Fig. 5 Iso-initial-dose-rate plotted at eight different planes parallel to the base of the source applicator for ^{103}Pd sources of unit air-kerma strength. The distance of each plane relative to the applicator base is –1 mm (A), 0 mm (B), 1 mm (C), 2 mm (D), 3 mm (E), 4 mm (F), 5 mm (G), and 6 mm (H). Note that plane A is 1 mm below the base of the applicator.

Fig. 6 Cumulative histogram plot of the initial dose rates within a cylindrical volume centered at the center of the source applicator.

Fig. 7 *In vivo* tumor volume growth under CLDRI of ^{125}I with an initial dose rate of 8 cGy/hr (open triangles) and no irradiation (solid circles).

Fig. 8 *In vivo* tumor volume growth under CLDRI of ^{125}I with an initial dose rate of 16 cGy/hr for eight rats and no irradiation (solid circles).

Fig. 9 *In vivo* tumor volume growth under CLDRI of ^{103}Pd with an initial dose rate of 16 cGy/hr for eight rats and no irradiation (solid circles).

Fig. 10 *In vivo* tumor volume growth under CLDRI of a mixture of ^{125}I and ^{103}Pd with an initial dose rate of 16 cGy/hr for eight rats and no irradiation (solid circles). The source strength of ^{125}I and ^{103}Pd were chosen such that it contribute half of the dose rate at each point.

Fig. 11 Surviving fraction as a function of dose using ^{125}I. The solid and open circles represent measured (using the *in vivo-in vitro* assay technique) and the solid line represents model calculated surviving fraction.

Fig. 12 Normalized dose rate as a function of time for irradiation with ^{125}I alone, ^{103}Pd alone, and with a mixture of ^{125}I and ^{103}Pd each contribute 50% of initial dose rate.

Table I. Comparison of dose measured by TLDs for six applicators

Applicator	Measured (cGy)	Calculated (cGy)	Relative Difference (%)	Standard Deviation
I	124.3	114.2	1.089	0.02
L	102.1	96.7	1.056	0.00
F	87.9	83.6	1.051	0.04
G	79.7	74.8	1.067	0.02
B	87.1	82.5	1.050	0.09
H	82.0	78.3	1.047	0.04

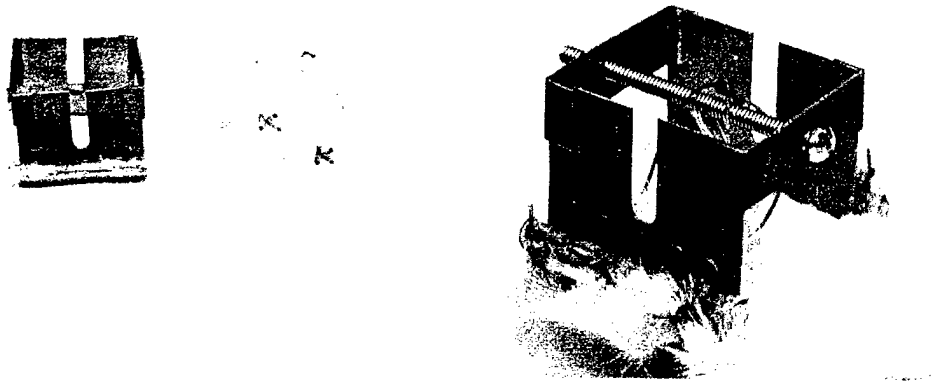

Fig. 1. Photography of the afterloading device developed for *in vivo* irradiation of BA1112 tumor grown on the head of a laboratory rat. Shown on the left is a matched pair of lightweight metallic helmet and the polystyrene radioactive source afterloader. Shown on the right is the helmet sutured on a rat's head. Note the string used to pull the tumor up into the center of the source applicator (not shown) during the irradiation experiment

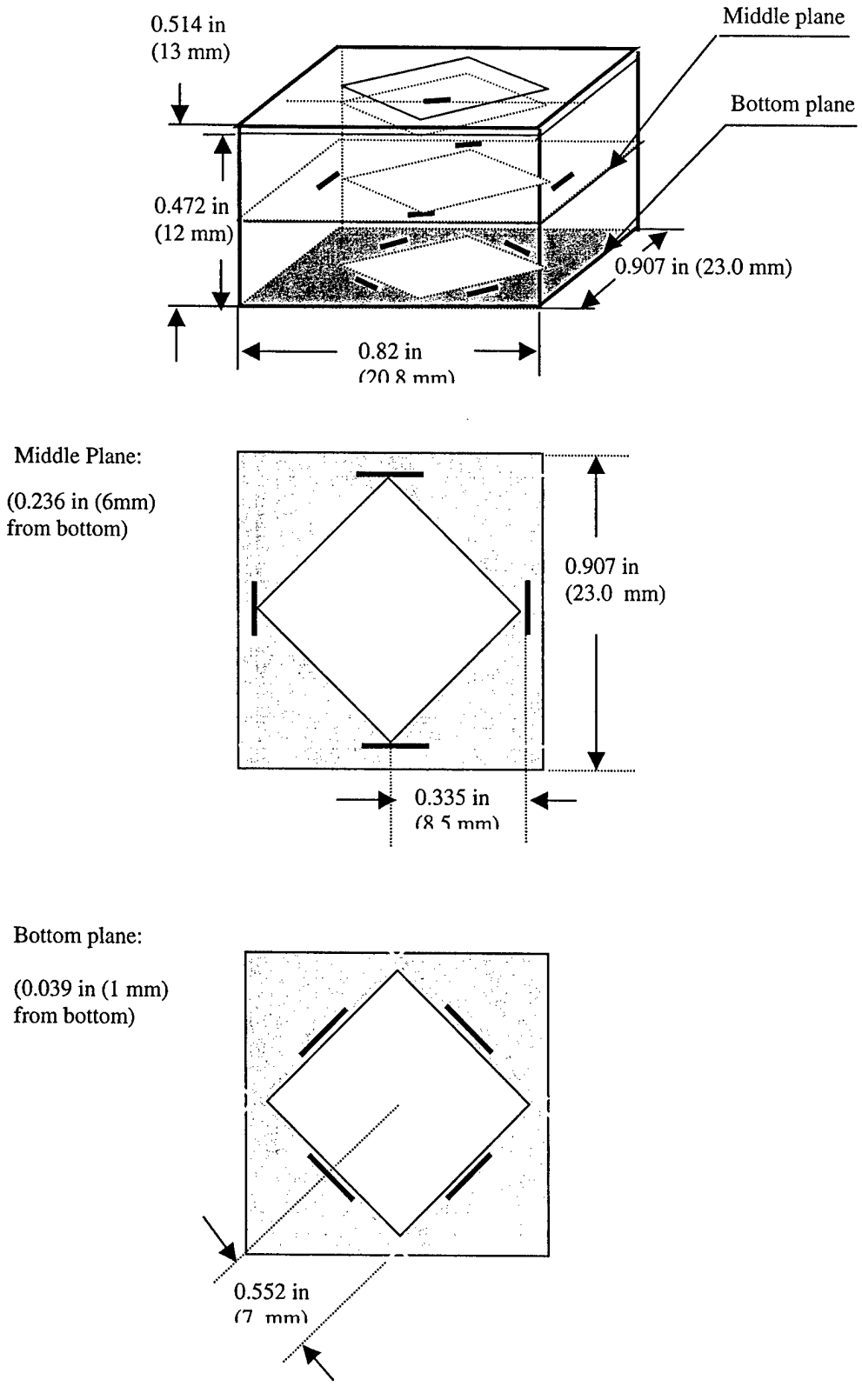

Fig. 2. Schematic drawing of the source afterloader for ^{125}I and ^{103}Pd brachytherapy sources

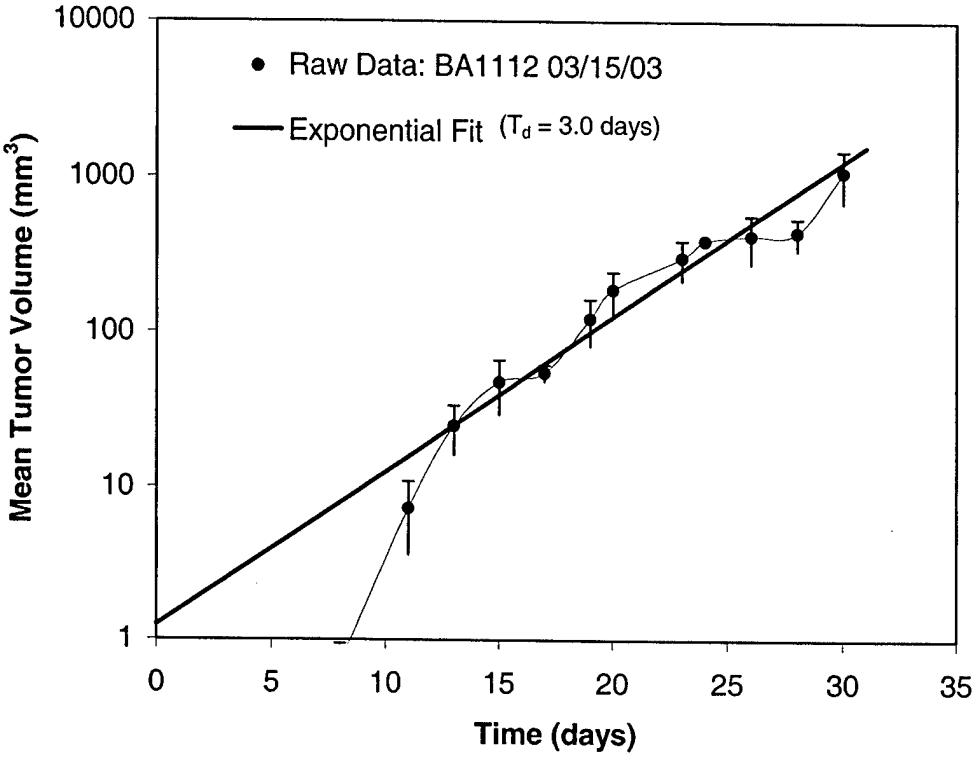

Fig. 3. BA1112 tumor volume growth characteristics. The tumor volume is measurable from approximately 10 days after inoculation of the BA1112 tumor cells to the rat. After a brief period fast volume growth, the tumor volume grows exponentially with an apparent volume-doubling time of approximately 3 days with no irradiation

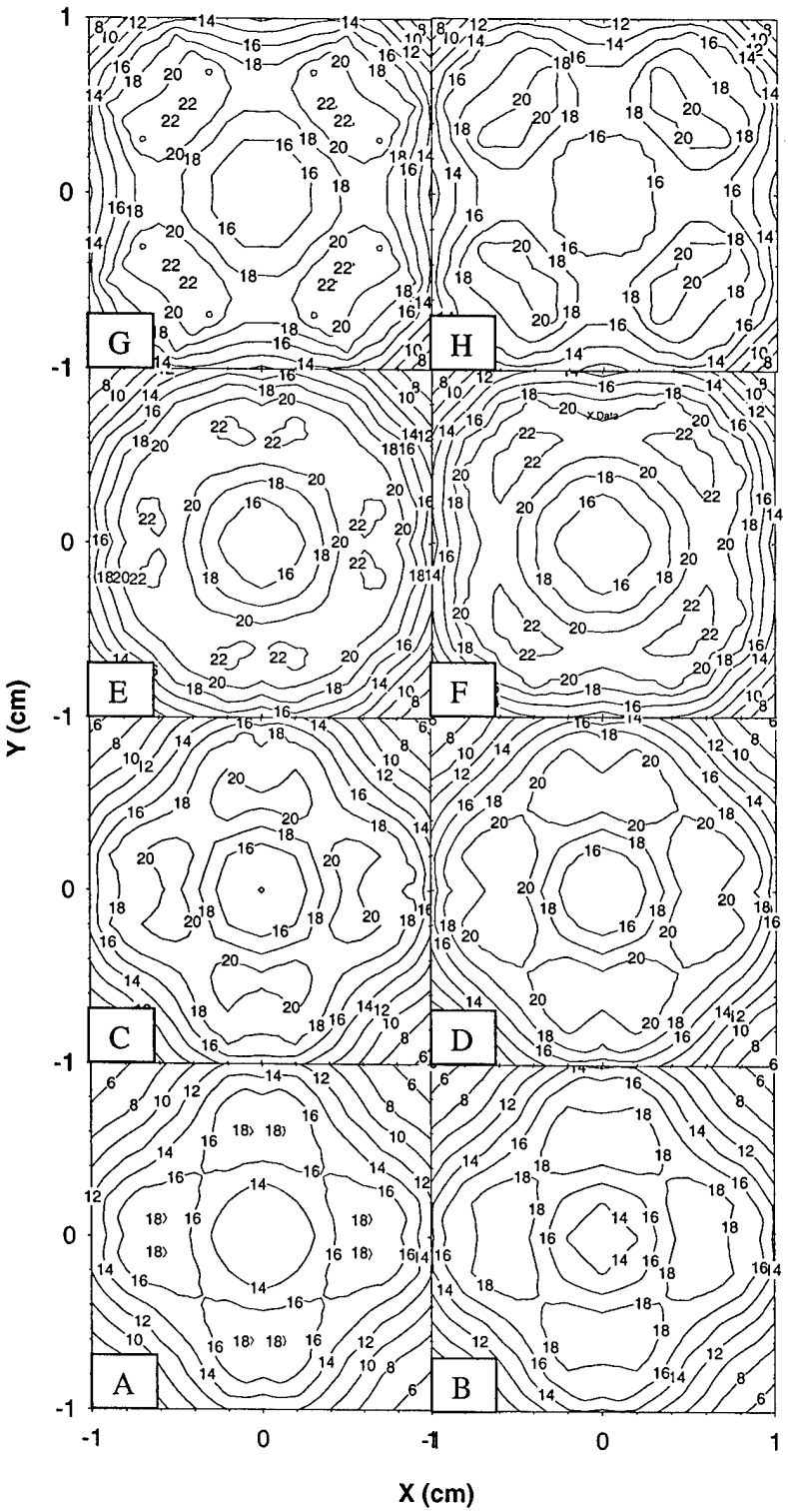

Fig. 4. Iso-initial-dose-rate plotted at eight different planes parallel to the base of the source applicator for ^{125}I sources of unit air-kerma strength

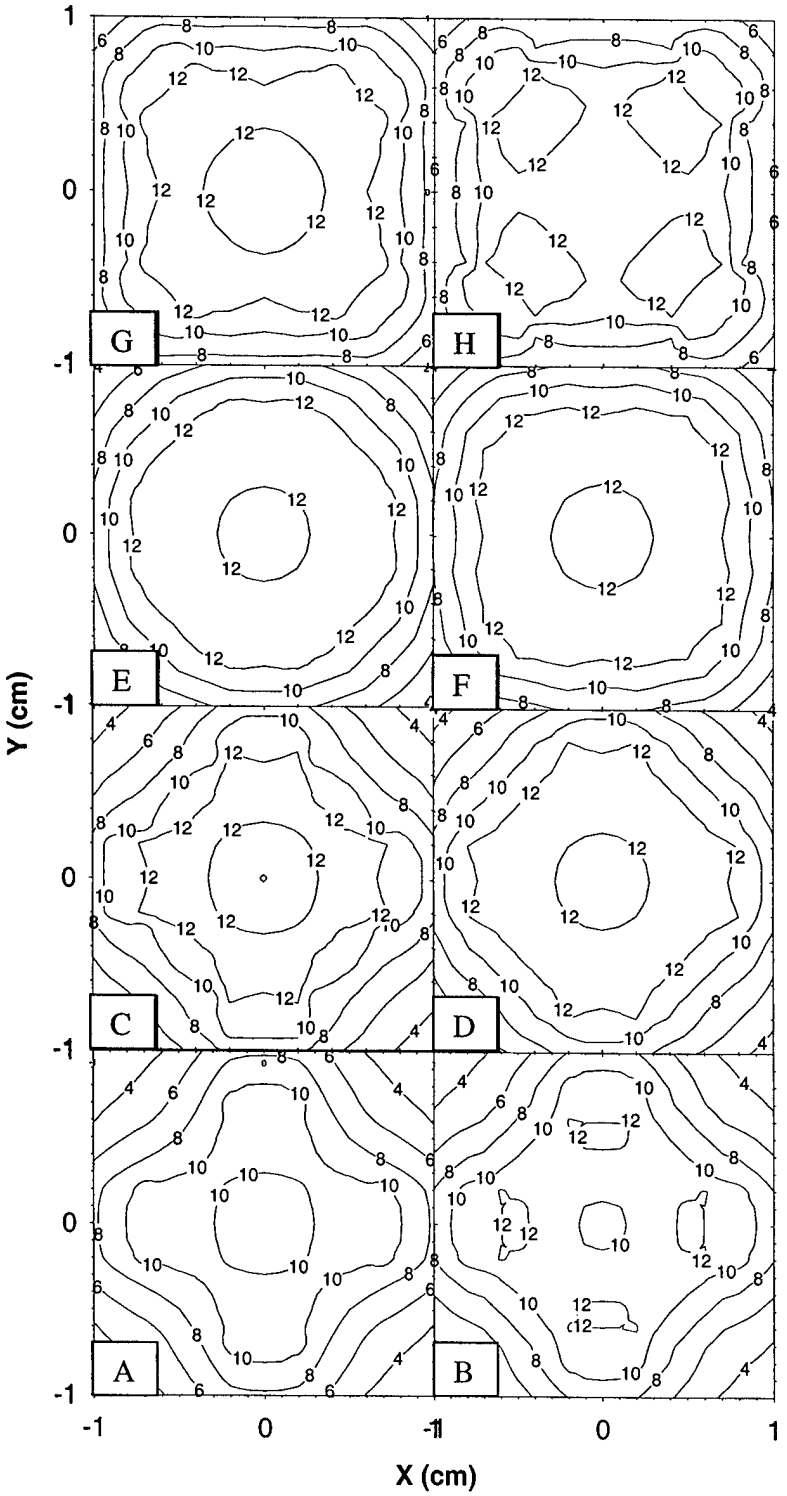

Fig. 5. Iso-initial-dose-rate plotted at eight different planes parallel to the base of the source applicator for ^{103}Pd sources of unit air-kerma strength

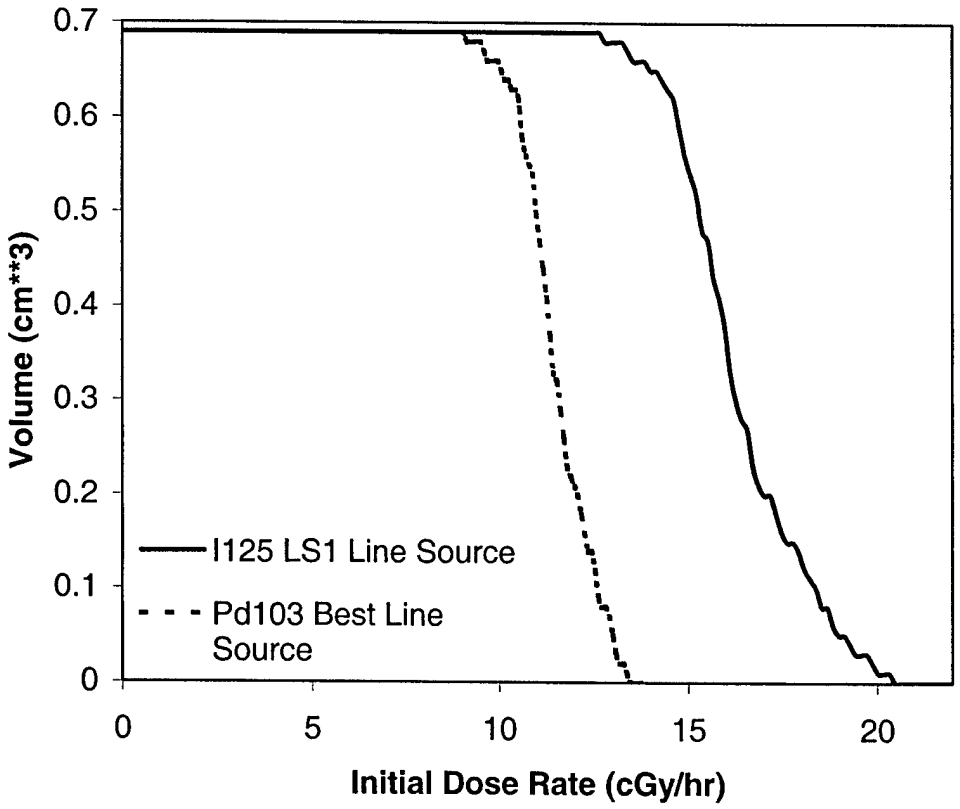

Fig. 6. Cumulative histogram plot of the initial dose rates within a cylindrical volume centered at the center of the source applicator

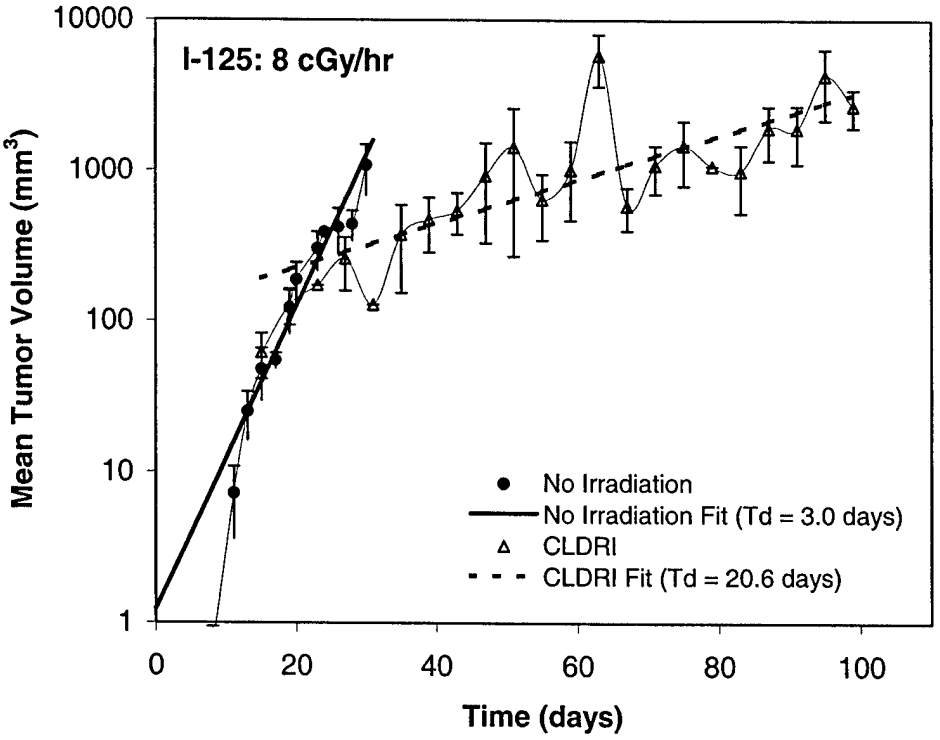

Fig. 7. *In vivo* tumor volume growth under CLDRI of ^{125}I with an initial dose rate of 8 cGy/hr (open triangles) and no irradiation (solid circles)

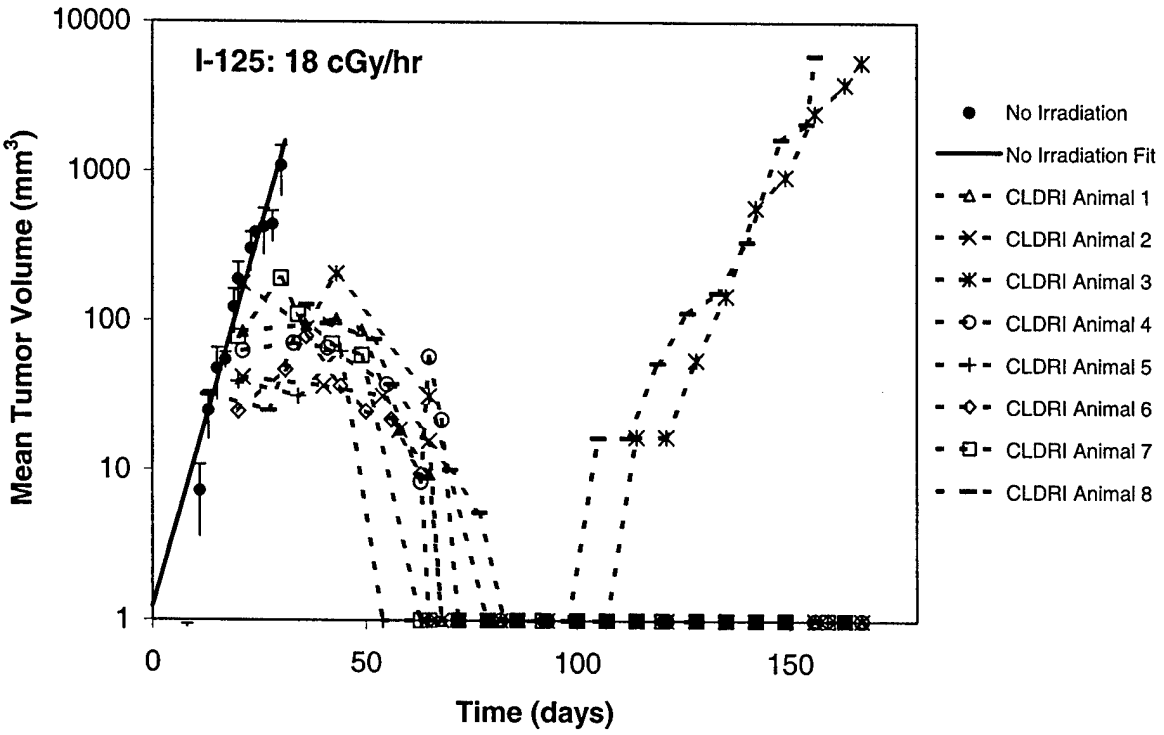

Fig. 8. *In vivo* tumor volume growth under CLDRI of ^{125}I with an initial dose rate of 16 cGy/hr for eight rats and no irradiation (solid circles)

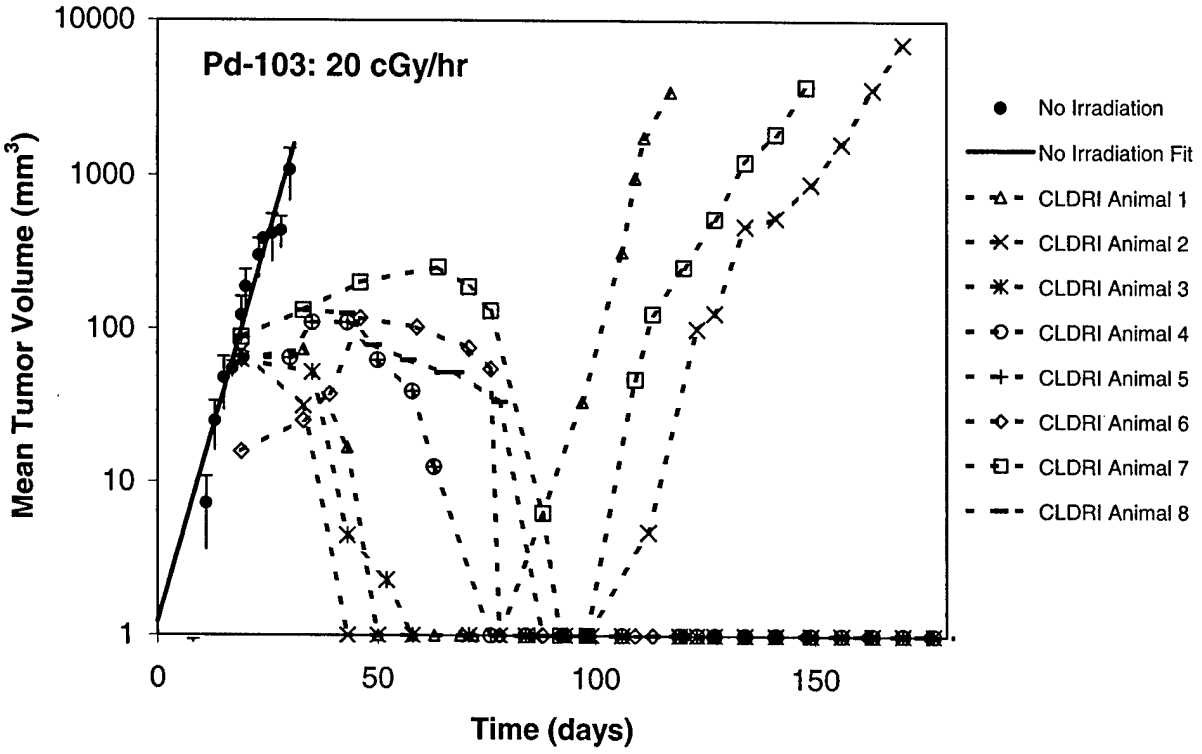

Fig. 9. *In vivo* tumor volume growth under CLDRI of ^{103}Pd with an initial dose rate of 16 cGy/hr for eight rats and no irradiation (solid circles)

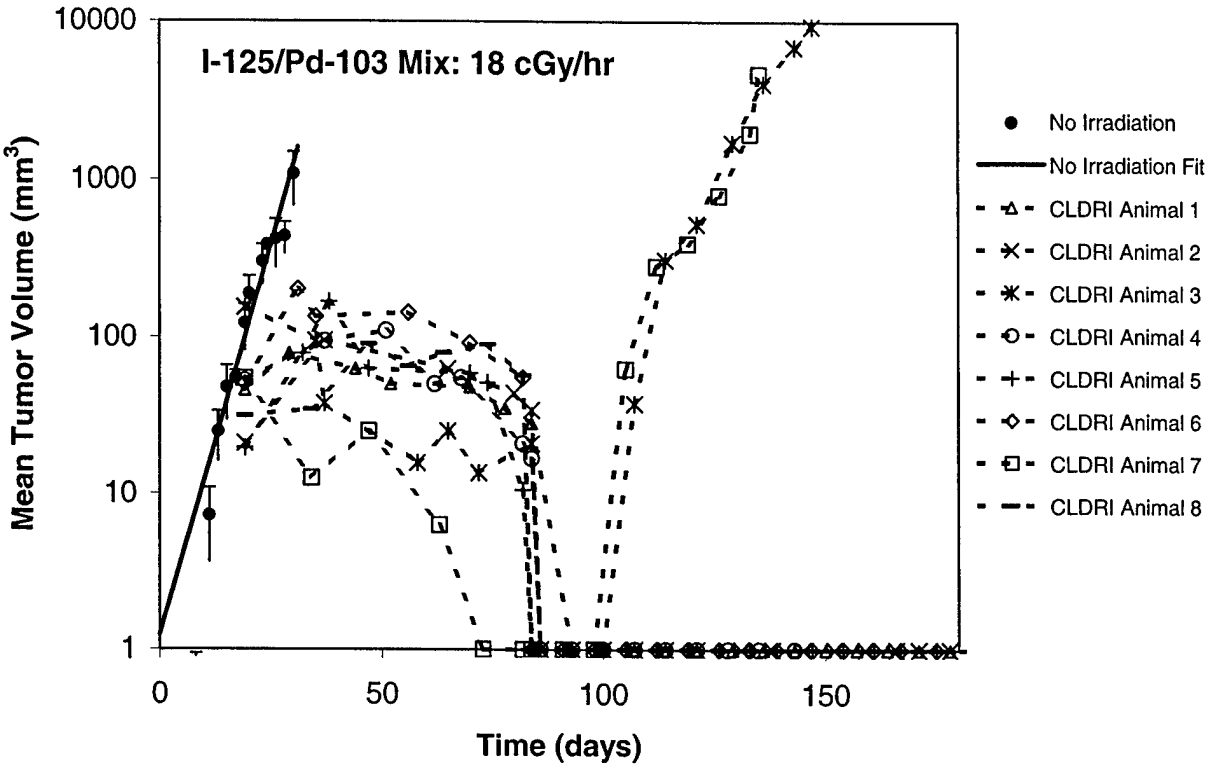

Fig. 10. *In vivo* tumor volume growth under CLDRI of a mixture of ^{125}I and ^{103}Pd with an initial dose rate of 16 cGy/hr for eight rats and no irradiation (solid circles). The source strength of ^{125}I and ^{103}Pd were chosen such that it contribute half of the dose rate at each point

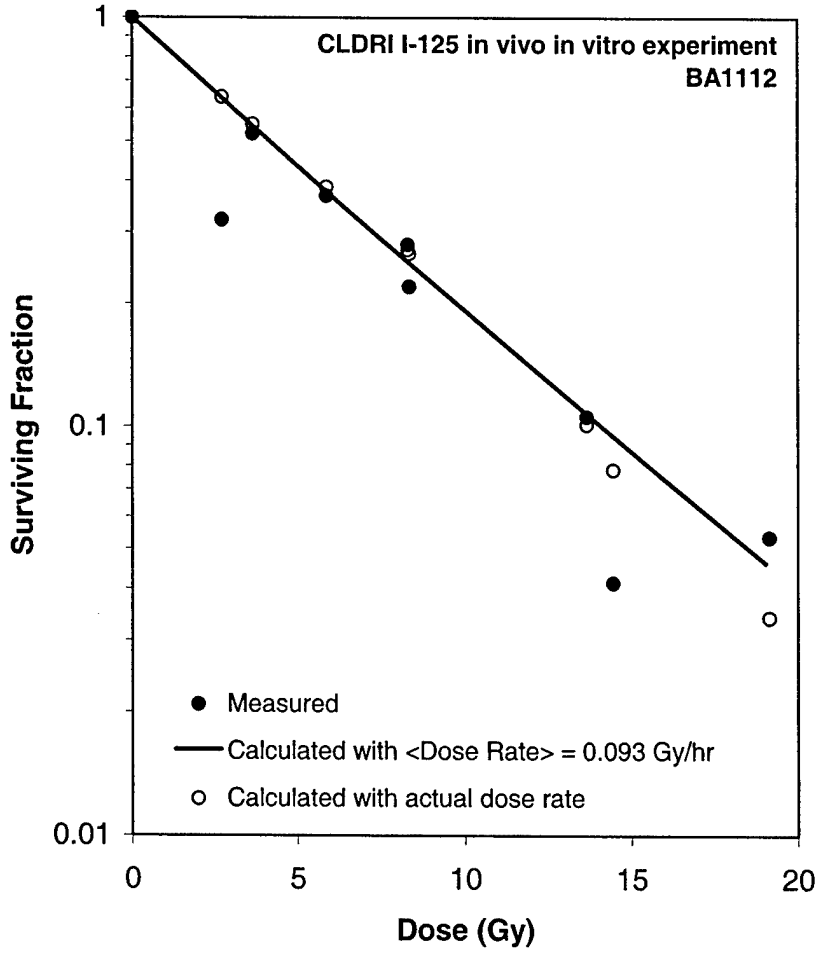

Fig. 11. Surviving fraction as a function of irradiated dose using ^{125}I. The solid and open circles represent measured (using the *in vivo-in vitro* assay technique) and the solid line represents model calculated surviving fraction

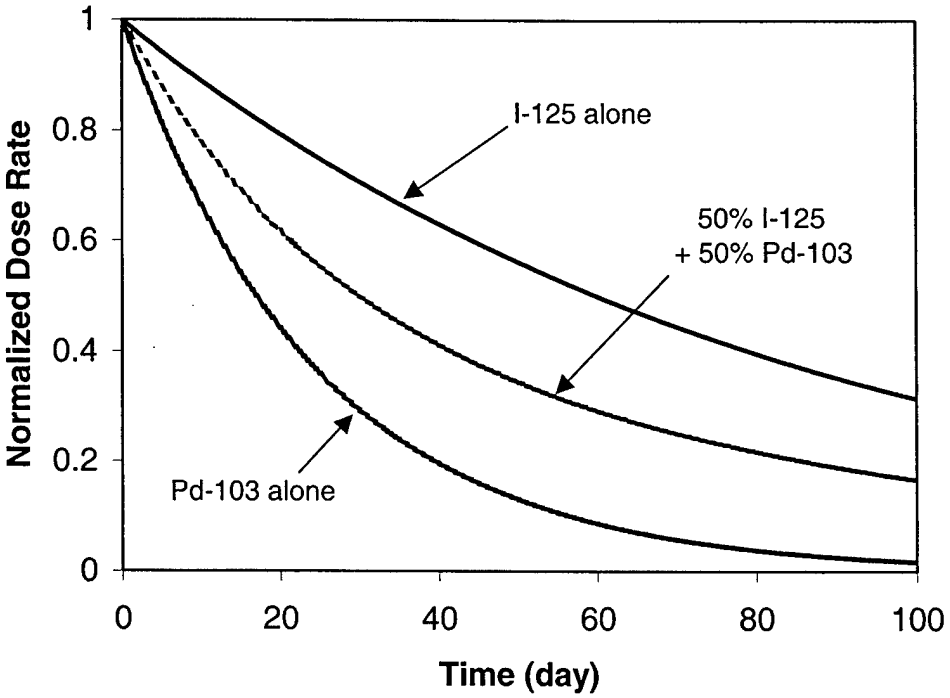

Fig. 12. Normalized dose rate as a function of time for irradiation with ^{125}I alone, ^{103}Pd alone, and with a mixture of ^{125}I and ^{103}Pd each contribute 50% of initial dose rate.

Relative biological effectiveness of ^{103}Pd and ^{125}I photons for continuous low dose rate irradiation of Chinese Hamster cells

Ravinder Nath, Paul Bongiorni, Zhe Chen, Jillian Gragnano, and Sara Rockwell

Department of Therapeutic Radiology, Yale University School of Medicine, 333 Cedar Street, New Haven, Connecticut 06510

Corresponding author:

Ravinder Nath, Ph.D.

203-785-2971 (tel)

203-688-8682 (fax)

ravinder.nath@yale.edu (email)

(Submitted to Radiation Research on March 31, 2004)

Supported in part by DOD grant no. DAMD 17-00-1-0052, awarded by the Department of Army

ABSTRACT

The purpose of this work was to compare the relative biological effectiveness of ^{103}Pd (21 keV photons) and ^{125}I (27 keV photons) sources at dose rates used in permanent implantation of tumors. Half life of ^{103}Pd is about four times shorter than that of the commonly used sources of ^{125}I. Clinical implants are usually prescribed to deliver 145 Gy at initial dose rate of about 7 cGy/hr for ^{125}I and 125 Gy at initial dose rate of 21 cGy/hr for ^{103}Pd. To investigate the effects of different photon energies and half lives of radionuclides used in permanent interstitial brachytherapy, monolayers of Chinese hamster lung cells (CCL-16) were irradiated *in vitro* by ^{103}Pd and ^{125}I sources in a polystyrene phantom. Colony formation ability of irradiated cells under aerobic conditions was measured for graded doses, at dose rates of 6 to 72 cGy/hr. Cells were in exponential growth during the irradiation and a correction for cell loss during the irradiation period was applied to the cell survival data. Cell survival curves from acute high dose rate irradiation (AHDRI) (over 30 Gy/hr) were also measured using nearly monoenergetic x-ray beams which were designed to simulate the mean energies of photons emitted by ^{125}I and ^{103}Pd and using a clinical 250 kVp x-ray beam. A profound dose rate effect is observed over the dose rate range of 6 to 30 cGy/hr. The slopes of the survival curves for ^{125}I increased dramatically as the dose rate increased from 6.89 to 19.1 cGy/hr. Similarly, the ^{103}Pd survival curve for 12.6 cGy/hr was considerably steeper than that for 6.86 cGy/hr. A reverse dose rate effect was observed for both radionuclides with its onset occurring at a dose rate of about 20-30 cGy/hr. The average RBE of ^{103}Pd relative to ^{125}I was 1.45, 1.41, 0.70, and 1.49 at dose rate of 6.86, 12.6, 19.0, and 26.7 cGy/h, respectively. Because ^{103}Pd implants are generally prescribed at a higher initial dose rate (21 cGy/h) than the corresponding ^{125}I implants (6.99 cGy/h), effects of both dose rate and photon energy on biological response should be considered together. For the CCL-16 cells, the RBE of ^{103}Pd at 19.0 cGy/hr relative to ^{125}I at 6.89 cGy/hr was estimated to be 2.3 ± 0.5.

Key words: ^{103}Pd, ^{125}I, RBE, dose rate effect, brachytherapy, permanent implantation, Chinese hamster cells, radiobiology

I. INTRODUCTION

The overall objective of this work was to determine the relative biological effectiveness of ^{103}Pd photons relative to that of conventional sources of ^{125}I for permanent brachytherapy implants. Many factors influence the relative efficacy of radiation delivered at different dose rates [1-4]. As the dose rate falls from the acute dose rates used in external beam radiotherapy (~ 1 Gy/min) to dose rates requiring more than a few minutes for the delivery of the radiation, repair of sublethal damage (SLDR) during irradiation becomes an important factor. As the halftime for SLDR generally is 30-90 minutes and SLDR is generally complete within 6 hrs, the effect of SLDR becomes evident as the treatment time increases from a few minutes to a few hours in duration. The cell population structure and cell proliferation during treatment influence the response of cells to continuous low dose rate irradiation (CLDRI) in a complex fashion. Because cells of different ages have different intrinsic radiosensitivities, radiation selectively kills cells of certain ages, leaving a surviving cell population enriched in cells of resistant ages. This partially synchronized population of radioresistant cells will progress through the cell cycle and, because of normal random variations in the progression rate, will eventually become randomly distributed through the cell cycle. For protracted CLDRI, this "redistribution" may occur during treatment, and will influence the effects of the later part of the radiation treatment. If the radiation treatment is long enough, cell proliferation will result in an increase in the size of cell population and produce a concomitant increase in the radiation resistance of the population. This scenario is further complicated by the fact that radiation also alters cell proliferation, primarily by producing damage which blocks the progression of cells through G_2 and damage that inhibits the entry of cells into the S phase and slows the progression of cells through the S phase. For acute high dose rate irradiation (AHDRI) with x-rays, the G_2 block is the primary effect at low radiation doses [5]. The duration of the G_2 block increases with increasing dose and varies with the age of the cell at the time of irradiation. S-phase delays become increasingly important at high radiation doses. Cell proliferation is clearly altered by CLDRI, but the exact nature of proliferative perturbations is less well defined for CLDRI than for AHDRI. The induction of a G_2 block, and the accumulation of large numbers of cells in this relatively radiosensitive phase during CLDRI, can also have a major impact on the cytotoxicity of the radiation. For some cell lines, this phenomenon can result in a "reverse dose rate effect;"[6] in this case decreasing the dose rate slightly causes more cells to accumulate in G_2 and thereby

results in greater cell kill. The overall pattern of the effect of dose rate on survival of cells irradiation *in vitro* has been described previously[2]. Because of the complex nature of the response of cells to CLDRI, it is important to investigate carefully the radiobiological implications of using new radioisotopes, such as ^{103}Pd.

In addition to the dose rate effects mentioned above, for low energy radioisotopes such as ^{125}I and ^{103}Pd, the RBEs for photons of different energies reflect the LETs of the secondary electrons released by the photons [5,7-8]. Secondary electrons from low energy photons have a higher LET than those from high energy photons. Generally for AHDRI cellular radiosensitivity increases with increasing LET; the survival curves become steeper (reflecting an increase in the amount of damage) and the shoulder becomes smaller (reflecting an increase in the proportion of non-repairable damage) [5,9-12]. For AHDRI using x-rays, it has been found that RBEs for progression delay generally are similar to or larger than those for cytotoxicity [5]. Also, for cells under the conditions of AHDRI, the LET influences the age-response function: the variation in cell survival with cell age decreases with increasing LET and becomes essentially flat at an LET of 100 keV/μ [9].

For these reasons and perhaps others, the RBEs for CLDRI with low energy photons may vary with dose rate in a manner that is complex and difficult to model. Cell survival curves comparing the effects of CLDRI by ^{125}I (27 keV photons, on average), ^{103}Pd (21 keV photons, on average), or ^{241}Am (60 keV photons) with the effects of higher energy photons from ^{192}Ir, ^{137}Cs, ^{60}Co, and ^{226}Ra have generally revealed RBEs for cytotoxicity in the range of 1.2 to 1.9 using various *in vitro* systems [9,13-24]. The change in the shape of the dose-response curve and the increased proportion of non-repairable damage influences the response at relatively high dose rates. Because of the flattening of the age-response curve (which decreases the influence of redistribution) and the relatively large RBE for progression delay (which increases the delay/Gy with higher LET radiations), the changes in the population structure, and the resulting variations in the radiosensitivity of the population, are different for radiations having different LETs. We lack the biological data necessary to fully interpret and model the effects of irradiation with photons of different energies. More biological data and stochastic cell kinetic models [25-28] of the type used in our previous studies [27] will therefore be necessary to interpret fully the RBE data. This work presents some of the critically needed biological data on the response of

mammalian cells *in vitro* irradiated by ^{103}Pd and ^{125}I sources at dose rates of clinical interest in permanent implantation.

II. MATERIALS AND METHODS

A. Chinese hamster cells

Characteristics of the Chinese hamster lung cells (DON Line, American Type Culture Collection CCL-26) and the details of our methodology have been described previously [22]. Chinese hamster cells are grown as monolayers in 75 cm^2 Falcon tissue culture flasks, in a humidified 95% air - 5% CO_2 atmosphere at 37°C. These cells are maintained in basal medium with Eagle's salts, supplemented with fetal calf serum (15% V/V), antibiotics (1% V/V), MEM vitamins (1% V/V) and L-glutamine (1% V/V). Under these conditions, the population doubling time during exponential growth is approximately 12 hr. Stock cultures are subcultured at 3-4 day intervals.

B. Cytotoxicity studies

All experiments were performed using cell monolayers that were prepared by plating cells, suspended from exponentially growing stock cultures, into 60-mm diameter Falcon tissue culture dishes. These cells were incubated for 18 hours prior to irradiation, to allow them to attach and to progress into exponential growth. The cells were seeded 18 hours prior to irradiation, to allow them to attach and to progress into exponential growth. Once the cells were in exponential growth, the growth medium was removed and replaced by fresh growth medium just before the beginning of the irradiations, which lasted 1 to 60 hr in CLDRI, and from several minutes to about half of a hour in AHDRI.

During irradiation, cells were maintained in a humidified 95% air-5% CO_2 environment at 37°C. Unirradiated controls were maintained analogously. After irradiation, the cells were washed with Hanks' balanced salt solution, trypsinized, and counted using a Coulter counter, equipped with a Channelizer to allow assessment of and correction for any changes in cell size. Cells were plated for colony formation in at least four dishes per data point and were allowed to grow in a humidified 95% air-5% CO_2 environment at 37°C for ten days. The colonies were then fixed, stained, and counted. To facilitate accurate counting, the experiments were planned to obtain approximately 120 colonies in each dish, by adjusting the number of cells plated per dish

appropriately. Controls incubated under identical conditions but receiving no irradiation were also examined.

The cell surviving fraction was calculated as the ratio of the plating efficiencies of the irradiated cells relative to those of unirradiated control cells plated at the same time as the irradiated cells. In these experiments, however, the numbers of cells in cultures irradiated with CLDRI were significantly lower than the numbers of cells in control cultures, even though the same numbers of cells were used to initiate the cultures, because of reduced rates of cell division in the irradiated cultures and because some cells died during the prolonged irradiations. The surviving fractions were therefore corrected to account for the deficit in cell number in the irradiated cultures, using the formula:

$$S = \frac{P_{\text{exptl}}}{P_{\text{control}}} \times \frac{C_{\text{exptl}}}{C_{\text{control}}} \qquad (1)$$

where P_{exptl} = plating efficiency of the experimental sample;

P_{control} = plating efficiency of the control sample;

C_{exptl} = number of cells harvested from the experimental sample at the end of irradiation time;

C_{control} = number of cells harvested from the unirradiated control sample assayed at the end of irradiation time.

Plating efficiencies (colonies formed/cells plated) for unirradiated cells were approximately 90% in the experiments reported here.

C. Irradiation technique - CLDRI

Cells in petri dishes were irradiated with especially designed ^{125}I and ^{103}Pd irradiators. The irradiators were made of a 20.3 x 20.3 x 10.2 cm polystyrene phantom with a centered hole (10.2 cm diameter), polystyrene source disks loaded with ^{125}I or ^{103}Pd sources, and polystyrene spacers for dose rate control. Figure 1 show a picture and a cross-sectional view of the ^{103}Pd irradiator. During an experiment, the petri dish was placed on top of the source disk or on top of a polystyrene spacer, depending on the dose rate required for the experiment. The polystyrene source disk has a diameter of 10 cm and a thickness of 1.25 cm. The ^{125}I irradiator was loaded with 26 ^{125}I sources (model 6702; Medi-Physics, Inc., Arlington Heights, IL), each with an initial activity of 40 mCi. Twenty-four of the ^{125}I sources were arranged in a circle with a diameter of 6 cm, and two sources were placed next to each other at the center of the circle. The

^{103}Pd source disk was loaded with 80 ^{103}Pd sources (model 200; Theragenics Corp., Norcross, Atlanta) with an initial activity of 1.9 mCi per source. The sources were arranged in three concentric circles with diameters of 6, 3.5, and 1.3 cm. Different dose rates spanning the range from 6 to 30 cGy/h were obtained by varying the thickness of the polystyrene spacers placed between the sources and the tissue culture dish. During the CLDRI experiment, the ^{125}I and ^{103}Pd irradiators were placed in a 37°C water-jacketed incubator and surrounded in lead foil of 1 mm thickness to shield the photons.

D. Irradiation technique – AHDRI

Acute high dose rate irradiations were performed using a clinical 250-kVp beam from an orthovoltage x-ray unit (Pantek DXT 300, CT). In addition, two heavily filtered x-ray beams were established on an orthovoltage x-ray unit (Pantek DXT 300, CT) to simulate the x-rays emitted by ^{125}I (27.2 – 35.49 keV with an average of 27.4) and ^{103}Pd (20 – 22.7 keV with an average of 20.5 keV) for AHDRI. The Pantek DXT 300 unit provides stable digital tube voltage control to as low as 20 kV. By optimizing the tube voltage (which determines the upper limit of the photon energy spectrum) and the amount of added filtration (which preferentially removes the low-energy bremsstrahlung photons), an x-ray beam with very narrow spectrum was obtained. The equivalent mono-energetic energy of the simulated beam was determined from the measured half-value-layer (HVL) of the beam according to Johns and Cunningham [29]. The HVL was measured under narrow beam condition for each combination of tube voltage and added filtration using an air-equivalent Spokas chamber (Exradin, Model No: A1 [0.5 ml, AE plastic]) and a set of calibrated aluminum sheets (Nuclear Associates). It should be noted that as more aluminum sheets were added into the beam during the HVL measurement, the effective energy of the resulting beam increased. To account for the non-uniform energy response of the Spokas chamber during the HVL measurement, the effective energy of the resulting beam at each aluminum thickness was determined and the energy response for the chamber was then obtained from an energy calibration curve for the Spokas chamber traceable to National Standard of Science and Technology. Figures 2a and 2b plot the relative exposure as a function of the thickness of the aluminum absorber for the simulated ^{125}I and ^{103}Pd beam. The simulated ^{125}I and ^{103}Pd beam were found to have a HVL of 1.85 and 0.84 mm aluminum, respectively, which correspond to equivalent mono-energetic energy of 27.5 and 20.5 keV, respectively. They are

approximately the same as the average energy of the photons emitted by ^{125}I and ^{103}Pd sources. The energy-homogeneity of the beam, as measured by the ratio of the 2nd HVL to the 1st HVL, was close to 90% for both beams indicating a narrow energy spread in the beams' photon energy spectra. The basic parameters of the simulated ^{125}I and ^{103}Pd beams are given in Table I. The clinical 250-kVp beam had a HVL of 1.85 mm Cu.

The output or dose rate for the simulated ^{125}I and ^{103}Pd x-ray beams will be low at the standard treatment dose (SSD of 50 cm) through the machine's adjustable collimator due to the low tube kV and added filtrations. To increase the output, the adjustable collimator was removed for the simulated beams. Without the adjustable collimator, the DXT300 unit produces a circular x-ray beam with a diameter of about 11 cm at 2 cm below the accessory mount. The polystyrene cell culture dish has a diameter of 5.5 cm that would be placed at the center of the x-ray beam. The beam uniformity over the 5.5 cm diameter circular region was within ± 5%.

E. Dosimetry techniques

The doses to the cells in the petri dish from the ^{125}I and ^{103}Pd irradiators were determined from the measured average dose to tissue culture medium in the dish using Fricke dosimetry [22], with a calculated correction for interface effects due to photoelectric effect in the tissue culture dish [22]. The uniformity of dose rate across the dish was verified by three independent means: LiF thermoluminescent dosimetry, film dosimetry and dose calculations by a computerized treatment planning package (Theraplan). In all cases, the dose uniformity across the dish was better than ±5%.

The output or dose rate of the clinical 250 kVp beam and the simulated ^{125}I and ^{103}Pd beams were determined by two independent dosimeters: $FeSO_4$ Fricke chemical dosimeter and the air-equivalent ionization chamber. The Fricke dosimeter uses the standard formulation (0.1 mM ferrous sulfate, 1.0 mM sodium chloride, 0.8 N sulfuric acid) under well established quality assurance program for the dosimeter system [22]. Since the $FeSO_4$ solution (similar to the amount of tissue culture used in experiments) is placed in the same polystyrene culture dish under exactly the same measurement geometry, doses measured by the Fricke dosimeter were used in the analysis of the experimental data. The interface correction due to photoelectric effect in the polystyrene culture dish was taken as approximately 1.0, in this case, since the cells are located upstream in the irradiation beam, as opposed to the irradiation geometry of the ^{125}I and

^{103}Pd irradiators. The radiation output of the three beams for acute irradiations was also checked against measurements using the air-equivalent Spokas chamber and a calibrated parallel-plate soft-energy chamber following the AAPM TG-61 calibration protocol [30]. The dose rate to the dish was determined to be 33.3 Gy/hr, 44.1 Gy/hr, and 38.9 Gy/hr for the simulated ^{103}Pd, the simulated ^{125}I, and the 250-kVp beams, respectively.

F. Determination of RBE

In this work, a in vitro cell surviving fraction of 0.01 (1% of survival) was chosen as the biological endpoint for comparing the relative biological effectiveness of a given irradiation condition on the Chinese hamster cells. The RBE was defined with respect to a standard reference irradiation condition as follows [31],

$$RBE = \frac{D_{250kV}(\dot{d}_R)}{D_T(\dot{d})} \qquad (1)$$

where $D_{250kV}(\dot{d}_R)$ is the dose required to reduce the cell survival to 1% by using 250 kVp x-rays under AHDRI with dose rate of $\dot{d}_R$ and $D_T(\dot{d})$ is the dose required to produce the same cell survival using ^{103}Pd under CLDRI with dose rate of $\dot{d}$. At low dose rates/low doses, the cell survival curve often exhibit only the linear portion of the linear-quadratic (LQ) curve. In these cases, the RBE can be calculated as

$$RBE = \frac{\alpha D_{250kV}}{-\ln S} \qquad (2)$$

where α is fitted linear coefficient of the LQ model and S is the surviving fraction, 0.01 in this work.

The RBE defined by Eq.(1) gives a direct relationship between the biological effectiveness of irradiations using the ^{103}Pd source and of the conventional 250-kVp AHDRI used in the clinic. This definition, however, lumps together the effects of dose rate and linear energy transfer (LET) on RBE. To separate the two effects, one may rewrite Eq.(1) as follows,

$$RBE = \frac{D_{250kV}(\dot{d}_R)}{D_T(\dot{d})} \equiv \frac{D_{250kV}(\dot{d}_R)}{D_T(\dot{d}_R)} \times \frac{D_T(\dot{d}_R)}{D_T(\dot{d})} \equiv RBE_{LET}^{Ref} \times DRF_T \quad (3)$$

where $RBE_{LET}^{Ref} = D_{250kV}(\dot{d}_R)/D_T(\dot{d}_R)$ describes the LET-induced RBE at the AHDRI dose rate and $DRF_T = D_T(\dot{d}_R)/D_T(\dot{d})$ is a dose rate factor for the test irradiation only and contains all the effects caused by the dose rate on RBE. With Eq.(3) the effects of LET and dose rate on RBE can be characterized independently. It should be pointed out that RBE_{LET} defined at the dose rate of test irradiation had been used by many authors in the literature. In such a definition, the additional dose rate dependence of RBE_{LET} arising from the difference of LET of the two comparing radiations cannot be readily discerned. See reference [32] for a detailed discussion.

III. RESULTS

A. Cell loss

The cell loss in irradiated cultures, described in the materials and methods section, was calculated as $(1 - C_{exptl}/C_{control})$ for all dose rates studied here. Figure 3 and 4 plot the cell loss measured at various dose rates for ^{125}I and ^{103}Pd CLDRI, respectively. These data were fitted with straight lines with no intercepts. The slopes of these lines, i.e. the rates of cell loss during irradiation, increased monotonically with increasing dose rate for both radioisotopes. The slopes were similar for the two radioisotopes. This confirms that the cell loss is a dose rate effect primarily related to the length of irradiation period.

B. Cell survival curves and RBE - AHDRI

Cell surviving curves for the CCL-16 Chinese hamster cell irradiated using the simulated ^{103}Pd and ^{125}I x-ray beams and using the 250-kVp x-ray beam under AHDRI condition are plotted in Fig. 5. The dashed lines represent the fit of the experimental data to the linear quadratic cell survival model. Note that the cell survival curves exhibit clear curvatures, indicating a significant contribution of cell killing from reparable damages. The doses required to produce a surviving fraction of 1% was 8.64, 10.09, and 10.86 Gy for the ^{103}Pd, ^{125}I, and 250 kVp x-ray beams, respectively. The RBE of the simulated ^{103}Pd and ^{125}I x-ray beams relative to the 250-kVp x-ray beam under AHDRI condition were found to be 1.26 and 1.08. Since the ^{103}Pd

photons have lower energy, therefore higher LET, the RBE of ^{103}Pd is higher than that of ^{125}I photons as expected. Relative to the ^{125}I, the ^{103}Pd photons are approximately 17% more effective in producing in vitro cell kill on the Chinese hamster cells under AHDRI.

C. Cell survival curves and RBE - CLDRI

Figure 6 and 7 illustrates cell survival curves obtained at different dose rates for CLDRI using ^{103}Pd and ^{125}I sources, respectively. The data for dose rates greater than 19.2 cGy/hr for ^{125}I were not shown in Fig. 7 for the sake of clarity. At these dose rates, the survival curves were essentially linear on the semi-log plot. These data were fitted to the linear-quadratic survival model. Because the quadratic term did not significantly improve the goodness of the fit, the survival data were fitted to a straight line with an intercept of 1.0 according to the following:

$$LnS = -\alpha D \qquad (4)$$

where S is the surviving fraction, D is the dose in Gy and α is the slope of the survival curve in Gy^{-1}. The values of α obtained from the fit are given in Table II and plotted in Fig. 8 for ^{103}Pd and ^{125}I. For cells irradiated by ^{103}Pd sources, the α increased as dose rate increased from 6.86 cGy/hr to 26.7 cGy/hr except a slight dip at dose rate of 19.0 cGy/hr. For cells irradiated by ^{125}I sources, α increased as dose rate increased from 6.89 to 19.1 cGy/hr, and then decreased as the dose rate increased further to 30.9 cGy/h. Beyond 30.9 cGy/hr, changes α were relatively small up to a dose rate of 72.5 cGy/hr.

The RBEs of ^{125}I and ^{103}Pd photons in CLDRI relative to 250 kVp x-rays in AHDRI were calculated following Eq.(2) for the 0.01 surviving fraction evaluation endpoint. The calculated RBEs are listed in Table III and its variation with dose rate is illustrated in Figure 9. The RBE of ^{103}Pd relative to AHDRI of 250 kVp x-rays decreased rapidly initially from a value of 1.84 at 26.7 cGy/h to 1.11 at 19.0 cGy/h. As the dose rate decreased further to 12.6 cGy/h, the RBE increased slightly to 1.16 and then decreased rapidly again to 0.72 at 6.86 cGy/h. The trend of the RBE of ^{125}I relative to AHDRI of 250 kVp x-rays appeared quite different from that of ^{103}Pd around the dose rate of 19 cGy/hr. For ^{125}I, the RBE started from a value of 0.5 at 6.89 cGy/hr and increased to 0.83 at 11.9 cGy/hr. The increase continued to a value of 1.58 at 19.1 cGy/hr and then decreased to 1.23 at dose rate of 30.9 cGy/h. Beyond 30.9 cGy/hr (the was no corresponding data available for ^{103}Pd in this range), the RBE leveled off with slight variation.

Note that when the dose rate increases to acute irradiation, the RBE will attain the value of 1.26 and 1.08, respectively.

For a direct comparison, the RBEs of ^{103}Pd photons relative to ^{125}I photons were calculated from Table III in two ways: (i) using ^{125}I at the same dose rate of ^{103}Pd for reference, and (ii) using ^{125}I at 6.86 cGy/hr as reference. The results are given in Table IV and Fig. 10. It is interesting to note that when similar dose rate were used in both ^{103}Pd and ^{125}I CLDRI the RBE of ^{103}Pd relative to ^{125}I was approximately 1.4 at dose rates of 6.86, 12.6, and 26.7 cGy/hr, but was only 0.7, a reduction by approximately a factor of 2, at the dose rate close to 19 cGy/hr. Nonetheless, as shown in the third column of Table IV, the ^{103}Pd photons with dose rate of 19 cGy/hr (close to what is used in clinical permanent seed implant) is still more effective, by a factor of more than 2, compared to ^{125}I photons delivered with the initial dose rate of 6.89 cGy/hr (commonly used in clinical permanent seed implants).

IV. DISCUSSION

Our results indicated that the biological effectiveness of the photons emitted by ^{103}Pd and ^{125}I relative to AHDRI 250 kVp x-rays is dependent on both the LET and the dose rate of irradiation. The dose rate dependence of RBE was complicated by the presence of reverse dose rate effects in the range of dose rates studied in this work for both ^{103}Pd and ^{125}I CLIDRI on Chinese hamster cells. In general, the RBE of ^{103}Pd photons was greater than that of ^{125}I. For ^{125}I, the RBE at AHDRI was 1.08 and increased gradually as dose rate decreased and was 1.2 to 1.4 in the range of 30 to 75 cGy/hr. Further decrease in dose rate resulted in an rapid increase of RBE initially to a value of approximately 1.6 and followed by rapid decrease of RBE to a value of 0.5 at 6.89 cGy/hr. For ^{103}Pd, we do not have data for dose rates from 30 to 75 cGy/hr. Nonetheless, the RBE changed from a value of 1.26 at AHDRI to a value of 1.8 as the dose rate decreased to 26.7 cGy/hr. A rapid reduction in RBE followed when the dose rate decreased further to 19.0 cGy/hr. After a slight increase of RBE at 12.6 cGy/hr, the RBE decreased as dose rate decreased further. The increase in RBE as dose rate decreased in the range of 12 to 30 cGy/hr is a manifestation of the reverse dose rate effect as discussed in the Introduction. The results shown in Table III and Fig.9 indicate that the onset of the reverse dose rate effect occurred at different dose rates for ^{103}Pd and ^{125}I CLDRI. . It seems to suggest that the onset of the reverse dose rate effect might be affected by the different LET of the ^{103}Pd and ^{125}I photons.

More carefully controlled experiments would be helpful to verify and determine the detailed dependence of the reverse dose rate effect as a function of dose rate.

The LET-dependence of the onset of reverse dose rate effect, if proven to be true, would have an impact on comparing the relative biological effectiveness of ^{103}Pd implants to the ^{125}I implants. For Chinese hamster cells, the RBE of ^{103}Pd photon relative to ^{125}I photons delivered at the same dose of 19.0 cGy/h (close to the 21 cGy/h initial dose rate currently used in ^{103}Pd permanent prostate implant) was only 0.7, a factor of two smaller than what was measured at other dose rates. Therefore, a meaningful clinical application of RBE requires a more systematic study of the RBE of the ^{103}Pd photons relative to ^{125}I over a range of clinically relevant dose rates. It would be interesting to find out if a reverse dose rate effect exists for human prostate cancer when irradiated by CLDRI of ^{103}Pd or ^{125}I photons and whether the onset, if exists, of the reverse dose rate effect occurs within the clinically relevant dose rates. Since the dose rate decreases continuous with time in permanent implants, the overall impact of LET-dependence of the reverse dose rate effect would be smaller than what was indicated from the in vitro CLDRI at relatively constant dose rates.

Because of its dose-rate dependence, it is important to compare the RBE of ^{103}Pd to ^{125}I with respect to their dose rates of clinical application. ^{103}Pd implants are generally prescribed at a higher initial dose rate (21 cGy/h) than the corresponding ^{125}I implants (6.99 cGy/h). Even though the RBE of ^{103}Pd relative to ^{125}I at the dose rate of 19.0 cGy/h was 0.7 while it was 1.45 when both were irradiated at the dose rate of 6.8 cGy/h, the clinically relevant comparison should be relative biological efficacy of ^{103}Pd photons delivered at 21 cGy/h to ^{125}I photons delivered at dose rate of 6.99 cGy/h. For the CCL-16 cells, the RBE of ^{103}Pd at 19.0 cGy/hr relative to ^{125}I at 6.89 cGy/hr was estimated to be 2.3 ± 0.5, different from either 1.4 or 0.7 determined with matched dose rates.

There are only limited data in the literature, which an indirect comparison to our measured RBE can be made. Ling et al [24] had measured the RBE of ^{103}Pd and ^{125}I relative to ^{60}Co with dose rates matched for the test and reference irradiations. From these data, the RBE of ^{103}Pd relative ^{125}I at a matched dose rate of 7 cGy/hr can be deduced and was 1.36 for in vitro CLDRI of REC:ras cells. Our measured value of 1.45 for the Chinese hamster cells at the dose rate of 6.86 cGy/hr was remarkably close to 1.36, keeping in mind that the cell lines are different. In addition, the RBE of ^{103}Pd relative 250 kVp x-rays for AHDRI of BA1112

rhabdomyosarcomas cells had been measured by Nath et al [32] to be 1.24. This value is also very close to what was measured in this work (1.26) for ^{103}Pd with AHDRI of the Chinese hamster cells. While the cell lines used in these experiments were different, the quoted measurements were aimed at quantifying the LET-induced RBE and the close agreements indicate that our basic experimental methodology is correct. Different cell lines, however, are believed to have different impact on the overall dose rate and LET dependence of RBE, for example, the presence of reverse dose rate effect as discussed earlier, whose impact has not been explicitly shown in the literatures.

The reduction of RBE as a function of dose rate also carries some interesting clinical implications for permanent implants. On the one hand, the dose rate of irradiation to organs at risk and normal tissues outside the target volume is always lower than that inside the target volume due to the rapid dose-fall-off around the low-energy photon sources. Therefore permanent implants would provide additional sparing, beyond that indicated by the planned physical dose, to the organs at risk and the surrounding normal tissues. By the same token, any "cold" spots of dose rate occurring inside the target volume would be worse biologically than what is indicated by physical dose alone. Therefore, both the dose and dose rate should be considered in the planning and evaluation of permanent implants. Ideally, the RBE_{LET}^{Ref} and the DRF_T should be build into the planning and evaluation software for brachytherapy.

V. CONCLUSION

The relative biological effectiveness of ^{103}Pd photons relative to that of conventional sources of ^{125}I was determined for Chinese hamster lung cell (CCL-16) at acute high dose rate irradiation and at continuous low dose rate irradiations at dose rates relevant to clinical permanent brachytherapy implants. At AHDRI, the ^{103}Pd photons are biologically more effective than the ^{125}I photons with a RBE of 1.17. For CLDRI, the RBE of ^{103}Pd varies with both the dose rate of ^{103}Pd and the dose rate of ^{125}I "reference" irradiation. When the dose rates of ^{103}Pd and ^{125}I were similar, the RBE of ^{103}Pd photons relative to ^{125}I was approximately 1.4 at dose rates of 6.86, 12.6, and 26.7 cGy/h, but was only 0.7 at the dose rate close to 19 cGy/h due to reverse dose rate effect. For clinically relevant dose rate, the ^{103}Pd photons with dose rate of 19 cGy/h is more effective, by a factor of more than 2, compared to ^{125}I photons used in clinical implants with initial dose rate of 6.89 cGy/h.

References

1. E.J. Hall, Radiation dose rate: a factor of importance in radiobiology and radiotherapy. Br. J. Radiol. 45, 81-97 (1972).
2. E.J. Hall, The biological basis of endocurietherapy, Endocur. Hyperthermia Oncol. 1, 141-152 (1985).
3. G.G. Steel, J.D. Down, J.H. Peacock, and T.C. Stephens, Dose-rate effects and the repair of radiation damage, Radiother. Oncol. 5, 321-331, (1986).
4. G.G. Steel, J.M. Deacon, G.M. Duchesne, , A. Horwich, L.R. Kelland, J.H. Peacock, The dose-rate effect in human tumour cells , Radiother. Oncol. 9, 299-310 (1987).
5. J.F. Scaife, The RBE of 137Cs-gamma, 250 kV and 100 kV x-rays for mitotic delay and survival in human kidneys cells, Int. J. Radiat. Biol. 15, 279-283 (1969).
6. J.B. Mitchell, J.S. Bedford, S.M. Bailey, Dose-rate effects on the cell cycle and survival of S3 HeLa and V79 cells, Radiat Res 79(3):520-36 (1979).
7. V.P. Bond, C.B. Meinhold, H.H. Rossi, Low-dose RBE and Q for x-ray compared to gamma-ray radiations, Health Physics 34(5):433-8 (1978).
8. W.K. Sinclair, Radiat Res 16, 369-383 (1962).
9. W.K. Sinclair, Radiat Res 16, 369-383 (1962).
10. M. Bistrovic, M. Biscan, T. Viculin, RBE of 20 kV and 70 kV X-rays determined for survival of V 79 cells, Radiotherapy & Oncology 7(2):175-80 (1986).
11. E.R. Hering, An investigation of changes in relative biological effectiveness (RBE) with depth for X ray beams generated between 100 and 250 kVp using the mouse foot as biological test system, Int J Radiat Oncol Biol Phys 12(5):815-21 (1986).
12. L. Zeitz, S.H. Kim, J.H. Kim, J.F. Detko, Determination of relative biological effectiveness (RBE) of soft X rays, Radiat Res 70(3):552-63 (1977).
13. M.L. Freeman, P. Goldhagen, E. Sierra, E.J. Hall, Studies with encapsulated 125I sources. II. Determination of the relative biological effectiveness using cultured mammalian cells, Int J Radiat Oncol Biol Phys 8(8):1355-61 (1982).
14. E.R. Hering, A comparison of the biological effect of 125I and 192Ir gamma rays on the roots of Vicia faba using a specially designed applicator, Brit J Radiol 53(627):255-8 (1980).
15. E.R. Hering, P.P. Le Roux, R. Sealy, A comparison of the biological effect of iodine 125 and tantalum 182 gamma rays using Vicia faba roots, Brit J Radiol 51(605):392-3 (1978).
16. E.R. Hering ER. Sealy GR. Dowman P. Blekkenhorst G. OER and RBE for 125I and 192Ir at low dose rate on mammalian cells. *Radiotherapy & Oncology. 10(3):247-52, 1987.*
17. E.R. Hering, G. Blekkenhorst, P. Dowman, OER and RBE for two types of iodine seed, Brit J Radiol 61(729):862 (1988).

18. D.K. Kwan, A.R. Kagan, A. Norman, Relative biological effectiveness of 125I in the induction of micronuclei in human peripheral blood lymphocytes, Radiother Oncol 4(2):163-6 (1985).

19. M.J. Marchese, E.J. Hall, B.S. Hilaris, Encapsulated iodine-125 in radiation oncology. I. Study of the relative biological effectiveness (RBE) using low dose rate irradiation of mammalian cell cultures, Am J Clin Oncol 7(6):607-11 (1984).

20. M.J. Marchese, E.J. Hall, B.S. Hilaris, Endocur. Hyperthermia Oncol. 1, 67-82 (1985).

21. M.J. Marchese, P.E. Goldhagen, M. Zaider, D.J. Brenner, E.J. Hall, The relative biological effectiveness of photon radiation from encapsulated iodine-125, assessed in cells of human origin: I. Normal diploid fibroblasts, Int J Radiat Oncol Biol Phys 18(6):1407-13 (1990).

22. R. Nath, P. Bongiorni, S. Rockwell, The RBEs of ^{125}I and ^{241}Am photons relative to ^{226}Ra photons for continuous low dose rate irradiations at dose rates of 0.17 to 0.73 Gy/hr, Endocur Hyperthermia Oncol 6, 81-91 (1990).

23. R.J. Schulz, P. Bongiorni, The dose rate dependence of the relative biological effectiveness of 241Am versus 226Ra gamma rays, Radiat Res 118(3):420-36 (1989).

24. M. Demeestere, S. Rockwell, A.J. Valleron, E. Frindel, M. Tubiana, Cell proliferation in EMT6 tumours treated with single doses of X-rays or hydroxyurea. II. Computer simulations, Cell Tissue Kinetics 13(3):309-17 (1980).J.B. Mitchell, J.S. Bedford, and S.M. Bailey, Radiat. Res. 79, 520-536 (1979).

25. Ling, CC, Li, WX, Anderson, L, The relative biological effectiveness of I-125 and Pd-103. Int. J. Radiat. Oncol. Biol. Phys. 32:373-378, 1995.

26. G.M. Hahn and R.F. Kallman, Radiat. Res. 30, 702-713 (1985).

27. C.R. King, R. Nath, and S. Rockwell, "Effects of Continuous Low Dose Rate Irradiation: Computer Simulations," Cell Tissue Kinet. 21, 339-351 (1988).

28. A.-J. Valleron and E. Frindel, Computer simulation of growing cell populations, Cell Tissue Kinet 6, 69-79 (1973).

29. Johns H and Cunningham J, The Physics of Radiology, 4th ed., Springfield: Thomas 1983.

30. Ma CM, Coffey CW, DeWerd LA, Liu C, Nath R, Seltzer SM, Seuntjens JP; AAPM protocol for 40-300 kV x-ray beam dosimetry in radiotherapy and radiobiology. Med Phys. 28:868-93 2001.

31. Hall EJ. Radiobiology for the radiologist. 4th ed. Philadelphia: Lippincott, 1994.

32. Nath R, Bongiorni P, Chen Z, Gragnano J, and Rockwell R, Dose rate dependence of the relative biological effectiveness of ^{103}Pd for continuous low dose rate irradiation of BA1112 rhabdomyosarcoma cells in vitro relative to acute exposures, submitted to Int. J. Radiat. Biol. 2004.

Figure Captions:

Figure 1 A photograph and a schematic cross-sectional view of the ^{103}Pd irradiator used for continuous low dose rate irradiation (CLDRI) of the CCL-16 cells in culture dishes. The polystyrene spacer is designed to produce different dose rates for the CLDRI experiments. The ^{103}Pd irradiator was placed in a 37°C water-jacketed incubator and surrounded by lead foil of 1 mm thickness (not shown in the sketch) to shield the photons emitted by ^{103}Pd during the experiments. The ^{125}I irradiator has the same design except the source-loading pattern on the source disk.

Figure 2 Relative exposures as a function of added filtration for the simulated ^{103}Pd (top panel) and ^{125}I (lower panel) beams established on an orthovoltage x-ray machine. The half-value-layer thickness was determined from these curves. Their equivalent mono-energetic photon energy and the basic operating parameters were given in Table I.

Figure 3 Cell loss measured at different dose rates of CLDRI with ^{125}I.

Figure 4 Cell loss measured at different dose rates of CLDRI with ^{103}Pd.

Figure 5 Cell survival curves of CCL-16 cells under acute high dose rate irradiations (AHDRI) by the simulated ^{103}Pd, simulated ^{125}I, a clinical 250-kVp x-ray beams. Open squares, circles, and filled triangles represent measured surviving fractions from the 250 kVp x-rays, the simulated ^{125}I x-rays, and the simulated ^{103}Pd x-rays, respectively. Lines represent fits to data using the linear-quadratic model.

Figure 6 Cell survival curves of CCL-16 cells under continuous low dose rate irradiation (CLDRI) by ^{103}Pd sources at dose rates of 6.86 (open diamonds), 12.6 (open circles), 19.0 (open squares), and 26.7 cGy/h (open triangles), respectively. Lines represent fits to data using the linear portion of the linear-quadratic model.

Figure 7 Cell survival curves of CCL-16 cells under continuous low dose rate irradiation (CLDRI) by ^{125}I sources at dose rates of 6.89 (open diamonds), 11.9 (open squares), 16.1 (open circles), and 19.1 cGy/h (open triangles), respectively. Lines

represent fits to data using the linear portion of the linear-quadratic model. For the sake of clarity, the data for dose rates greater than 0.192 Gy/hr is not shown here. However, the slopes of the cell survival curves at higher dose rate are shown in Fig. 8

Figure 8 The fitted α co-efficient for ^{125}I (open circles) and ^{103}Pd (closed circles) as a function of the dose rate. The dashed lines were drawn to help distinguish the two data sets. The error bars represent the values of $\alpha \pm$ one standard deviation.

Figure 9 RBE (relative to acute high dose rate irradiation of 250 kVp x-rays) of ^{125}I (open circles) and ^{103}Pd (closed circles) photons as a function of the dose rate. The dashed lines were drawn to help distinguish the two data sets.

Figure 10 The RBE of ^{103}Pd photons relative to ^{125}I photons at the same dose rates (filled circles) The dashed line were drawn for easy visualization. Error bars represent one standard deviation.

Table I. Radiation characteristics of the simulated x-ray beams

	kV	mA	Added Filter (mm AL)	Beam HVL (mm AL)	Energy Homogeneity (%)	Equivalent Energy (keV)	<E> from isotope (keV)
I-125 Simulated	43	20	3.545	1.851	86.9	27.45	27.4
Pd-103 Simulated	29	25	1.826	0.82	88.6	20.5	20.5

Note that the homogeneity index for the beam energy was defined as the ratio of the second HVL to the first HVL. For a mono-energetic beam, it equals to 100%. Both the ^{125}I and ^{103}Pd simulated beams have a homogeneity index close to 90%.

Table II. Fitted α for CLDRI

^{125}I		^{103}Pd	
Dose Rate (cGy/h)	**α* (Gy^{-1})**	**Dose Rate (cGy/h)**	**α* (Gy^{-1})**
6.89	0.210 ± 0.046	6.86	0.304 ± 0.053
11.9	0.348 ± 0.046	12.6	0.491 ± 0.058
16.1	0.380 ± 0.044	19.0	0.471 ± 0.059
19.1	0.670 ± 0.047	26.7	0.781 ± 0.09
30.9	0.523 ± 0.026		
55.0	0.596 ± 0.040		
72.5	0.527 ± 0.040		

* The error limits for the values of α are standard errors.

Table III. RBE of ^{103}Pd and ^{125}I photons relative to 250 kVp x-rays

^{125}I		^{103}Pd	
Dose Rate (cGy/h)	RBE	Dose Rate (cGy/h)	RBE
6.89	0.50	6.86	0.72
11.9	0.82	12.6	1.16
16.1	0.90	19.0	1.11
19.1	1.58	26.7	1.84
30.9	1.23		
55.0	1.41		
72.5	1.24		
AHDRI	1.08	AHDRI	1.26

Table IV. RBE of ^{103}Pd photons relative to ^{125}I.

Dose Rate (cGy/h)	Relative to ^{125}I at same dose rate	Relative to ^{125}I at 6.86 cGy/h
6.86	1.44	1.44
12.6	1.41	2.32
19.0	0.70	2.22
26.7	1.49	3.68
AHDRI	1.17	2.52

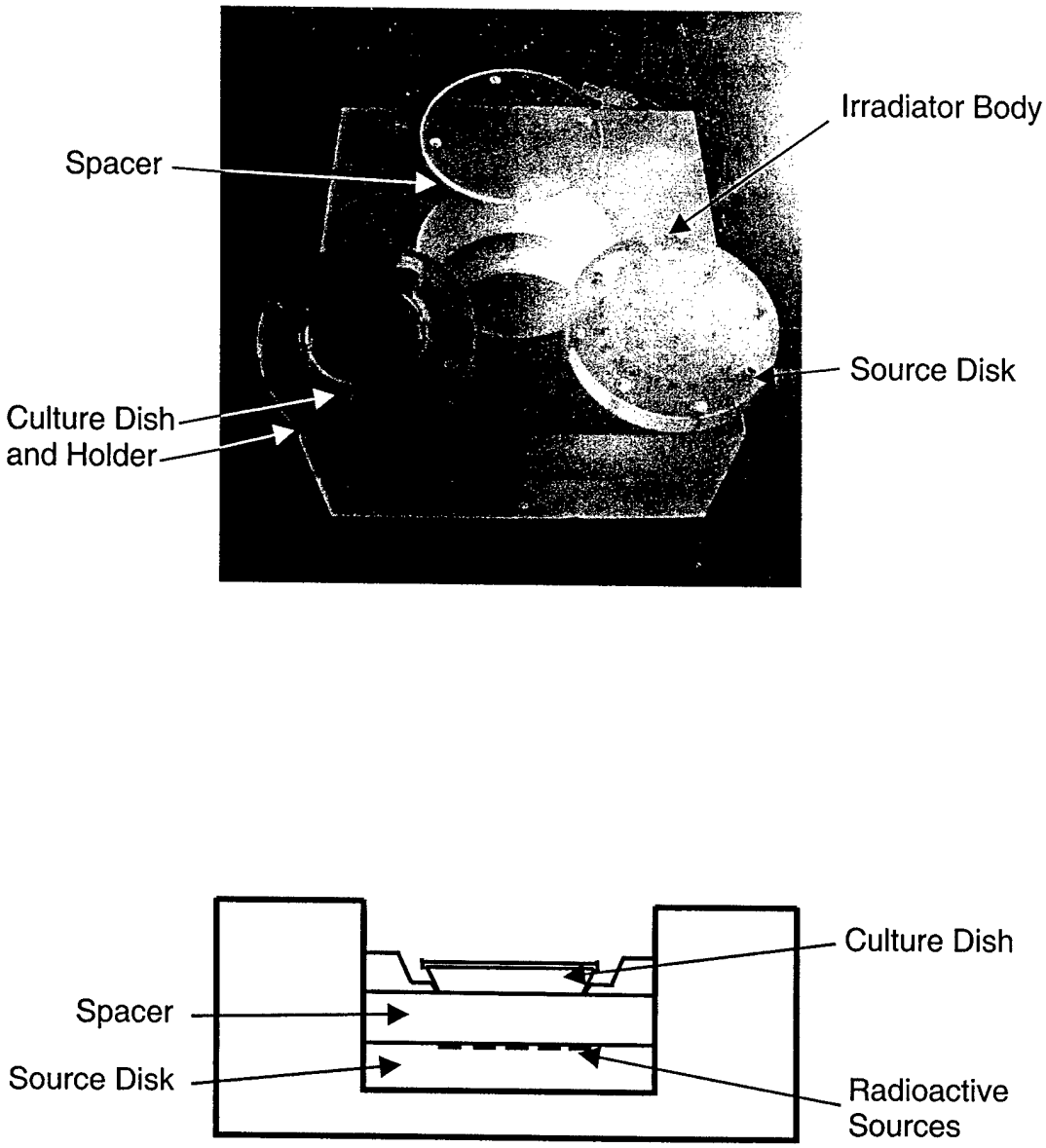

Fig. 1. A photograpy and a schematic cross-sectional view of the ^{103}Pd irradiator used for continuous low dose rate irradiation (CLDRI) of the CCL-16 cells in culture dishes. The polystyrene spacer is designed to produce different dose rates for the CLDRI experiments. The ^{103}Pd irradiator was placed in a 37°C water-jacketed incubator and surrounded by lead foil of 1 mm thickness (not shown in the sketch) to shield the photons emitted by ^{103}Pd during the experiments. The ^{125}I irradiator has the same design except the source-loading pattern on the source disk.

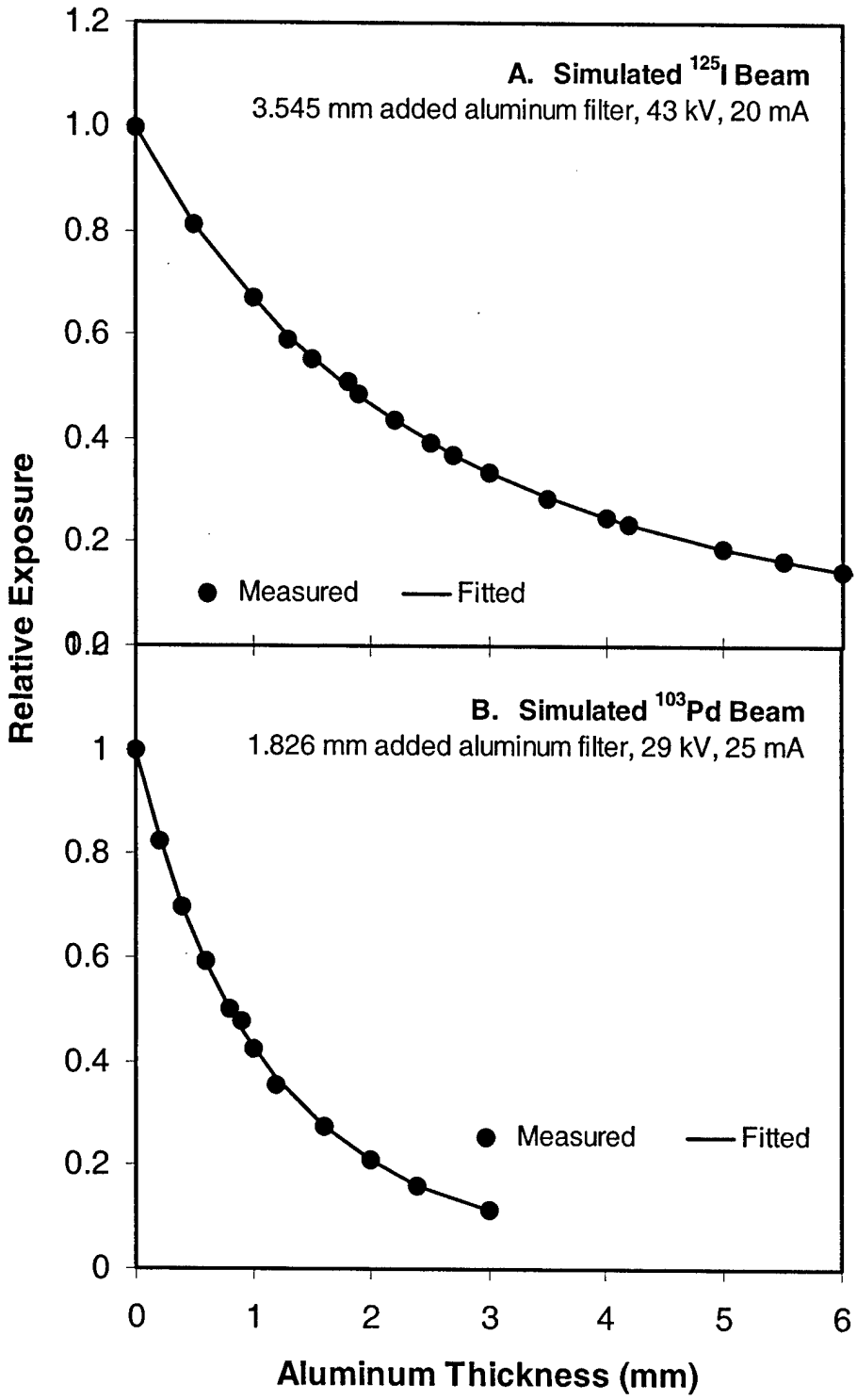

Fig. 2. Relative exposures as a function of added filtration for the simulated ^{103}Pd (top panel) and ^{125}I (lower panel) beams established on an orthovoltage x-ray machine. The half-value-layer thickness was determined from these curves. Their equivalent mono-energetic photon energy and the basic operating parameters were given in Table I.

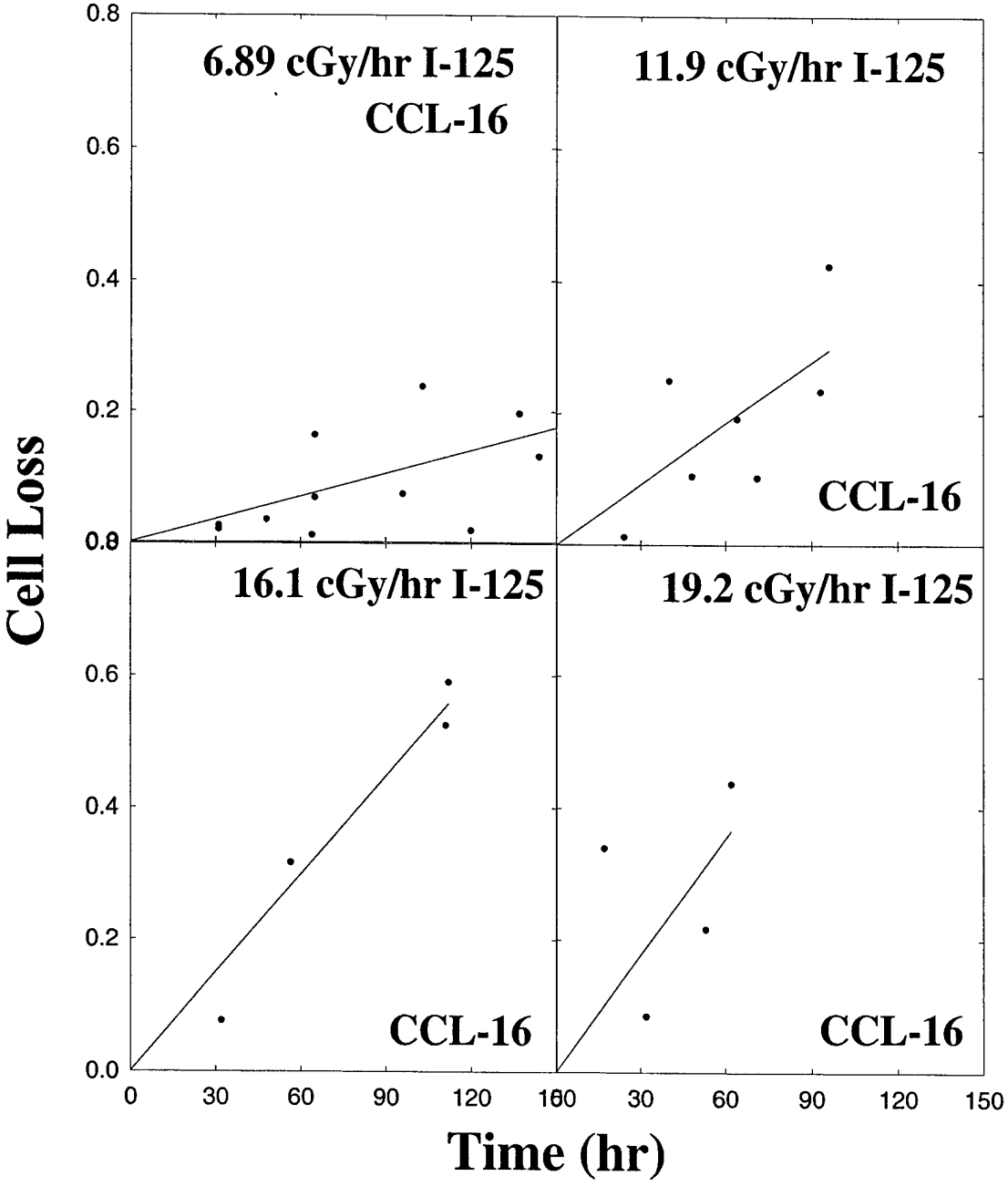

Fig. 3. Cell loss measured at different dose rates of CLDRI with ^{125}I

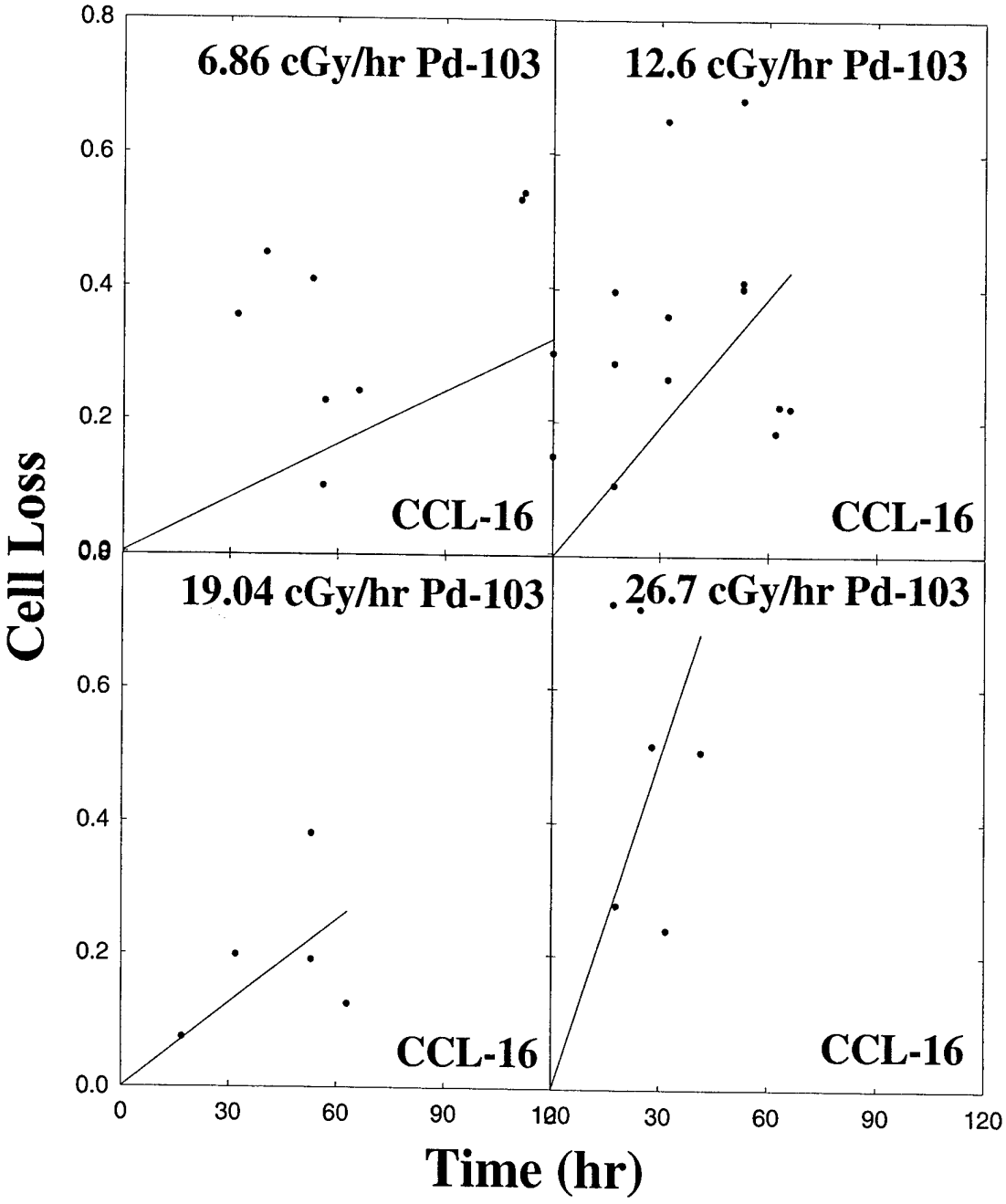

Fig. 4. Cell loss measured at different dose rates of CLDRI with ^{125}Pd

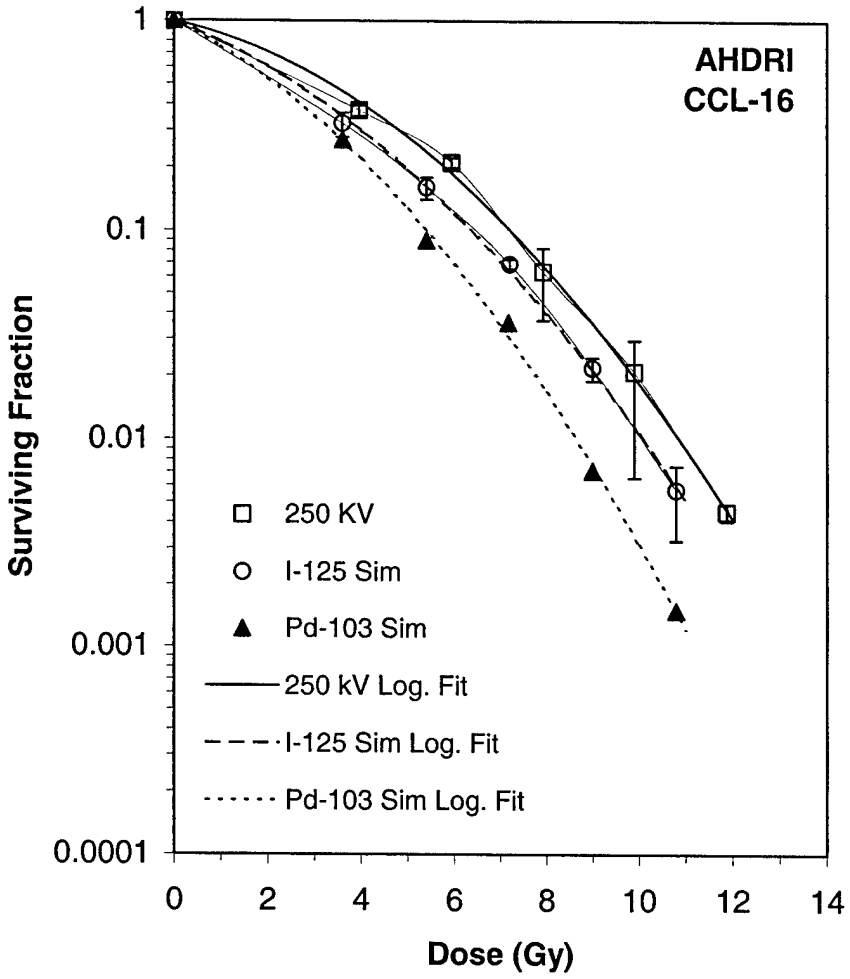

Fig. 5. Cell survival curves of CCL-16 cells under acute high dose rate irradiations (AHDRI) by the simulated ^{103}Pd, simulated ^{125}I, a clinical 250-kVp x-ray beams. Open squares, circles, and filled triangles represent measured surviving fractions from the 250 kVp x-rays, the simulated ^{125}I x-rays, and the simulated ^{103}Pd x-rays, respectively. Lines represent fits to data using the linear-quadratic model.

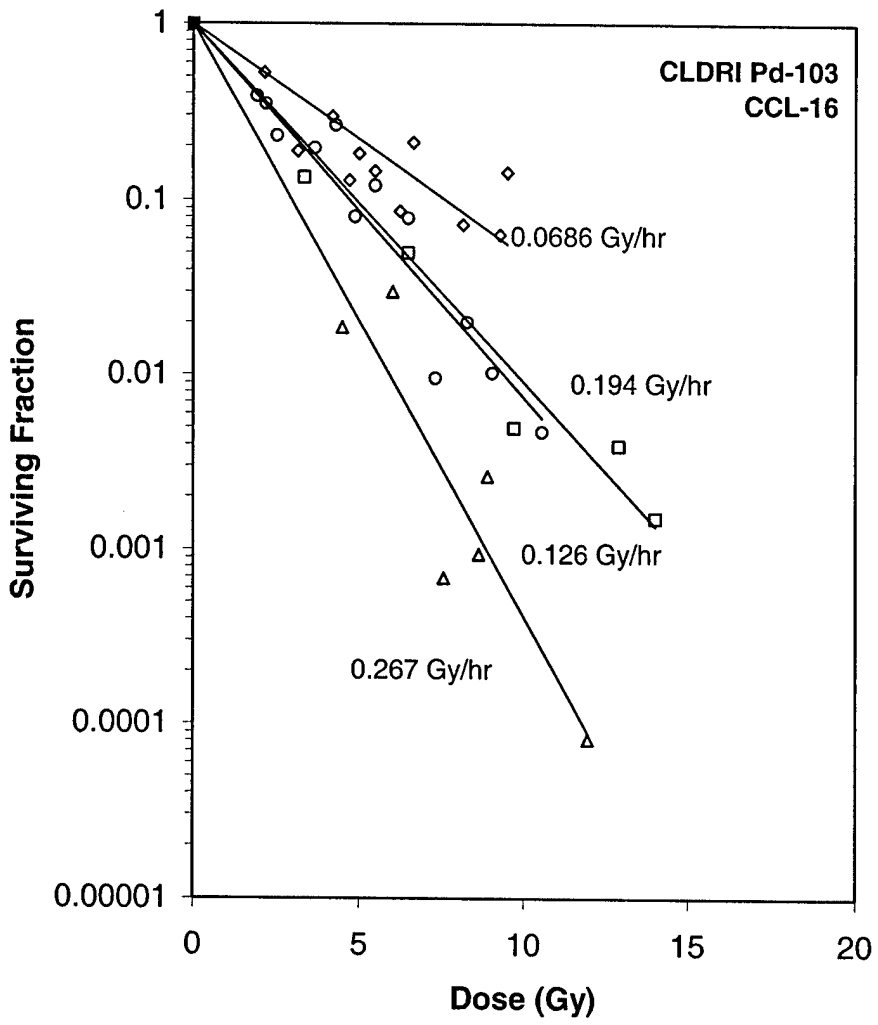

Fig. 6. Cell survival curves of CCL-16 cells under continuous low dose rate irradiation (CLDRI) by ^{103}Pd sources at dose rates of 6.86 (open diamonds), 12.6 (open circles), 19.0 (open squares), and 26.7 cGy/h (open triangles), respectively. Lines represent fits to data using the linear portion of the linear-quadratic model.

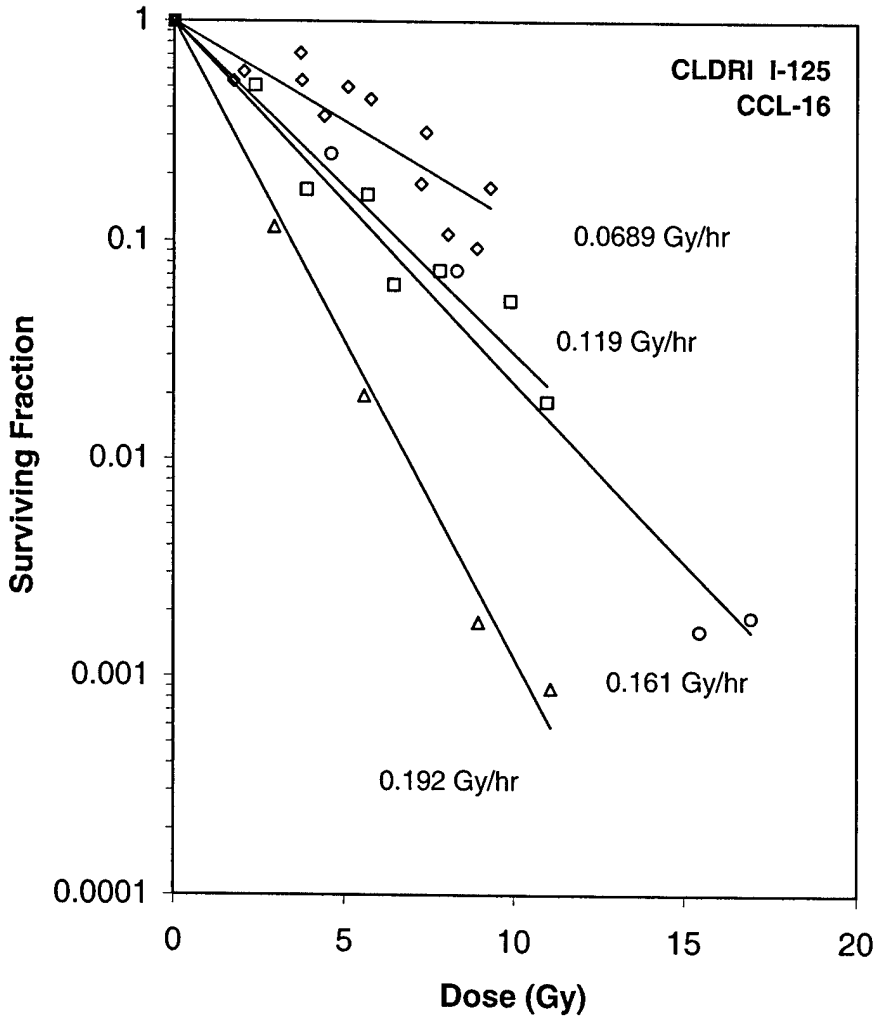

Fig. 7. Cell survival curves for ^{125}I photon irradiations. For the sake of clarity, the data for dose rates greater than 0.192 Gy/hr is not shown here. However, the slopes of the cell survival curves at higher dose rate are shown in Fig. 8.

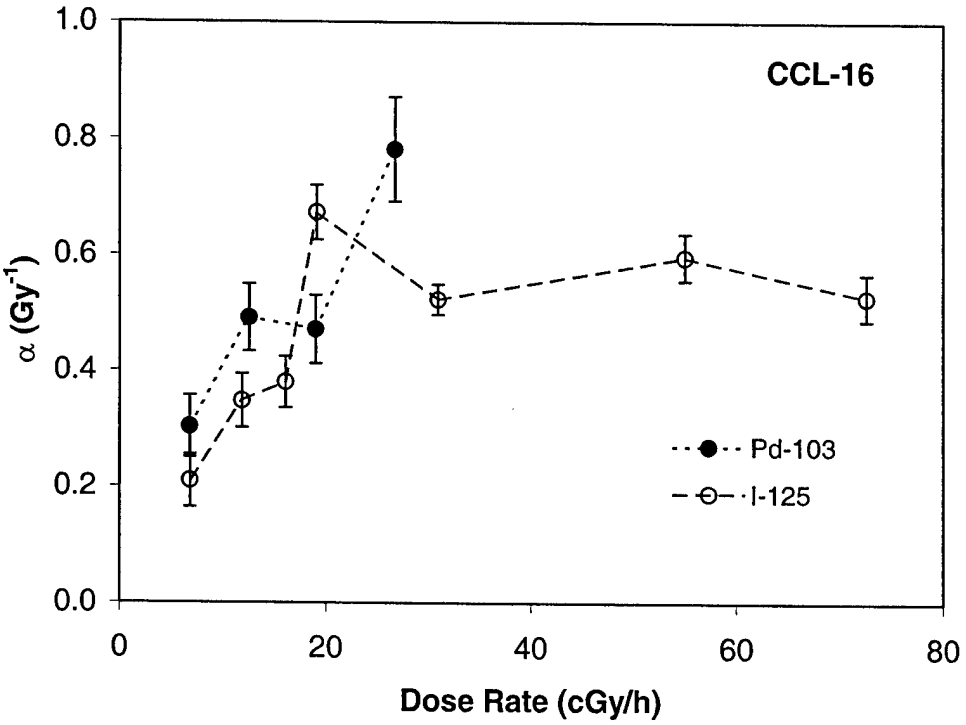

Fig. 8. The fitted α co-efficient for ^{125}I (open circles) and ^{103}Pd (closed circles) as a function of the dose rate. The dashed lines were drawn to help distinguish the two data sets. The error bars represent the values of α ± one standard deviation.

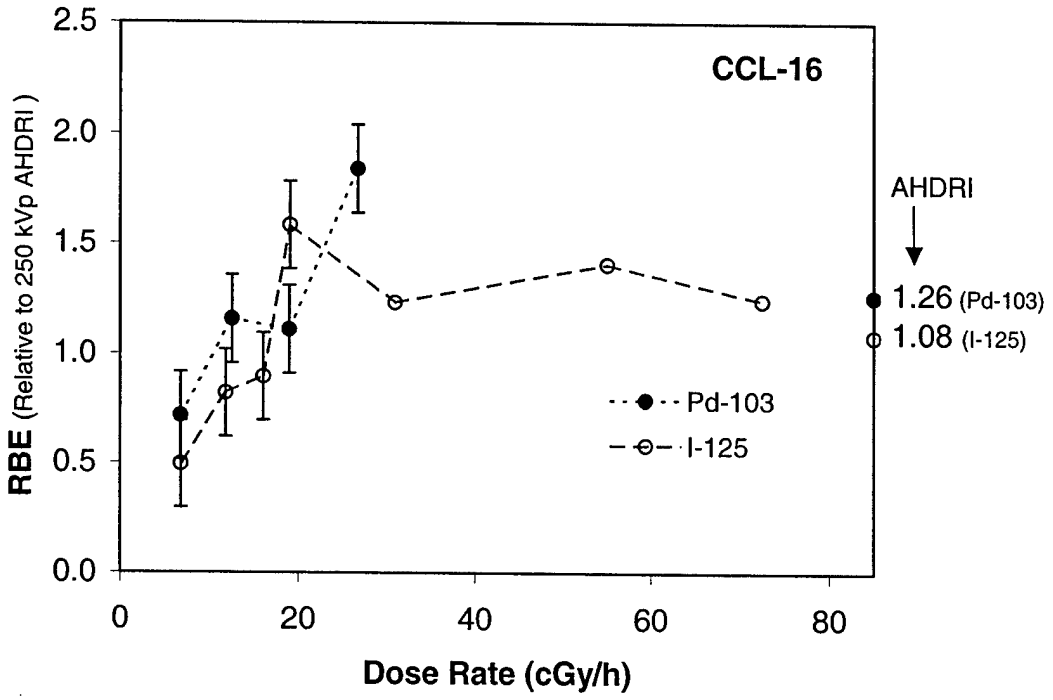

Fig. 9. RBE (relative to acute high dose rate irradiation of 250 kVp x-rays) of ^{125}I (open circles) and ^{103}Pd (closed circles) photons as a function of the dose rate. The dashed lines were drawn to help distinguish the two data sets.

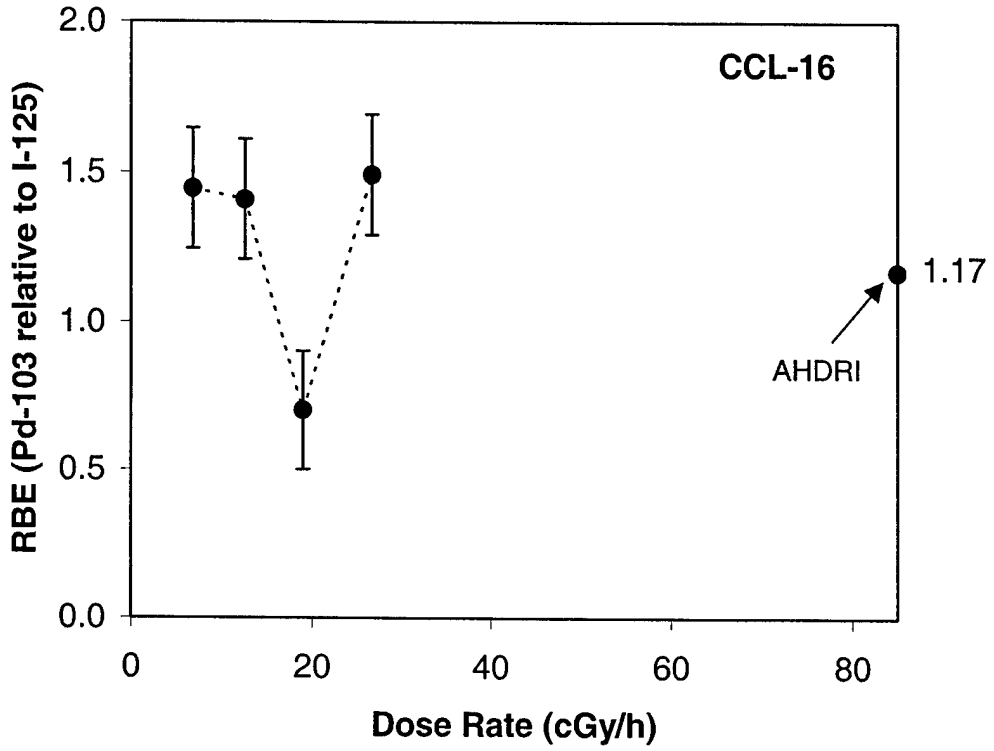

Fig. 10. The RBE of ^{103}Pd photons relative to ^{125}I photons at the same dose rates (filled circles) The dashed line were drawn for easy visualization. Error bars represent one standard deviation.